NASA Contractor Report 189221

Creep Fatigue Life Prediction for Engine Hot Section Materials (Isotropic)

Final Report

R.S. Nelson, G.W. Levan, and P.R. Harvey
United Technologies Corporation
Pratt & Whitney
Commercial Engineering

August 1992

Prepared for
Lewis Research Center
Under Contract NAS3–23288

National Aeronautics and Space Administration

PREFACE

This Final Report covers the activities completed under the optional program of the NASA HOST Contract, "Creep Fatigue Life Prediction for Engine Hot Section Materials (Isotropic)", under Contract NAS3-23288. The time period covered is from May 1987 through February 1989. The objective of this effort was to improve the high temperature crack initiation prediction technology for gas turbine hot section components. This program was initiated under the direction of Dr. Gary R. Halford, who served as the original NASA Program Manager. Dr. Michael A. McGaw served as the NASA Program Manager from 1989 to the conclusion of the program. The Program Manager at United Technologies Corporation was Mr. Richard S. Nelson who also served as prinicipal investigator, having responsibility for the life prediction model development and oversight of most of the technical tasks. Mr. Gregory W. Levan directed the metallographic examinations of the test material and specimens and provided interpretation of the results. For the subject time period, Mr. Peter R. Harvey was responsible for the technical effort under Task VI, Multiaxial Stress State Model; Task XII, Final Verification and Evaluation of the Alternate Material Protective Coating System/Component Combination; and Task XIV, Cyclic Damage Accumulation (CDA) Computer Program.

TABLE OF CONTENTS

TABLE OF CONTENTS (Continued)

SECTION 1.0
SUMMARY

A series of high temperature, strain controlled fatigue tests have been completed to study the effects of complex loadings such as thermomechanical fatigue, multiaxial loading, and imposed mean stresses along with reactive environments. These tests used the cast nickel-base superalloy B1900+Hf (with and without coatings) as a baseline alloy, wrought INCO 718 as an alternative alloy.

The B1900+Hf tests completed during this period included 29 environmental tests using various atmospheres (75 psig oxygen, purified argon, or block exposures). These showed that even small amounts of oxygen can cause life degradation, often non-linear with exposure. Twenty mean stress tests performed at the University of Rhode Island explored the effects of creep fatigue interaction by directly controlling mean stress and strain range at temperatures well into the creep regime.

The majority of the specimen tests completed during this period were of wrought INCO 718, including tensile, creep, stress rupture, TMF, multiaxial, and mean stress tests. These results were used to calibrate a CDA model for this alloy and to develop modifications or corrections to the CDA model to handle additional failure mechanisms. The Socie parameter was found to provide the best correlation for INCO 718 multiaxial loading.

Extensive microstructural evaluations were completed for many specimens in this program using optical, Scanning Electron Microscopy (SEM), and Transmission Electron Microscopy (TEM) techniques. These techniques were used to categorize failure modes and to correlate the various types of dislocation configurations with fatigue capability. Crack initiation lives were determined using surface replication techniques; tensile load drop lives were recorded automatically by the test rig software. Life prediction models were then developed based on this information.

SECTION 2.0
INTRODUCTION

2.1 CONTRACT OBJECTIVES

The overall operating cost of the modern gas turbine engine is greatly influenced by the durability of combustor and turbine structural components operating at high temperatures. Inadequate durability results in reduced engine efficiency, increased maintenance costs due to premature repair and replacement, and expensive corrective redesigns. To increase the durability of these components, more accurate structural analysis and life prediction methods must be developed for components operating at higher temperatures. However, improvements in the state-of-the art technology for elevated temperature durability prediction have been hampered by: 1) the severe operating conditions of the engine; 2) the inability of current analytical and life prediction tools which have been successfully used in the design of lower temperature components to predict complex material behavior and interaction of damage mechanisms of components at elevated temperatures; and 3) the high cost of engine development testing which prohibits the accumulation of adequate failure data and local operating conditions required for the systematic development and calibration of durability prediction models.

This contract began as part of the NASA Hot Section Technology (HOST) program which was aimed at developing improved life prediction technology for structures operating at elevated temperatures. It investigated fundamental approaches to high temperature crack initiation life prediction, identified modeling strategies and developed specific models for component relevant loading conditions. The program was a 6-year, 2-part effort (2-year base program plus a 4 year optional program) that considered two isotropic hot section materials and protective coating systems. Under the base program, various life prediction approaches for high temperature applications were investigated, and basic models for simple cycle, isothermal loading conditions were selected and developed. Models that addressed thermomechanical cycling, multiaxial loading conditions, non steady cumulative loading, environmental effects and cyclic mean stress were developed under the optional program. Finally, to demonstrate the applicability of these models to other materials, additional tests were performed on an alternative material.

This report details the activities completed under the optional portion of NASA Contract NAS3-23288, "Creep Fatigue Life Prediction for Engine Hot Section Materials (Isotropic)", during the period from May 1987 through February 1989. The specific areas covered include the following technical tasks:

Task V - Thermal-Mechanical Cycling Model
Task VI - Multiaxial Stress State Model
Task IX - Environmental Attack Model
Task X - Protective Coating Models
Task XI - Cyclic Mean Stress Model
Task XII - Final Verification and Evaluation of Alternative Material/Protection Coating System/Component Combination
Task XIV - Cyclic Damage Accumulation (CDA) Computer Program

2.2 OVERVIEW OF PREVIOUS CONTRACT ACTIVITY

This section provides a brief review of the progress made during the first five years of this contract effort. It describes the early work performed during this period of the HOST contract and serves as background for the work covered by this report. The data generated during the base program will not be repeated in this report but may be found in the Second Annual Report (Moreno et al, 1984) and in the previous two Interim Reports (Nelson et al, 1986 and 1992).

The following materials were recommended and approved for use in both the base and option portions of the program:

Base Material	=	Cast B1900 + Hf	(PWA 1455)
Alternate Material	=	Wrought INCO 718	(AMS 5663)
Coatings	=	Diffusion Aluminide	(PWA 273)
		MCrAlY Overlay	(PWA 286)

Details of the selection and characterization of these materials and of the preparation and testing of the specimens will be presented in Section 3.0.

Twenty-one tensile tests were completed on PWA 1455, covering the temperature range from room temperature to 1093°C (2000°F). Figure 1 shows typical stress-strain response curves for the standard strain rate of 0.005 min^{-1}. Also, 19 specimens were creep tested at temperatures from 649°C (1200°F) to 982°C (1800°F). Both test data and post-test metallurgical examination of these monotonic specimen tests were used to understand the deformation mechanisms active at various temperatures for this material.

Nearly 100 isothermal fatigue tests were conducted on PWA 1455 during the base program covering the temperature range from 538°C (1000°F) to 982°C (1800°F), with the bulk of the tests being run at 871°C (1600°F). Additional variables studied included strain range, ratio, and rate, as well as hold time effects. A crack initiation life was inferred for each specimen by means of surface replicas taken during companion tests conducted at the same conditions. The definition of initiation was chosen to be the generation of a 0.76 mm (0.030 in.) surface length crack. With an aspect ratio of 2:1, this surface length corresponds to a crack depth of several grain diameters in the cast PWA 1455, and is considered to represent the point at which the crack may be analyzed using fracture mechanics concepts for "large cracks".

Many specimens were examined metallographically using optical, SEM, and TEM techniques to determine failure sites, crack paths, and dislocation networks. No statistically significant difference could be seen between failures which originated at internal pores and those which originated at carbides. The initiation and propagation modes (transgranular or intergranular) were shown to be a function of both temperature and strain rate. Figure 2 shows that there is a greater tendency toward intergranular behavior as temperature increases and strain rate decreases. The appearance of the dislocation networks created by various loading conditions suggested that the maximum stress achieved during the initial cycling was very important to the subsequent fatigue capability of the material.

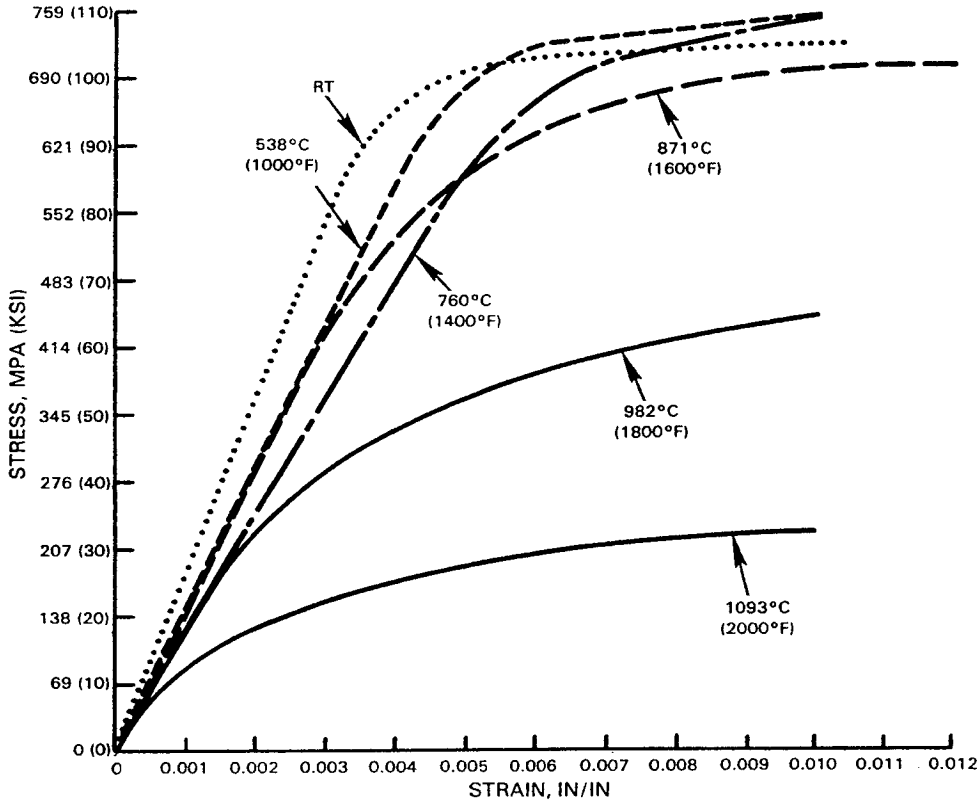

Figure 1.- Monotonic Tensile Response, $\dot{\epsilon} = .005\ \text{min}^{-1}$.

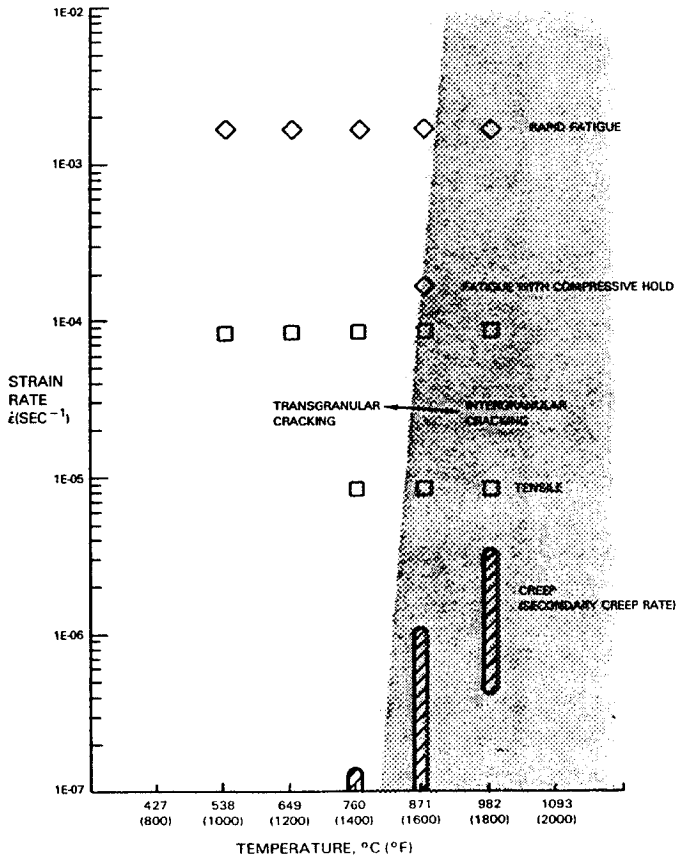

Figure 2.- Cracking Map for B1900+Hf.

The life prediction approach developed during the base program is called Cyclic Damage Accumulation (CDA). One of the fundamental assumptions of the CDA model is that the damage capacity is related to the grain dislocation structure. Determination of the grain capability must therefore include consideration of the entire loading history of the specimen, especially the maximum stress excursions. In particular, it was assumed that the grain cyclic capability can be calculated from the maximum stress attained in the initial loading cycle and the amount of primary creep strain that could have been developed if that stress level had been held constant. It was further assumed that, for temperatures below 649°C (1200°F) where little or no creep occurs, the grain cyclic capability would be represented by the residual inelastic strain (percent elongation) measured following a tensile test. The result of these two assumptions is that grain cyclic capability varies as a function of temperature and stress as shown in Figure 3.

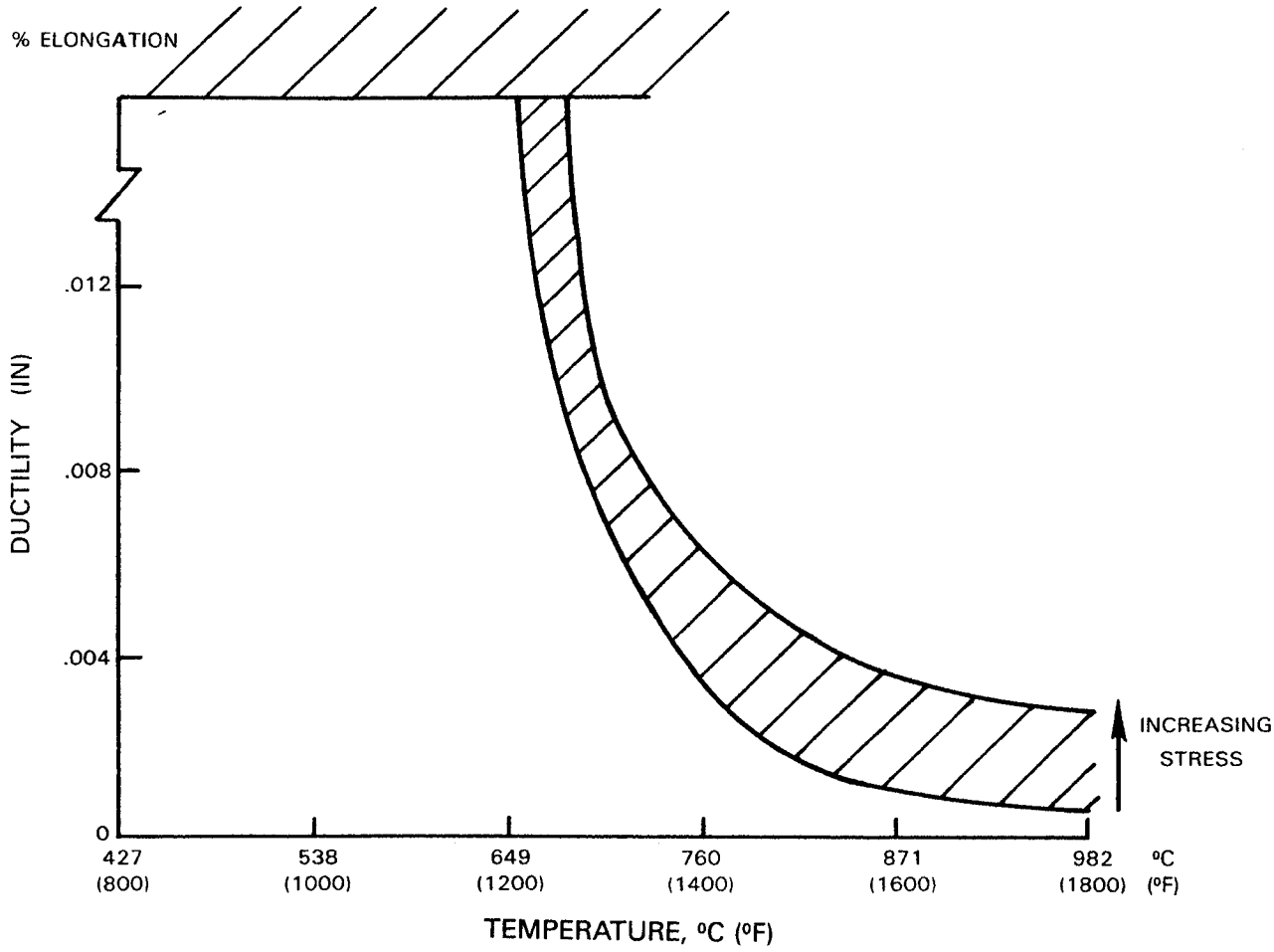

Figure 3.- Assumed Grain Cycle Fatigue Capability

Another feature incorporated in the CDA life model was the use of damage ratios rather than absolute damage levels. By plotting the available data for cycles having either time-independent or time-dependent damage, it was possible to arrive at the following mathematical form of the CDA model:

$$\bar{\varepsilon}_p - \int_0^{N_i} \left(\frac{dD}{dN}\right)_{REF} \left\{ \left(\frac{\sigma_T}{\sigma_{T,REF}}\right)\left(\frac{\Delta\sigma}{\Delta\sigma_{REF}}\right) + \left[\left(\frac{\Delta\sigma_{REF}}{\Delta\sigma}\right)\left(\frac{\sigma_T}{\sigma_{T,REF}}\right)\right]^{B'} \left[\left(\frac{t}{t_{REF}}\right)^{C'} - 1\right] \right\} dN = 0$$

Where:

$\bar{\varepsilon}_p$	=	primary creep strain ductility
$\left(\frac{dD}{dN}\right)_{REF}$	=	reference cyclic damage rate
σ_T	=	maximum tensile stress
$\Delta\sigma$	=	stress range
t	=	time = 0.5 * (total cycle period + hold times)
N_i	=	initiation life
REF	=	reference values
B'	=	stress exponent in primary creep power law
C'	=	time exponent in primary creep power law with shifted time origin

This equation was then calibrated using the baseline fatigue data and used to generate life predictions for various verification cycles. Sensitivity studies were also conducted to determine the effects of crack size to grain size ratio, definition of initiation, choice of reference condition, and data requirements for life predictions. Preliminary work was also done on possible means of using this or a similar equation to predict intergranular cracking as well as transgranular.

During the initial part of the optional program, work began on the expansion of the basic CDA life prediction method to account for the effects of thermomechanical fatigue, multiaxiality, cumulative damage, environment, coatings, and mean stresses. The B1900+Hf specimen database was significantly expanded during this time to provide clear data regarding material behavior under such complex conditions. Under Task IV, eighteen additional isothermal fatigue verification tests were completed and are covered by the previous report. These tests explored the effects of hold times with R=0 or high strain range, R-ratios at low strain rate and high temperature, load control, and surface finish. The 26 base material multiaxial tests were completed during the previous reporting periods. Similarly, the investigation of environmental effects began during the last period and is covered in detail in this report. Two literature reviews, covering state-of-the-art life prediction methods for both multiaxial stresses and environmental effects, were also included in an earlier report (Nelson et al, 1986).

Prediction of initiation life under conditions of thermomechanical fatigue (TMF) is one of the most important practical applications of any advanced creep-fatigue life model since conditions of simultaneously varying strain and temperature are typical of what is experienced by many components of modern turbomachinery and powerplants. To understand the behavior of B1900+Hf under TMF conditions, 30 uncoated TMF specimen tests were completed. These simulated many types of strain-temperature cycle paths, including in-phase, out-of-phase, "dogleg" (non-isothermal holds), and elliptical cycles. The results shown in

Figure 4 are typical of the effects produced by such variables for which successful life models must be able to account. The modifications to the CDA model which were initiated at this time will enable it to accept completely arbitrary histories of stress-strain-temperature and thereby make accurate TMF life predictions.

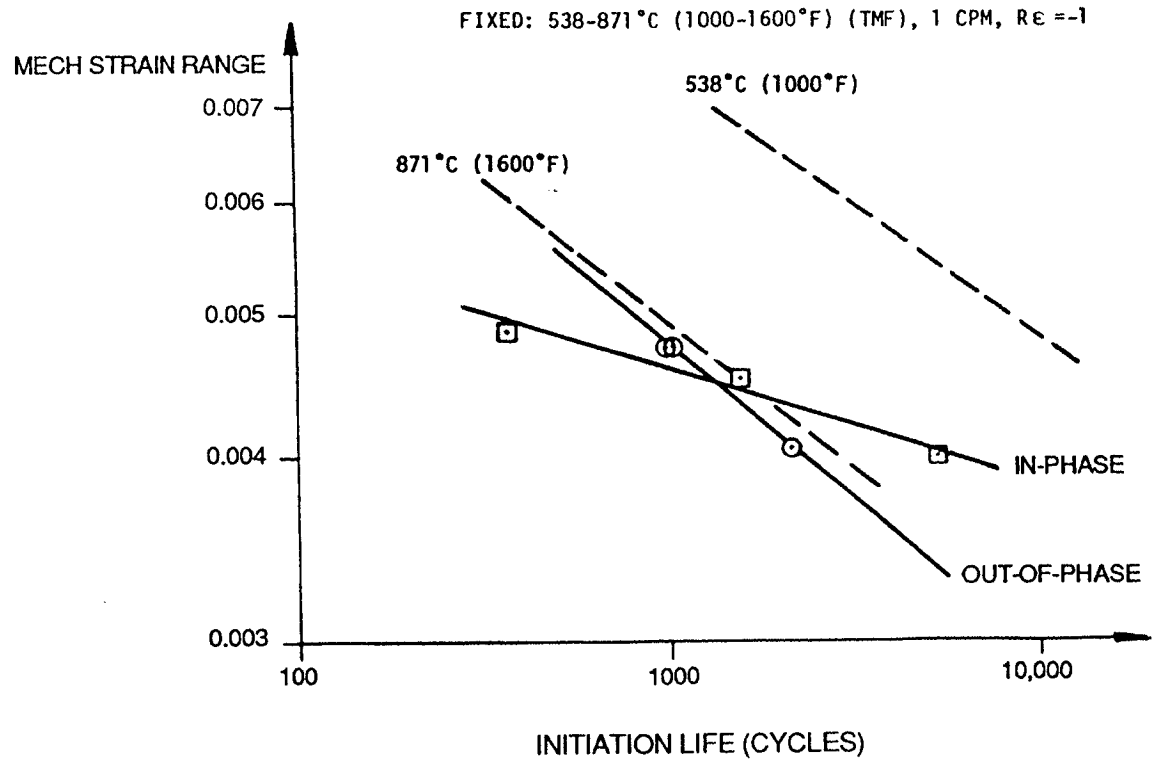

Figure 4.- TMF Results for In-Phase and Out-of-Phase Cycles.

Under Task VII, 50 cumulative damage tests were completed, including block tests (strain ratio, temperature, and hold time), sequenced tests (strain range and rate), and interrupted tests (prior creep and interspersed exposure time). An interaction curve for the block strain ratio results are shown in Figure 5, where the level of prior loading and its duration are seen to have pronounced effects on the life of subsequent block loading. This effect is easily captured using the CDA concept of primary creep ductility, since this variable depends on the prior loading history. The cumulative damage tests also showed the need to incorporate a non-linear damage accumulation function to predict sequence effects correctly. This required the introduction of two modifications of the original form of the CDA model: the concept of ductility fraction, and the non-linear rate modifier function, G(N/Ni).

The ductility fraction concept permits the primary creep strain ductility to vary during the course of the test by bringing it under the integral. The ductility fraction, f_ϵ, is defined as the fraction of the available ductility which has been consumed:

$$Ductility\ Fraction, f_\epsilon = \frac{Ductility\ Exhausted}{Available\ Ductility} \quad (2)$$

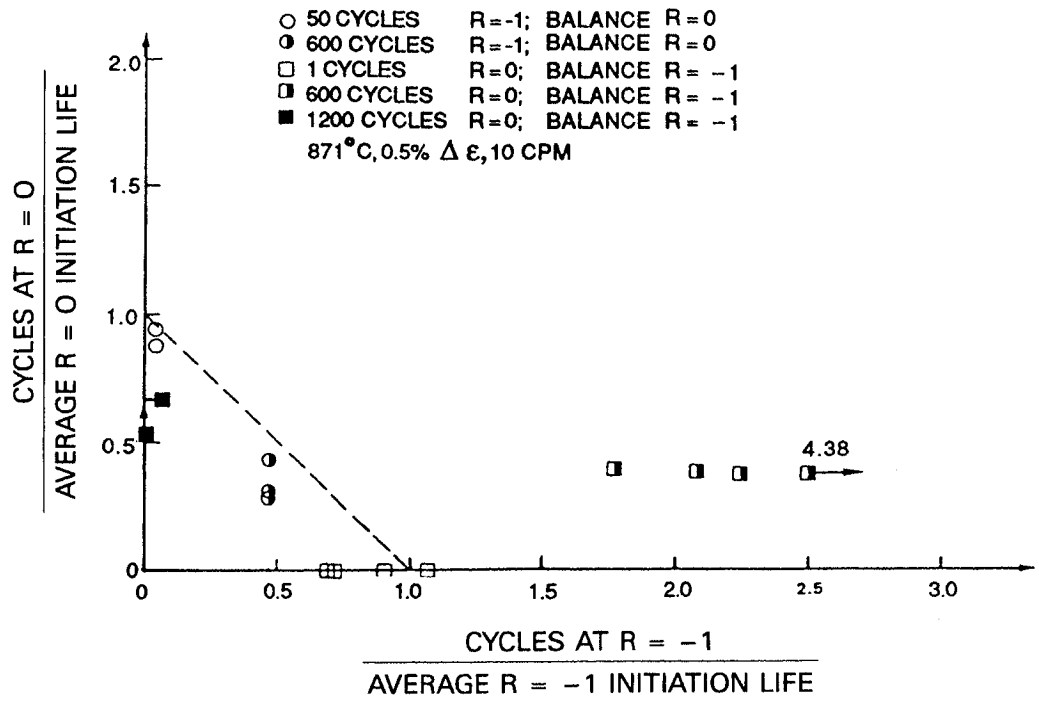

Figure 5.- Interaction Diagram for Strain Ratio Block Tests.

The equation used to calculate this quantity may be written as follows, using CDA nomenclature:

$$f_\varepsilon = \int_0^{N_i} \left(\frac{1}{\bar{\varepsilon}_p}\right)\left(\frac{dD}{dN}\right)_{REF} F(\sigma_T, \Delta\sigma, t)\,dN \tag{3}$$

where:

$$F(\sigma_T, \Delta\sigma, t) = \left(\frac{\sigma_T}{\sigma_{T,REF}}\right)\left(\frac{\Delta\sigma}{\Delta\sigma_{REF}}\right) + \left[\left(\frac{\Delta\sigma_{REF}}{\Delta\sigma}\right)\left(\frac{\sigma_T}{\sigma_{T,REF}}\right)\right]^{B'}\left[\left(\frac{t}{t_{REF}}\right)^{C'} - 1\right] \tag{4}$$

It can be seen that when f_ϵ reaches 1, N will equal the predicted initiation life, Ni. Note also that the current initial ductility is now inside the integral, which permits the algorithm to switch from one loading condition to another which has a different initial ductility.

We may also rewrite equation 3 to perform the integration over f_ϵ instead of N, and at the same time introduce a non-linear function G(N/Ni) which has the property that its integral over the interval from 0 to 1 is always 1, no matter what values are chosen for its constants:

$$N_i = \int_0^1 \left[\frac{\bar{\varepsilon}_p}{\left(\frac{dD}{dN}\right)_{REF} F(\sigma_T, \Delta\sigma, t)}\right] G\left(\frac{N}{N_i}\right) df_\varepsilon \tag{5}$$

The function G(N/Ni) chosen for the initial trials of this method is a combination of a power law and a linear function:

$$G\left(\frac{N}{N_i}\right) = (1 - LF)(M+1)\left[1 - \left(\frac{N}{N_i}\right)\right]^M + LF \tag{6}$$

The effect of the inclusion of the non-linear function G(N/Ni) on the CDA life prediction for a strain ratio block test is shown by Figure 6. This plot shows how the ductility fraction increases as a function of cycles, both for linear and non-linear damage accumulation. In this case the non-linear prediction is lower than the linear prediction, because the basic damage rate (slope of the linear accumulation line) during the first block of the test is lower than the rate during the second block. This causes the ductility to be consumed earlier with the non-linear function than without it, and the net result is a lower prediction. The opposite effect is seen in Figure 7, where reversal of the order of the blocks causes the non-linear life prediction to be higher than the linear one. Note that this is the same effect which was observed during the specimen testing.

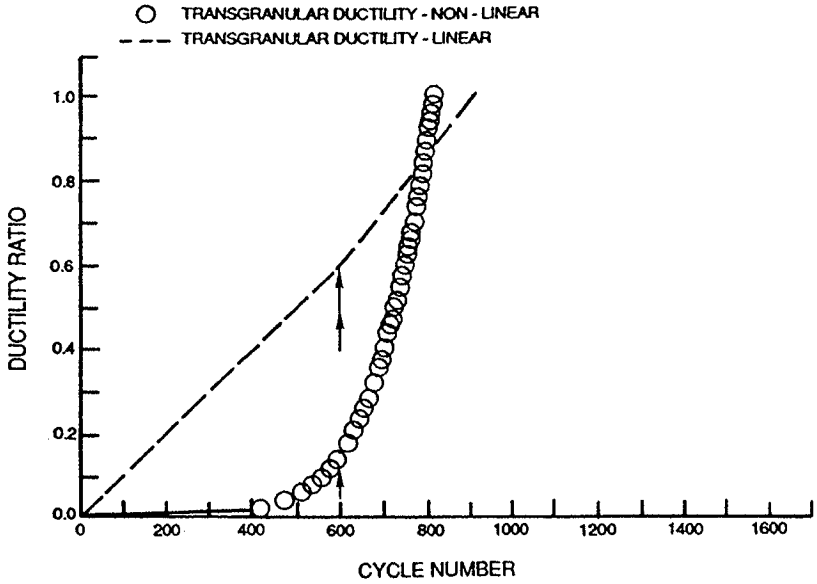

Figure 6.- Example of Lower Life Prediction with Non-Linear Accumulation.

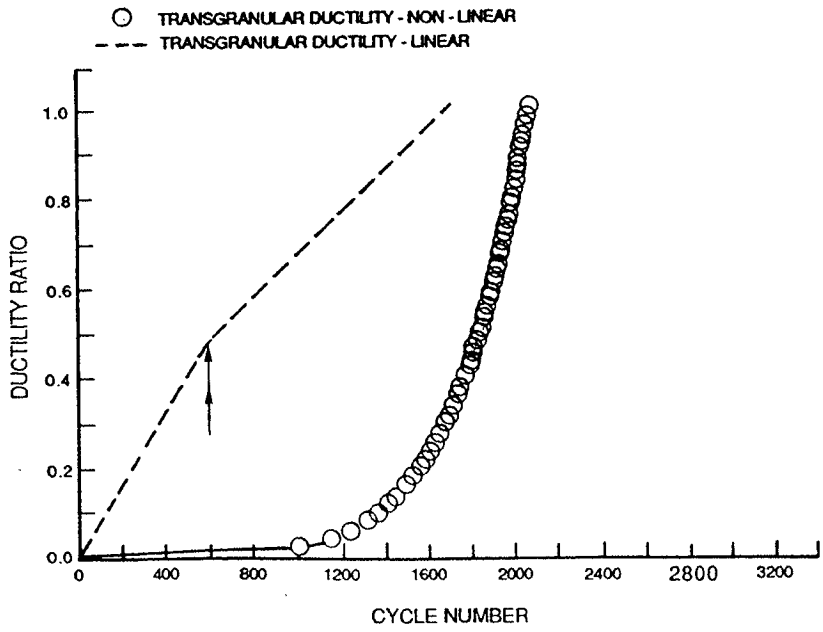

Figure 7.- Example of Higher Life Prediction with Non-Linear Accumulation.

3.0 EXPERIMENTAL PROGRAM

TASK V - THERMOMECHANICAL MODEL DEVELOPMENT

Fifty-five thermomechanical fatigue (TMF) tests were completed the course of the contract (12 specimens with PWA 286 overlay coating, 11 specimens with PWA 273 diffusion coating, and 32 uncoated specimens) for the development of a thermal mechanical cycling model to predict the influence of simultaneous cycling of both temperature and mechanical strain on the cyclic crack intiation lifetimes of materials, coatings and components. Specimen testing of both coated and uncoated samples were reported by Nelson, et al (1986, 1992). Various modifications to the CDA life prediction model were evaluated for TMF life prediction.

Modifications to CDA Model

The effectiveness of solving for the coefficients of the equations necessary to predict the strain constituents of an arbitrary TMF history was further enhanced. A least-squared fitting routine was used to further constrain the problem of determining a unique set of coefficients. The algorithm was used in conjunction with the optimizer, ADS, to determine a reasonable starting point from which the optimizer could quickly solve for the coefficients. In addition, a means of calculating improved, consistent design gradients was implemented and worked extremely well with ADS (Vanderplaats et al, 1983).

A program was developed which accesses the data banks of the Data Analysis System for HOST (i.e. DASH). This enabled retrieval of specimen data in a straightforward, simple manner such as that for several test conditions, along with the strain prediction code, to determine the coefficients of the strain constituent equations. The inelastic strain prediction equations were updated with an algorithm that calculated an inelastic strain component using a coupled differential equation. The update improved the performance of the coefficient prediction program by providing additional stability or less sensitivity to the strain prediction algorithm.

A system was developed which incorporated models created to predict component lives. Although the program was dedicated to assist in the search for proper coefficients of the strain prediction code, it evolved into a useful design tool.

The life prediction model was also enhanced through inclusion of the Walker viscoplastic strain equations in the strain prediction code and by providing material temperature dependence support for TMF cycles, where previously, isothermal cycles were analyzed to determine the strain constituent equation coefficients. Furthermore, the optimizer system was revised to a constrained rather than unconstrained minimization by confining the strain equations to correctly predict available monotonic creep data.

Predicted coefficients for isothermal specimen tests for temperatures ranging from 538°C (1000°F) to 1093°C (2000°F) were fitted for temperature dependence. The results showed the optimizer had difficulty with uncovering a unique solution because some coefficients did not show a smooth transition with temperature. Nevertheless, appropriate coefficient values were determined by curve fitting the temperature data.

Various methods of calculating the variation of the predicted coefficients with temperature were evaluated. Data obtained from Southwest Research Institute on this alloy for step strain rate and step temperature testing provided the guidance necessary to select a proper temperature interpolation scheme for TMF life prediction.

Preliminary correlations based on the CDA method were presented at a NASA-sponsored TMF Workshop. Figures 8 and 9 present these results for all the uncoated and coated TMF specimens, respectively. These correlations demonstrated the usefulness of the basic damage equations and further refined the methods for the final life prediction model.

Several alternative forms of the equation for time-independent damage were evaluated to improve the predictive capability of the CDA model. The initial form of this equation was written as:

$$N_{i_{time\text{-}indep}} = A\ \Delta\varepsilon^{b}\left(\frac{\Delta\sigma}{\Delta\sigma_{Ref}}\right)\left(\frac{\sigma_T}{\sigma_{T_{Ref}}}\right) \tag{7}$$

By combining the two reference stresses with the reference damage rate constants, the equation was rewritten as:

$$N_{i_{time\text{-}indep}} = A'\ \Delta\varepsilon^{b}\Delta\sigma\ \sigma_T \tag{8}$$

where:

$$A' = \frac{A}{\Delta\sigma_{Ref}\cdot\sigma_{T\ Ref}}$$

The correlative capability of equation (8) was compared to several other possible formulations which are functions of the same cyclic variables. Each equation was evaluated against rapid cycle fatigue data from the specimens tested under isothermal conditions at 1000°F and 1600°F. These equations and the results of the correlations are given in Table I. As expected, the two formulations with the best correlation coefficients were those with all three parameters and separate constants for each parameter. Further, the exponential form of the maximum stress, as found in equation (12) of Table I, had a slight edge over the basic power law in equation (11) of Table I. It is worthy to note that, under the limiting conditions of pure elastic or pure plastic material behavior, equation (12) reduced to the classical Manson-Coffin law based on total strain. Further development of the TMF prediction model used equation (12) coupled with a modified time-dependent term.

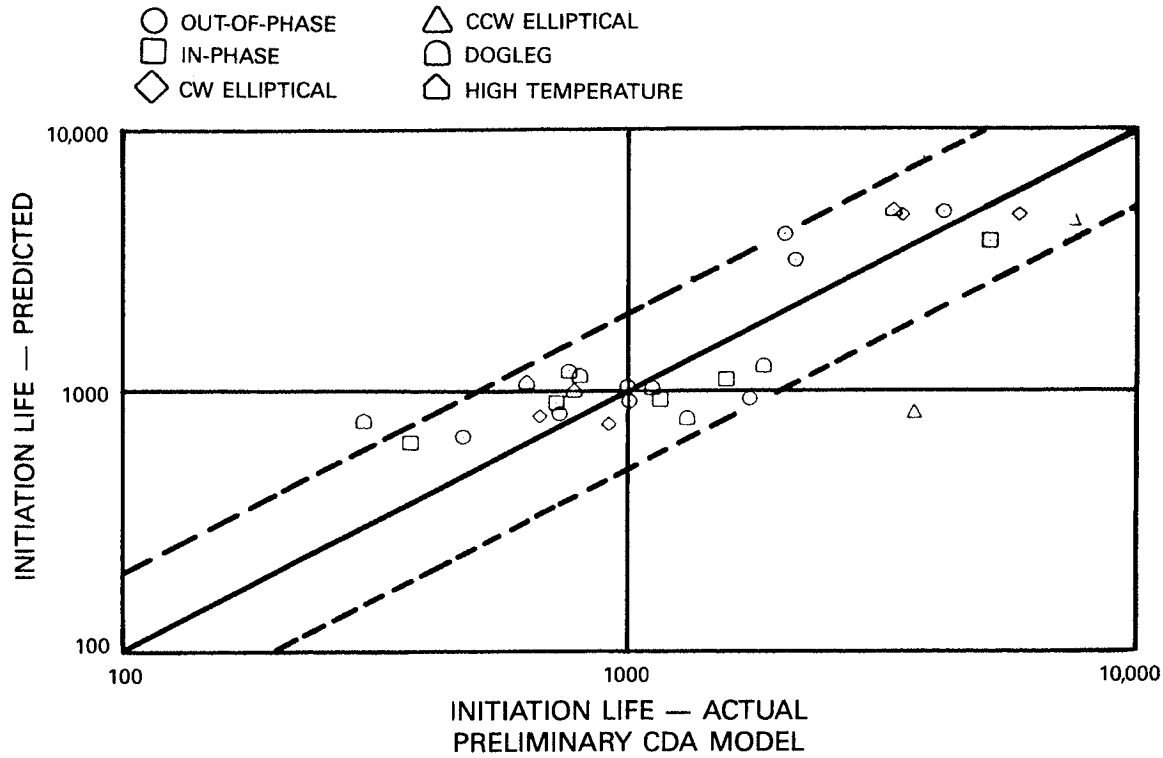

Figure 8.- TMF Life Model Comparisons for Uncoated PWA 1455.

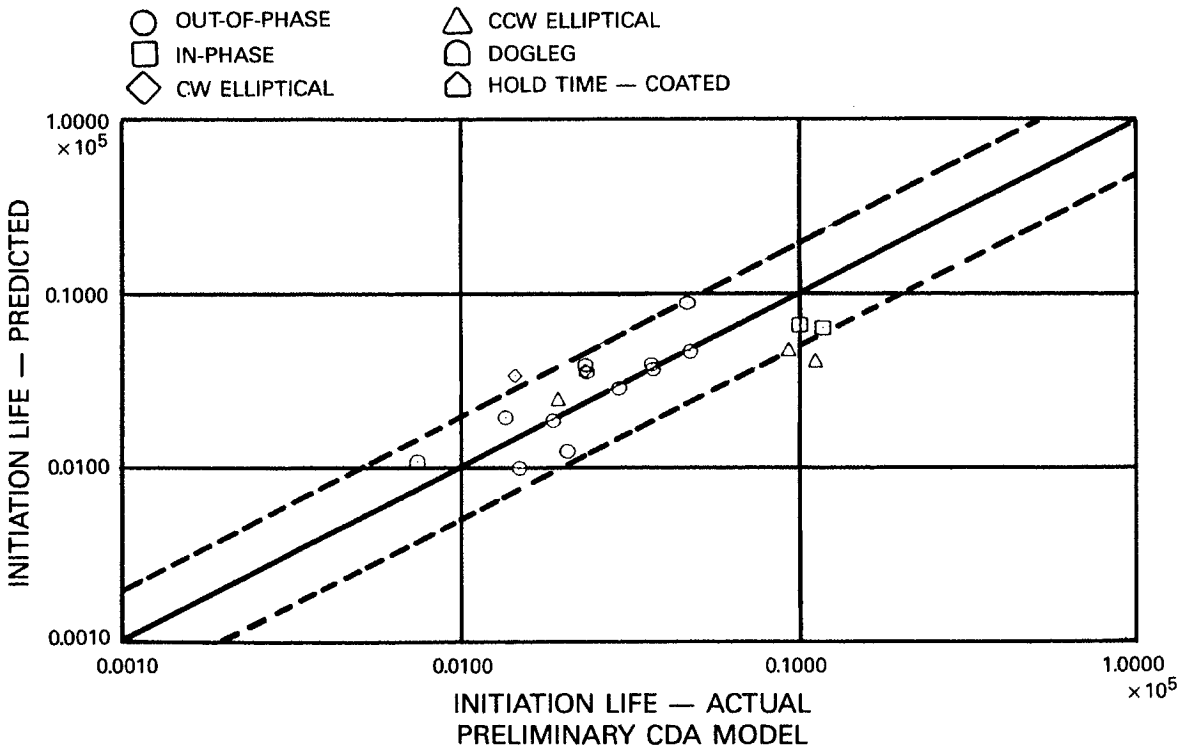

Figure 9.- TMF Life Model Comparisons for Uncoated PWA 1455.

TABLE I.- COMPARISON OF TIME-INDEPENDENT DAMAGE EQUATIONS

No.	Equation	Correlation Coefficient (R^2) 538°C(1000°F) Data	871°C(1600°F) Data
1	$N_i = A\Delta\varepsilon^{n_1}\,\Delta\sigma\,\sigma_T$ (Base CDA Version)	.9451	.7614
2	$N_i = A\Delta\varepsilon^{n_1}$	.9499	.7994
3	$N_i = A\,\Delta\sigma^{n_1}$	.9106	.7569
4	$N_i = A\,\sigma_T^{n_1}$	.6601	.2605
5	$N_i = A\,\Delta\varepsilon^{n_1}\,\Delta\sigma^{n_2}$	.9747	.8988
6	$N_i = A\Delta\varepsilon^{n_1}\,\sigma_T^{n_2}$	.9854	.9388
7	$N_i = A\,\Delta\sigma^{n_1}\,\sigma_T^{n_2}$	.9819	.9470
8	$N_i = A\Delta\varepsilon^{n_1}\,10^{n_2\sigma_m}$	.9826	.9281
9	$N_i = A\Delta\varepsilon^{n_1}\,10^{n_2\sigma_T}$	.9858	.9396
10	$N_i = A\Delta\sigma^{n_1}\,10^{n_2\sigma_T}$	.9839	.9507
11	$N_i = A\,\Delta\varepsilon^{n_1}\,\Delta\sigma^{n_2}\,\sigma_T^{n_3}$	.9869	.9537
12	$N_i = A\,\Delta\varepsilon^{n_1}\,\Delta\sigma^{n_2}\,10^{n_3\sigma_T}$	.9877	.9563

Various forms of time-dependent damage terms capable of predicting trends seen during specimen testing were evaluated, including methods which have the ability to discern correctly the effects of cycle path on initiation life. Modifications to the transgranular portion of the CDA model were developed which allowed the life predictions to be independent of temperature. This enabled evaluation of variable temperature component loadings and provided the framework to develop the final TMF life model. The most promising technique was an extension of the original CDA technique of computing stress ratios relative to reference conditions. This technique enabled one fatigue law to be used for all temperatures and hence permitted life predictions to be made directly for variable temperature loadings.

A new equation for the non-linear damage accumulation rate based on the basic damage rate is as follows:

$$G\left(\frac{n}{Ni}\right) = (1 - f_L)(\beta + 1)\left(\frac{n}{Ni}\right)^{\beta} + f_L \qquad (9)$$

where: β = damage rate exponent

$$= \left(\frac{B}{dD/dN_{base}}\right)^{\alpha}$$

and: α = rate ratio exponent = 0.76
B = reference damage rate value = 0.0042
f_L = linear fraction = 0.10

As with the previous G(n/Ni) function, the improved non-linear function integrated to a value of 1.0 under continuous cycling at constant conditions. However, this new equation did not require that the life prediction based on linear accumulation be known in order to perform the integration. Instead, the basic damage rate was used dynamically to provide an instantaneous value for the linear damage rate life. This caused the damage rate to change as damage accumulated as shown in Figure 10. The current values for the constants in the non-linear equation are shown above and are based on experience with the B1900+Hf data.

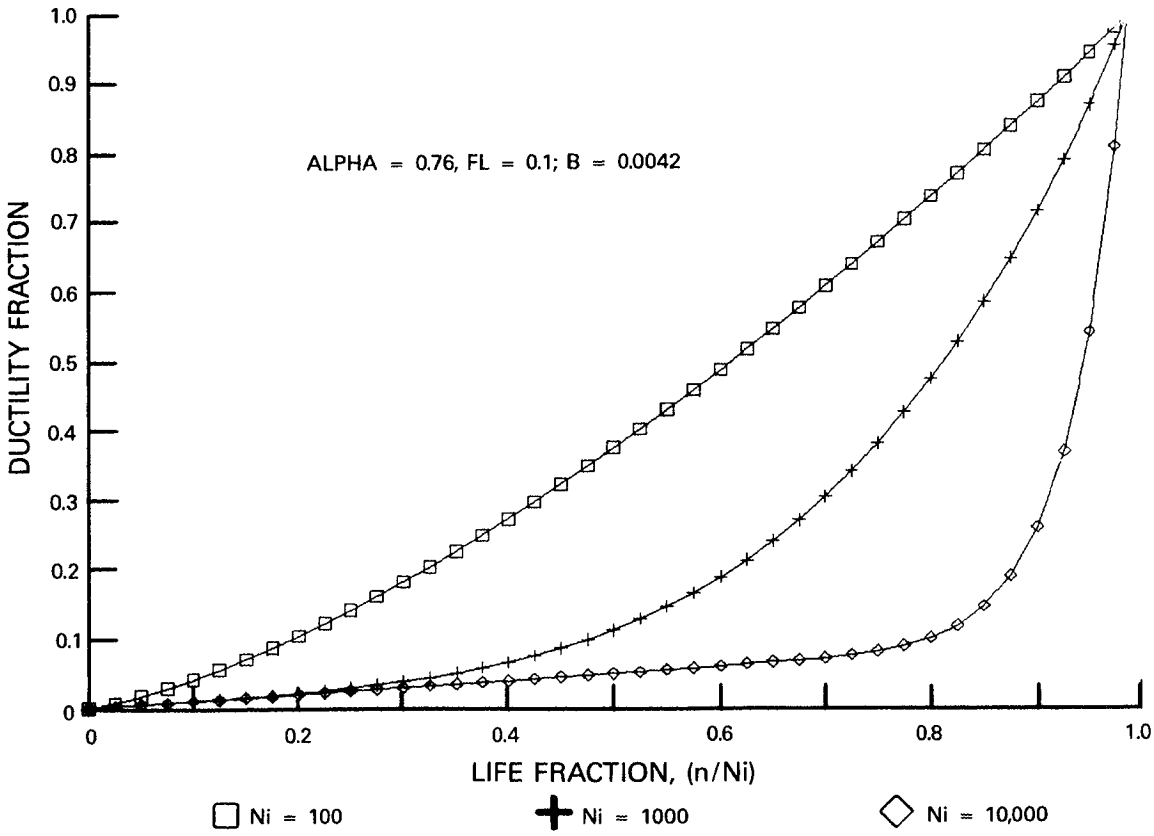

Figure 10.- CDA Non-Linear Damage Equation.

Derivation of new equations to handle evolution of the primary creep strain ductility under conditions of varying temperature was also investigated. The method chosen was similar to that for the stress range ratio; namely, computation of a maximum tensile stress ratio instead of using absolute values. The algorithm considered all the maximum tensile stress ratios from each cycle completed up to and including the present cycle. This was then used to characterize the current primary creep strain ductility, also as a ratio instead of an absolute value. The net result was a history parameter which captured the effect of prior loading on the dislocation structure present in the material. This permitted correct prediction of complex loading situations such as R-ratio block tests, sequenced tests, and TMF tests.

TASK VI - MULTIAXIAL STRESS STATE MODEL

This task consisted of tasks conducted on thin-walled (0.050") tubular specimens to obtain crack initiation data for the development and verification of a multiaxial stress state creep fatigue life prediction model. Twenty-six strain controlled PWA 1455 multiaxial fatigue tests were completed and reported by Nelson, etal (1992).

A detailed review was made of the test data for the PWA 1455 multiaxial specimens, including both replica data and computer files. It was found that 50% load drop lives were based on load range instead of tensile load, as used for all other experiments, resulting in a longer test run than was expected. Fortunately, load histories were recorded that were used to determine the actual 50% tensile load drop lives which were then used to estimate the initiation lives for those specimens which did not have replicas (half of the tests). The final revised initiation and separation lives are shown in Table II for all PWA 1455 multiaxial specimens. Comparison plots of this data based on principal strain range for 538°C(1000°F) and 871°C(1600°F) data are shown in Figures 11 and 12, respectively. This information was used to revise the multiaxial life prediction methods in the CDA model.

The major conclusions of this task are as follows:

1. Strain range and cycle type were both shown to be significant factors in determining multiaxial life. The phase angle between axial strain and torsional strain was also important, although frequently there was little interaction between the two.

2. The best parameter for multiaxial life prediction for the PWA 1455 data is still maximum principal strain range which agrees with experimentally observed crack directions.

TABLE II
PWA 1455 MULTIAXIAL FATIGUE TESTS

Test No.	Spec. No.	Temp. (°C)	Freq. (CPM)	$\Delta\epsilon$ (%)	$\Delta\gamma$ (%)	Phase Angle (Deg)	Initiation Life (Cycles)	Separation Life (Cycles)
1	204	871	10.0	±0.185	±0.260	0	350	714[1]
2	203	↓	↓	0.0	±0.404	–	8100	10,820
3	217			±0.250	0.0	–	1107	2040
4	216			±0.250	±0.375	90	1313	1973
5	218			±0.147	±0.220	0	6615	9450[1]
6	219			0.0	±0.361	–	40,000	62,000[2]
7	221	538		0.0	±0.675	–	1739	2213
8	222	871		±0.200	0.0	–	9629	15,864
9	220	538		±0.338	0.0	–	1790	2815
10	223	↓		±0.255	±0.382	0	1708	2880
11	202			±0.338	±0.506	90	240	431[1]
12	201			±0.260	0.0	–	4100	5941
13	215		1.0	±0.338	±0.506	90	486	873
14	214	↓	10.0	±0.250	±0.375	90	5210	8625
15	205	871	↓	±0.147	±0.220	90	11,434	15,389[1]
16	209	538		0.0	±0.500	–	20,188	23,590
17	226	871		±0.178	±0.267	0	5811	8208
18	207	↓	1.0	±0.250	±0.375	90	327	834
19	227		10.0	±0.200	±0.300	90	13,794	18,565
20	213		1.0	±0.220	±0.330	90	1911	4368
21	211	538	1.0	±0.250	±0.375	90	1454	2408
22	225	↓	10.0	±0.189	±0.283	0	6164	9580
23	206		10.0	±0.338	±0.506	90	1417	2544
24	212	871	10.0	0.0	±0.500	–	2377	3745
25	210	↓	1.0	0.0	±0.400	–	5400	7500[2]
26	228		10.0	±0.302	±0.452	0	56,000[2]	80,000[2]

Notes: 1. Data not included in correlations (dross, etc.)
2. Test discontinued; life estimated

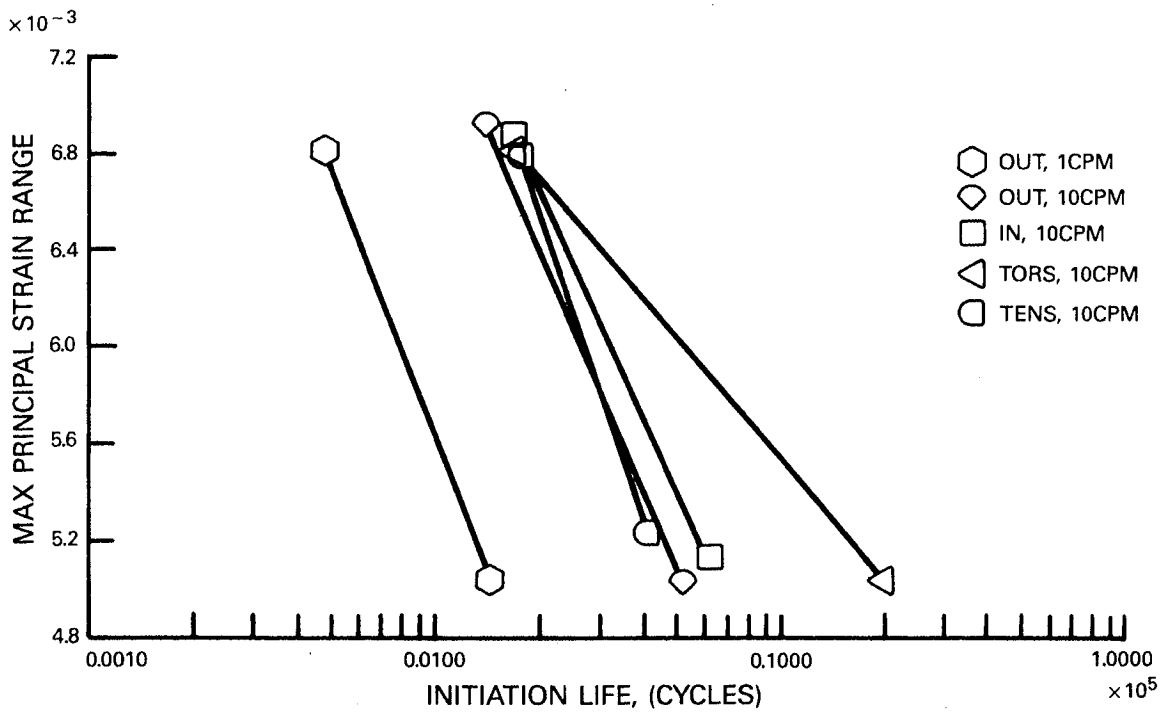

Figure 11.- PWA 1455 Multiaxial Test Data - 538°C(1000°F).

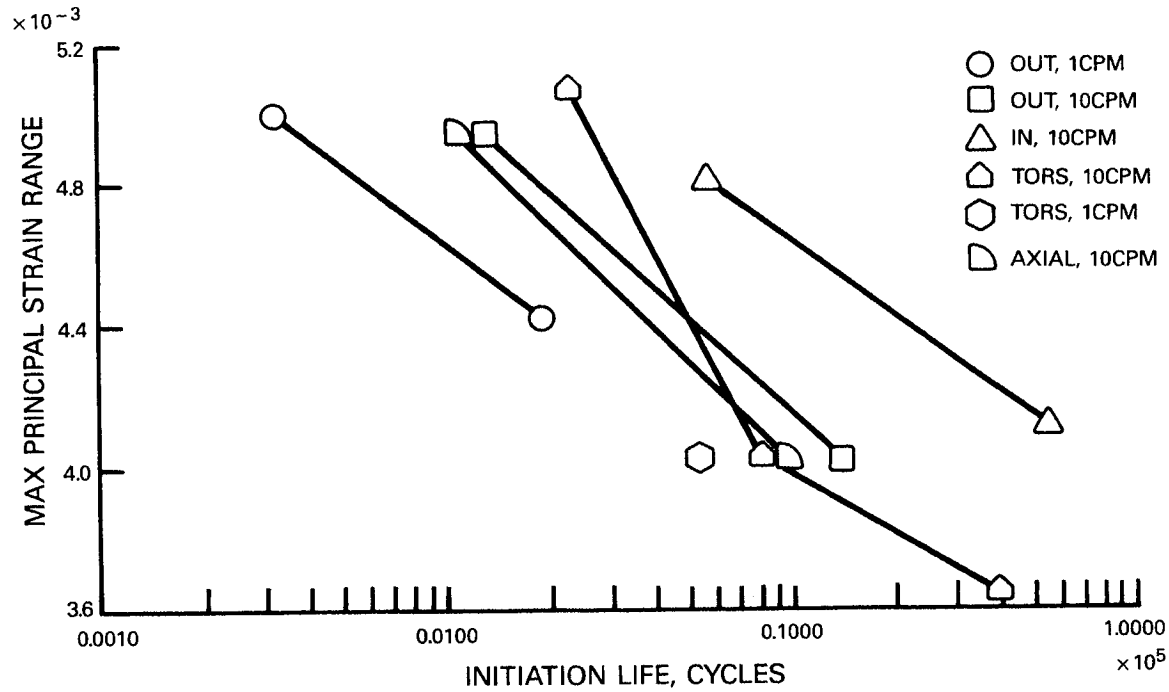

Figure 12.- PWA 1455 Multiaxial Test Data - 871°C(1600°F).

TASK IX - ENVIRONMENTAL ATTACK MODEL

This task encompassed testing of B1900+Hf smooth baseline fatigue test specimen in three different environments: laboratory air, high pressure oxygen and high purity argon, in support of the development of an environmental attack model. Previous work on this test was reported by Nelson et al (1992) Data for each of the 29 specimens tested under this task are given in Appendix A. The complete matrix of the 16 specimens tested using fixed environments is shown in Table III. The matrix of the 13 specimens tested under block environmental conditions is shown in Table IV.

TABLE III.- FIXED ATMOSPHERE ENVIRONMENTAL TEST MATRIX

Conditions				Argon[1]			Lab Air			75 Psia Oxygen		
Temp (°C)	$\Delta\epsilon$ (%)	R_ϵ	$\dot{\epsilon}$ (Sec^{-1})	Spec ID	Ni (Cycles)	Nf (Cycles)	Spec ID	Ni (Cycles)	Nf (Cycles)	Spec. ID	Ni (Cycles)	Nf (Cycles)
871	0.5	-1	$1.67x10^{-4}$	137C	521	1544	124D	1350	5632	111C	674	2245
			$1.67x10^{-4}$				123A	560[2]	1443[2]			
			$1.67x10^{-3}$							136D	900	5940
			+ 1min tensile hold									
		0	$1.67x10^{-4}$							139B	150	1186
982	0.4	-1	$1.67x10^{-4}$	137D	256	522	123B	1320	2493	111D	559	1216
			$1.67x10^{-4}$	143A	487	993	137A	989	2105	112A	460	1000
			$1.67x10^{-3}$				124B	1560	4464	112C	924	2641[3]
		0	$1.67x10^{-4}$							143D	280	808
		-1	$1.67x10^{-3}$ +1min tensile hold							143C	200	1259

Notes: 1. Argon was purified (see text(, but traces of water may have remained inside the test chamber.
2. Shop air; foreign substances apparently reduced these lives.
3. Failed prematurely at 958 cycles; life estimated from replica data.

TABLE IV.- TEST MATRIX FOR PWA 1455 ENVIRONMENTAL BLOCK TESTS

Condtions				Block 1	Lab Air, Then Oxygen				Oxygen, Then Lab Air			
Temp (°C)	$\Delta\epsilon$ (%)	R_ϵ	$\dot{\epsilon}$ (sec^{-1})	Fraction (% Ni)	Spec ID	Block 1 (Cycles)	Ni (Cycles)	Nf (Cycles)	Spec ID	Block (Cycles)	Ni (Cycles)	Nf (Cycles)
871	0.4	-1	$1.67x10^{-3}$	50%	140B	1800	18833	32753	140A	1800	14017	27218
	0.5		$1.67x10^{-3}$	25%					136B	363[1]	2019	6026
			$1.67x10^{-4}$	10%					138B	80	837	2263
			$1.67x10^{-4}$	25%	142B	300	597	2093				
			$1.67x10^{-4}$	50%	142C	600	901	3278	142A	300	427	2033
982	0.4	-1	$1.67x10^{-3}$	10%					144C	100	735	1442
			$1.67x10^{-3}$	50%	144A	800	806	1521	144B	500	848	1542
			$1.67x10^{-4}$	10%					143B	50	716	1301
			$1.67x10^{-4}$	50%	139D	800	470	1119	138C	260	624	1301

Note: 1. Specimen 136B initially ran at 1 cpm for the first 63 cycles.

Baseline Laboratory Air Screening Tests

Microstructural observations were made on Specimen 124B which was tested in laboratory air at 982°C(1800°F), 12 cpm, $\Delta\epsilon = \pm 0.20\%$ and had initiation and separation lives of 1560 and 4464 cycles, respectively.

SEM micrographs of the fracture surface of specimen 124B are shown in Figure 13. This specimen had two initiation sites, with the major site having porosity at its origin as indicated by the arrows in Figures 13a and 13b. The fracture path appears to be transgrannular. Extensive oxidation of the fracture surface occurred as shown in Figure 13c. The oxide appears rounded and featureless and this is believed to be caused by rubbing of the opposing fracture surfaces that occur due to the R=-1 loading conditions. In areas where the rubbing action did not take place, the oxide had a crystalline appearance.

High Pressure Oxygen Testing

The fracture surface of specimen 111C, 871°C(1600°F), $\Delta\epsilon$ = 0.5%, R=-1, 1 cpm, 60 psi O_2, 2245 cycles), is shown in Figure 14. This specimen had three initiation sites which are indicated by the arrows in Figure 14a. The major initiation site is on the extreme left, a higher magnification view of this area is shown in Figure 14b. The fracture path appears to be transgrannular. Figure 14c shows the heavy oxide buildup in the area of the initiation site. The oxide appears to be rounded, a result of rubbing that occured due to R=-1 loading. Based on SEM observations alone, it was not possible to positively identify the nature of the fatigue origin. Some porosity was noted in the general area of the initiation site; however, it was not at the origin.

Results of X-ray energy spectroscopy (XES) in the initiation site showed areas that are higher in Al, Ta, and Cr than the surrounding regions, indicating the presence of a casting impurity and/or carbides. The extensive oxidation of the fracture surface prevented a positive identification.

The fracture surface of specimen 111D (982°C)(1800°F), $\Delta\epsilon$=0.4%, 1.25 cpm, 60 psi O_2, 1216 cycles) is shown in Figure 15. This specimen had two initiation sites. The primary initiation is shown in Figures 15a and 15b. The fracture surface is heavily oxidized and the oxide has the rounded appearance that is typical of R=-1 loading. The crack path appears to be transgrannular. Figure 15c is a higher magnification view of porosity located near the center of the specimen, away from the initiation sites. The internal area of the pore was not subject to the mechanical damage that can occur during an R=-1 test and shows the crystalline features the oxide develops if it grows unimpeded. Results of XES indicated the presence of carbides (indicated by arrows in Figure 15b) in the area of the initiation site.

Typical SEM micrographs of specimen 112A [982°C(1800°F), $\Delta\epsilon = \pm 0.20\%$, 1.25 cpm, 60 psig O_2, initiation life = 460 cycles, separation life = 1000 cycles] are shown in Figure 16. Oxidation of the fracture surface prevented detailed examination; however, the area of the initiation site and the majority of fatigue crack propagation appear transgrannular.

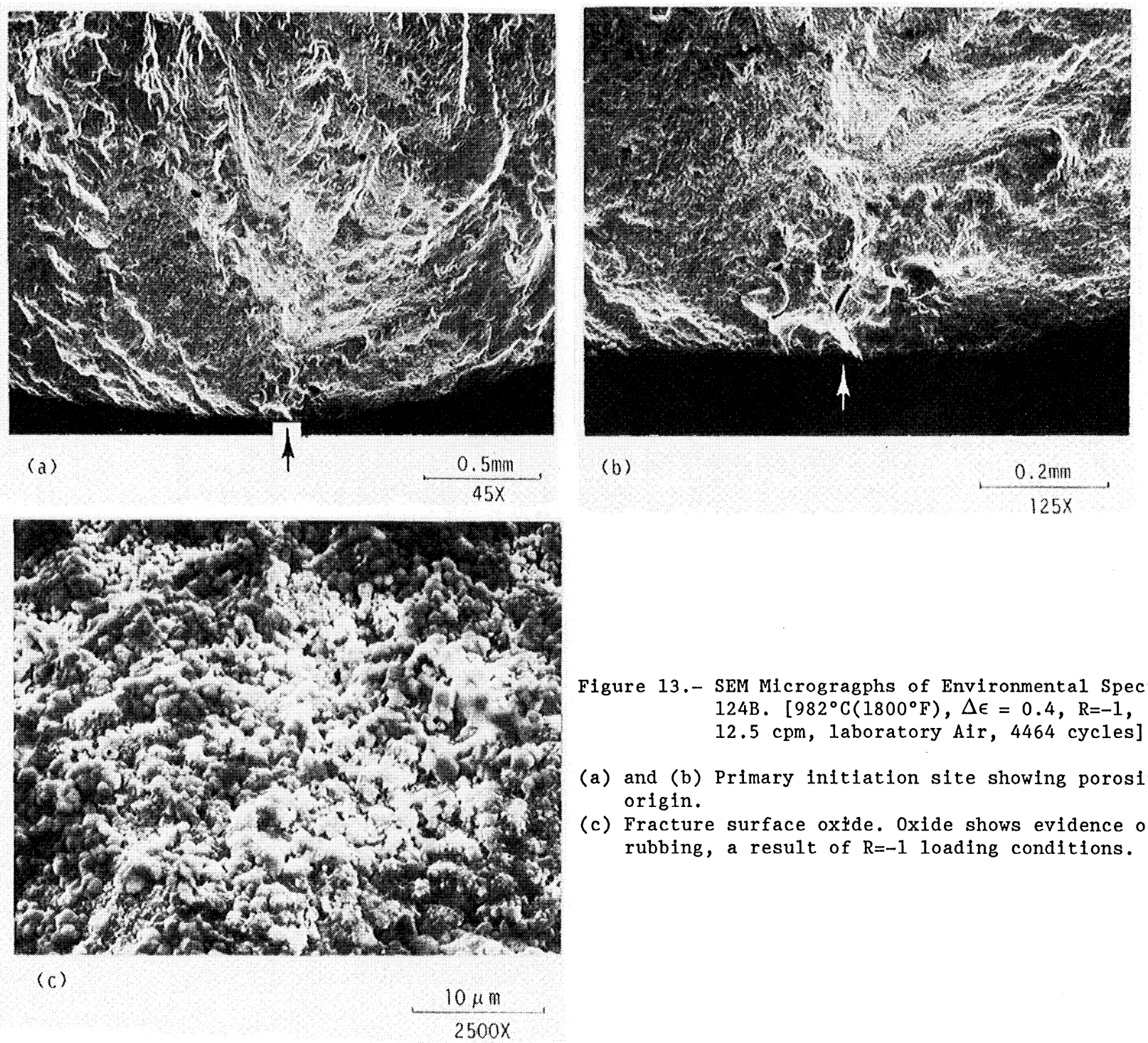

Figure 13.- SEM Micrograghs of Environmental Specimen 124B. [982°C(1800°F), $\Delta\epsilon$ = 0.4, R=-1, 12.5 cpm, laboratory Air, 4464 cycles]

(a) and (b) Primary initiation site showing porosity at origin.
(c) Fracture surface oxide. Oxide shows evidence of rubbing, a result of R=-1 loading conditions.

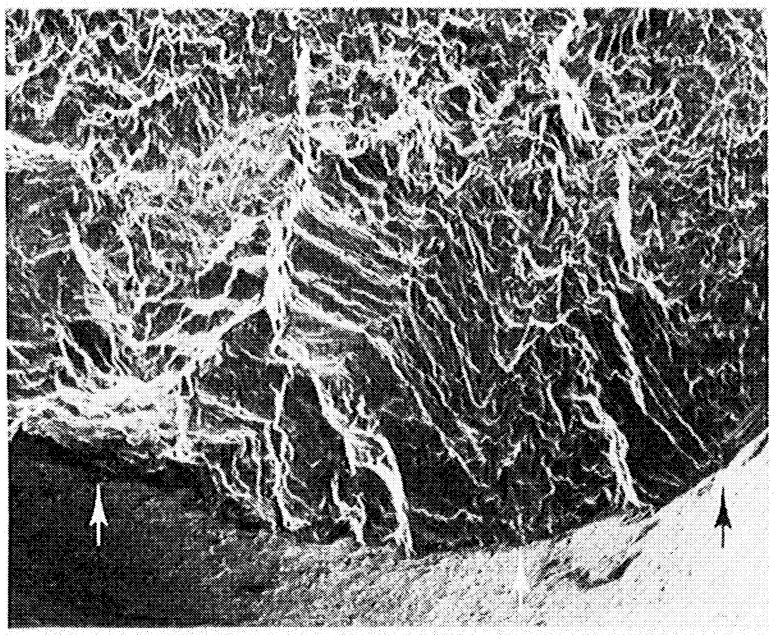

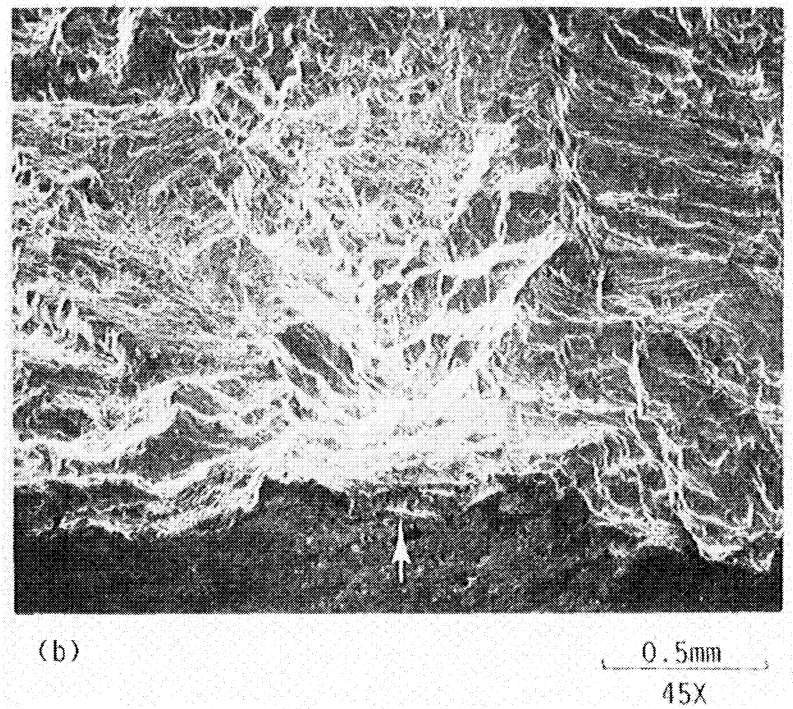

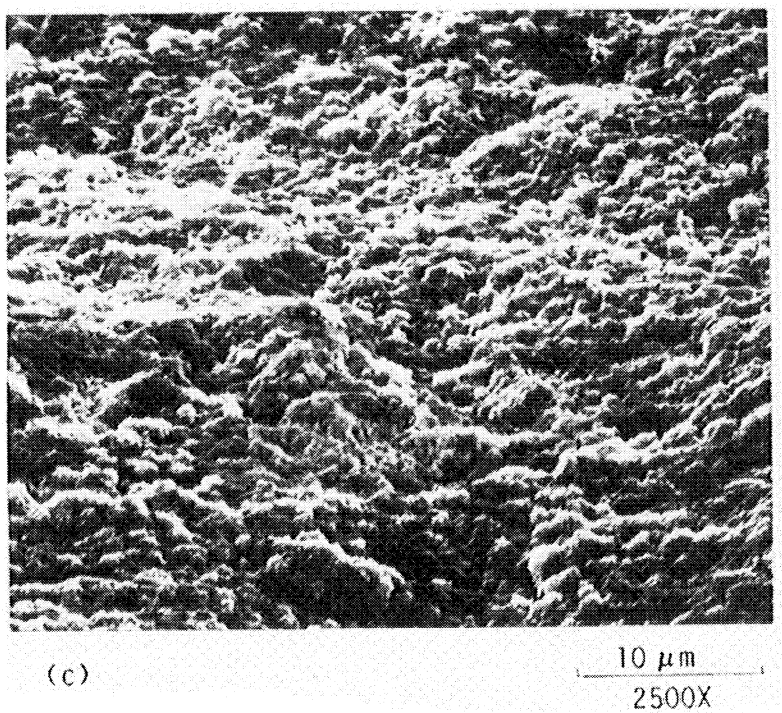

Figure 14.- SEM Micrograghs of Environmental Specimen 111C. [871°C(1600°F), $\Delta\epsilon$ = 0.5, R=-1, 1 cpm, 60 psi O_2, 2245 cycles]

(a) Arrows indicate three initiation sites. The primary initiation site is on the extreme left.
(b) Higher magnification of primary initiation site.
(c) Fracture surface oxide. Oxide shows evidence of rubbing, a result of R=-1 loading.

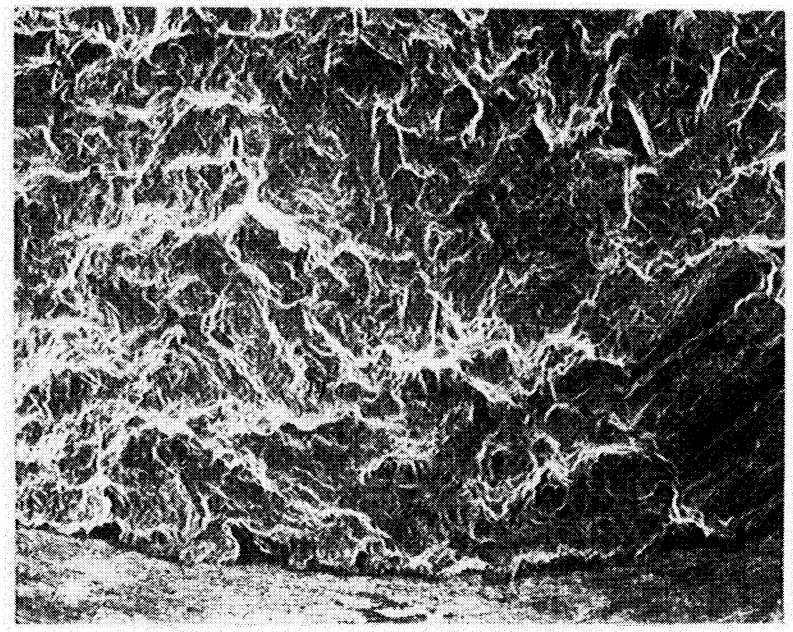

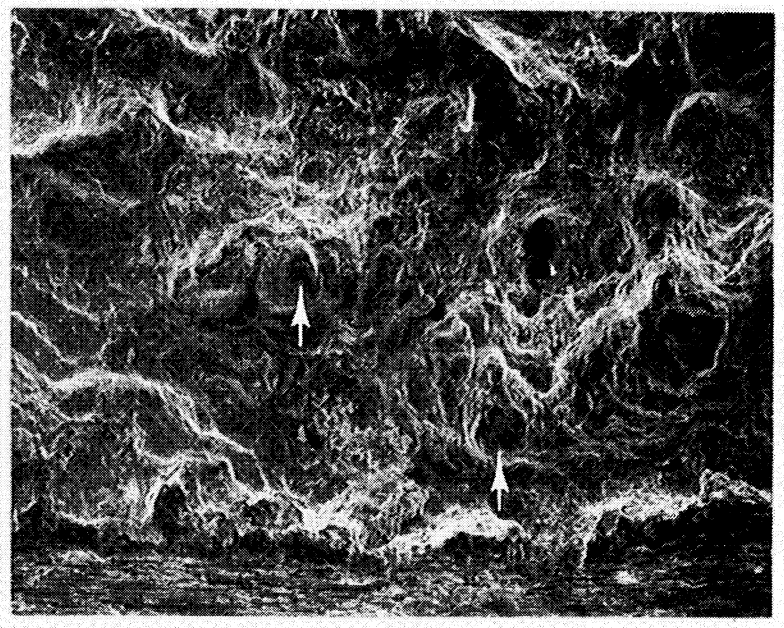

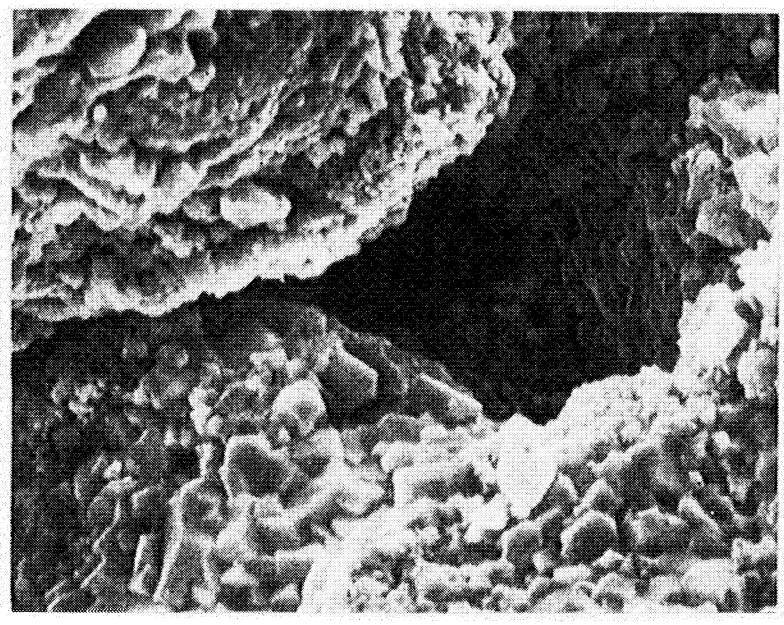

Figure 15.- SEM Micrograghs of Environmental Specimen 111D. [982°C(1800°F), $\Delta\epsilon$ = 0.4, R=-1, 1 cpm, 60 psi O_2, 1216 cycles]

(a) and (b) Primary initiation site, carbides detected by XES are indicated by arrows.
(c) Fracture surface oxide in vicinity of porosity showing rounded features where rubbing has occurred due to R=-1 loading conditions and crystalline features where no rubbing has occurred.

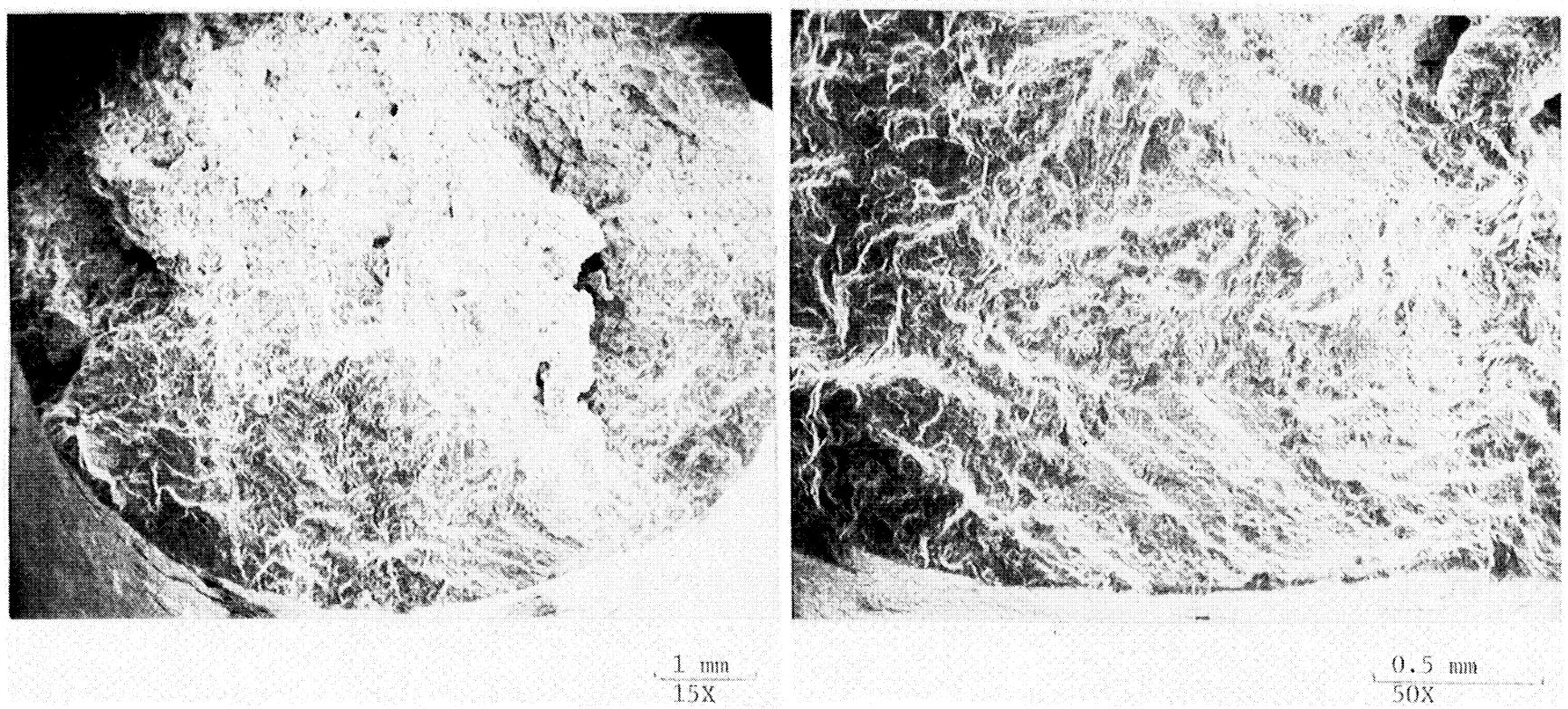

Figure 16.- SEM Micrographs of Fracture Surface of Environmental Specimen 122A. [982°C(1800°F), 0.4% strain range, R=-1, 1.25 cpm, 60 psig O_2, 1000 cycles]

Purified Argon Testing

Specimen 137C was run in the environmental chamber at 871°C(1600°F), 0.5% strain range, R=-1, and 1 cpm under a slight positive pressure of argon (to make sure the seal leakage would be outward). No replicas were taken during the test to avoid delay associated with opening the chamber and subsequent resealing and repressurization. Using replica data from similar tests, the initiation life was estimated as 521 cycles. The separation life was 1544 cycles. This life was unexpectedly low relative to other specimens tested either in lab air or in moderate pressure oxygen. The specimen surface appeared to be oxidized despite the argon atmosphere, and it is probable that some type of contaminant was present during the test.

Specimen 137D was run in the environmental chamber at 982°C (1800°F), 0.4% strain range, R=-1, and 1.25 CPM under a slight positive pressure of argon (to make sure the seal leakage would be outward). As with the first test, no replicas were taken during the test. Using replica data from similar tests, the initiation life was estimated as 256 cycles. The separation life was 522 cycles. Once again, this was unexpectedly low relative to other specimens previously tested either in lab air or in moderate pressure oxygen.

Optically, the appearance of specimen 137D (10 psig Ar) indicated that an extensive buildup of oxidation occurred during testing which was apparently the result of a contaminated Ar atmosphere. This fitted in well with the low lives of the Ar tests as compared to the 60 psig O_2 tests. Typical SEM micrographs of 137D are shown in Figure 17. The buildup of contamination on the fracture surface was responsible for the light band shown in Figure 17a which is a fluorescence effect that occurred when examining a nonconductive substance such as an oxide. The extent of oxide formation is evident in Figure 17b which shows the side surface of the sample in an area where the oxidation spalled off in two locations. Figure 17c is a higher magnification view of the light band shown in Figure 10a. It can be seen that the oxide buildup prevents detailed examination of the fracture surface; however, the initiation site and the majority of fatigue crack propagation appear to be transgranular.

Longitudinal sections were made through the initiation areas of specimens 137D and 112A in order to compare the amount of oxidation occurring in the Ar and O_2 atmospheres. Optical micrographs of the polished and etched sections are shown in Figure 18. Both samples show depletion zones at their fracture surfaces and side surfaces, a result of oxidation. The O_2 tested sample has a thicker depletion zone than the Ar sample (8 μm vs 4 μm, measured on the side surface of the sample) as well as a more extensive buildup of oxide. These differences may be a reflection of the lower partial pressure of oxygen and the shorter exposure for the Ar test.

The R=-1 loading conditions of these tests resulted in mechanical damage occurring to the oxide in most areas of the fractures and this may limit the final thickness the oxide layers can attain on the fracture surfaces regardless of the test environment.

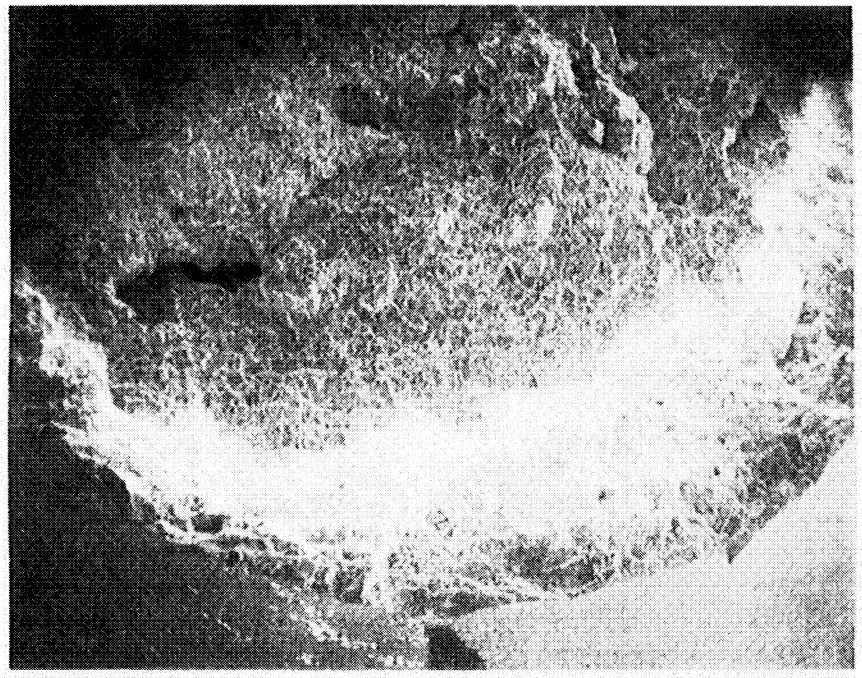

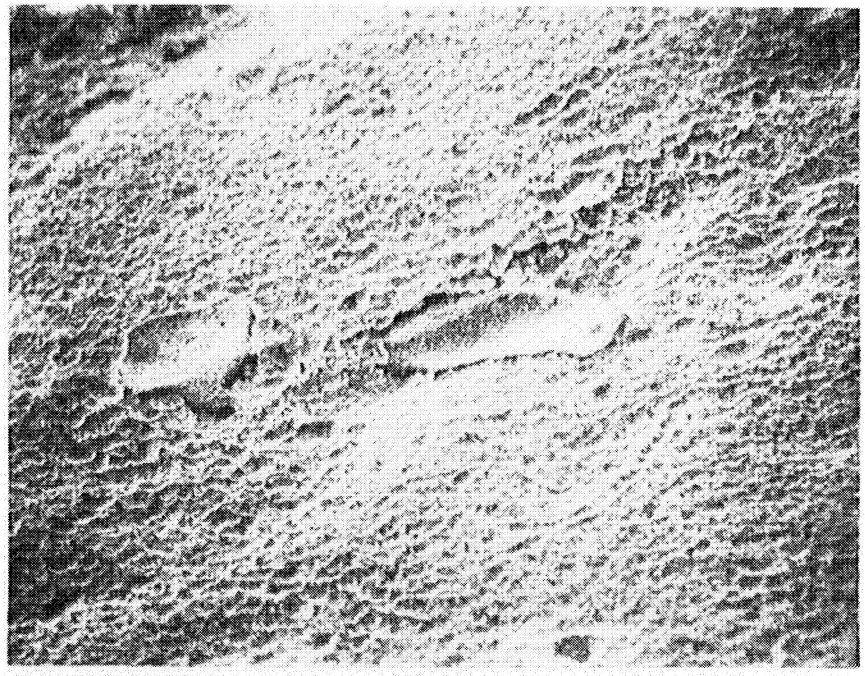

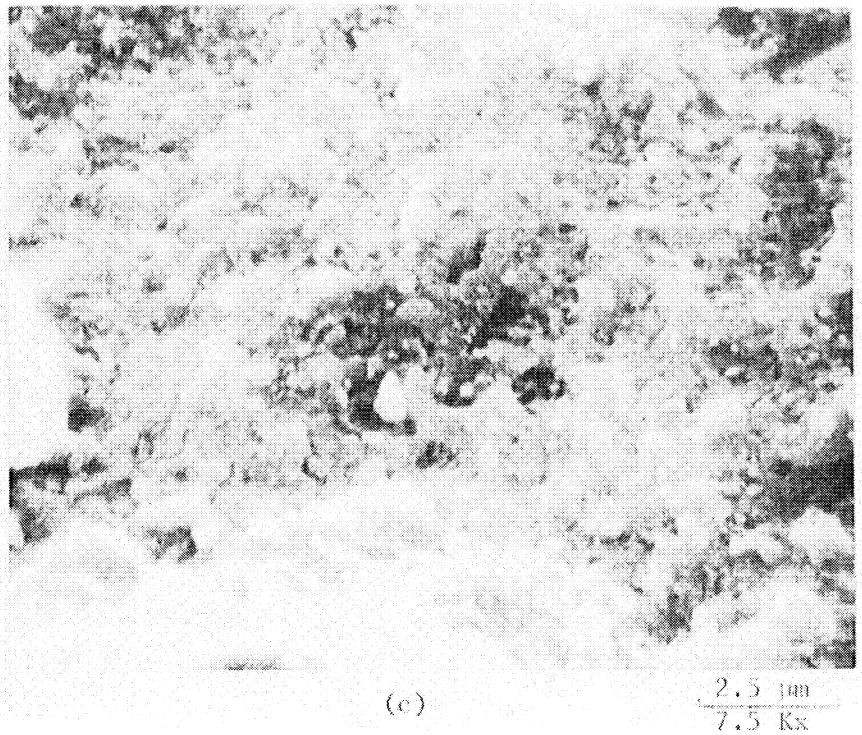

Figure 17.- SEM Micrograghs of Environmental Specimen 137D. [982°C(1800°F), 0.4% strain range, R=-1, 1.25 cpm, Ar, 522 cycles to failure]

(a) Overall view of fracture surface. Light band is the result of oxidation of the fracture surface.
(b) View of side surface of specimen showing extensive buildup of oxidation.
(c) Appearance of oxidation within light band shown in (a).

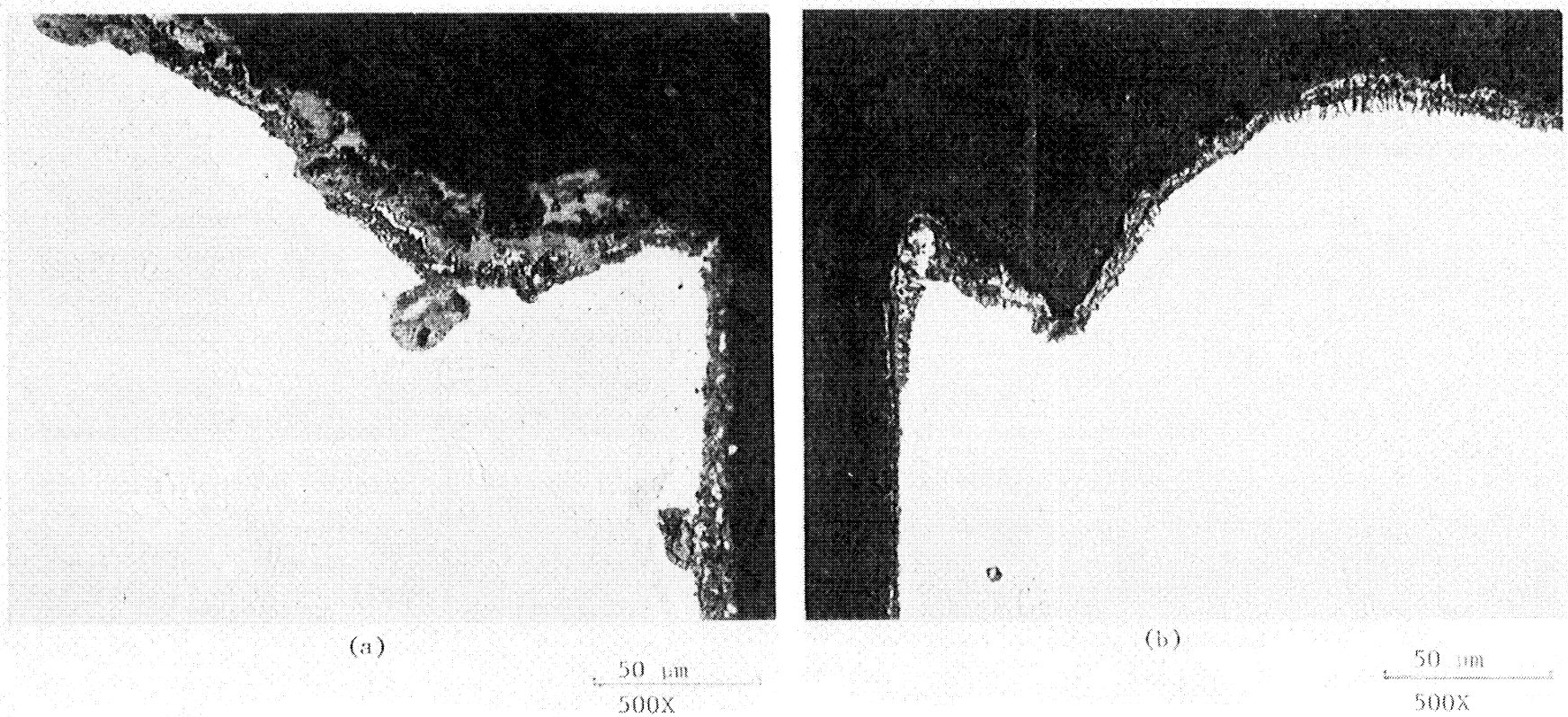

Figure 18.- Optical Micrographs of Longitudinal Sections Through Initiation Sites of:
(a) 112A. [982°C(1800°F), 0.4% strain range, R=-1, 1.25 cpm, 60 psig O_2, 1000 cycles]
(b) 137D. [982°C(1800°F), 0.4% strain range, R=-1, 1.25 cpm, 10 psig Ar, 520 cycles]
Both specimens show depletion layers, however, there is a more extensive oxide buildup on 112A.

Several techniques were evaluated to eliminate the effect of stray oxygen during the argon screening tests. These included a more aggressive titanium getter design, revisions to the chamber cooling scheme, reduction of leakages, and an increased argon flow rate. None of these techniques were successful in insuring a clean specimen surface after long exposures in argon at elevated temperatures. The design of the P&W environmental chamber assummed a slight positive pressure of argon would guarantee outflow at all joints. This was not the case and it appears that the chamber must first have a good vacuum which can be sealed and held before the chamber is backfilled with argon. This technique, coupled with a clean chamber interior, should be used for future environmental testing in inert atmospheres.

Because of the failures resulting from the argon trials, the remaining environmental tests were performed in an aggressive oxygen atmosphere instead of inert argon because it was felt the pressurized oxygen environment would generate data relevant to the actual conditions found in engine hot sections while eliminating the problems encountered during the argon tests.

Environmental Block Tests at 871°C(1600°F)

At this point in the experimental program, a fire occurred inside the environmental chamber. Apparently the cooling water to the induction coil (made of copper) was blocked off, causing the coil to overheat and burn fiercely in the pure oxygen. The feed-through for the induction coil was also destroyed by the heat, but the rest of the equipment, including the water-cooled extensometer, was not damaged. Repairs to the environmental rig included replacement of the induction power feed-through and thorough cleaning of all contaminated surfaces.

Testing resumed with Specimen 138B run at 871°C (1600°F), 0.50% strain range, R=-1, and 1 CPM in pressurized oxygen for 80 cycles, followed by lab air for the remainder of the test. The resulting initiation life was 837 cycles, and the separation life was a total of 2263 cycles. This test is similar to specimen 142A, except that the number of cycles run in oxygen was 300 instead of 80. The lives of these two tests were similar, with 427 and 2033 cycles for 142A.

Specimen 142A was run under similar conditions as 138B, except that a longer exposure of 300 cycles in oxygen was used for the first block. The remainder of the test was run in lab air. After the oxygen cycling, a crack of 0.015" was observed on the surface; the crack reached 0.030" in length by 427 cycles, and the final separation life was a total of 2033 cycles.

Specimen 142B was run under the same cyclic conditions as specimen 142A but with the order of the atmospheres reversed. It was run in lab air for 300 cycles, at which time a 0.012" surface crack occurred; the remainder of the test was then run in 60 psig oxygen. The initiation life was 597 cycles, and the final separation life was 2093 cycles. Though perhaps not statistically significant in view of the scatter observed during the baseline testing, it is interesting to note that the 60 psig oxygen environment apparently lowered both the initiation life and the propagation life, as expected. The effect on initiation was somewhat higher, with the life for the "oxygen first" test being about 70% of the "air first" test.

Specimen 142C was run at 871°C(1600°F), 0.50%, R=-1, and 1 CPM, using lab air for 600 cycles and pressurized oxygen for the remainder of the testing. The initiation life was 901 cycles, and the final separation life was 3278 cycles. As expected, these lives were somewhat higher than what was observed from specimen 142B, which was tested using 300 cycles in lab air instead of 600 cycles. A comparison of these specimens was made to each other to help determine the effect of the oxygen exposure.

Specimen 136B was to have been run at 871°F (1600°F), 0.50% strain range, R=-1, and 10 CPM using pressurized oxygen for 300 cycles followed by lab air for the remainder of the test. However, this specimen was inadvertantly run at 1 CPM instead of 10 CPM; this was discovered after 63 cycles and the test was restarted using the correct parameters. After a total of 363 cycles in oxygen (63 at 1 CPM and 300 at 10 CPM), the specimen had a 0.006 in. surface crack. The initiation life to 0.030 in. surface length was 2019 cycles, and the final separation life was a total of 6026 cycles. The effect of prior cycling at the slow rate on the life results were evaluated during the final model correlations.

Specimen 140A was run at 871°C (1600°F), 0.40%, R=-1, and 12.5 CPM, using pressurized oxygen for 1800 cycles and lab air for the remainder of the testing. The initiation life was 14,017 cycles, and the final separation life was 27,218 cycles. Curiously, these lives are both roughly 3X higher than what was observed during the baseline testing in lab air at the same conditions.

Specimen 140B was run at 871°C (1600°F), 0.40% strain range, R=-1, and 12.5 CPM in lab air for 1800 cycles followed by pressurized oxygen for the remainder of the test. No visible cracks on the specimen surface crack were seen after the lab air portion of the test. The final initiation life to 0.030-in. surface length was 18,833 cycles, and the separation life was a total of 32,753 cycles. This test was similar to specimen 140A, except that the order of the atmospheres was reversed. That test had lives of 14,017 and 27,218 cycles, indicating a slight but not statistically significant tendency for the oxygen-first test to have lower lives.

Environmental Block Tests at 982°C(1800°F)

Specimen 143B was run at 982°C (1800°F), 0.40%, R=-1, and 1.25 CPM, using pressurized oxygen for 50 cycles and lab air for the remainder of the testing. The initiation life was 716 cycles, and the final separation life was 1301 cycles. The separation life was identical to that observed for specimen 138C which was run at the same conditions, except with 260 cycles in the oxygen block; the initiation lives were also comparable.

Specimen 138C was run at 982°C (1800°F), 0.40%, R=-1, and 1.25 CPM, using pressurized oxygen for 260 cycles and lab air for the remainder of the testing. The initiation life was 624 cycles, and the final separation life was 1301 cycles. These lives were quite similar to those of specimen 143B which was run under similar conditions but with only 50 cycles in the initial oxygen environment. Specimen 139D was run at the same conditions but with the atmospheres reversed: lab air for 800 cycles, followed by pressurized oxygen for the remainder of the test. Surface replicas taken during the first portion of this test showed that the crack initiation occurred at 470 cycles, before

the switch to the oxygen environment; the final separation life was 1119 cycles. Note that the lives of both of these specimens were somewhat lower than the lives of the specimen run continuously in lab air at these conditions (137A; 989 & 2105 cycles); this is within the scatter for this material.

SEM micrographs of the primary initiation site of specimen 139D are shown in Figure 19. This specimen had one primary initiation site and two smaller initiation sites, all located on the outside diameter of the specimen. A secondary crack was also present at the primary initiation site and is indicated by the arrows in Figures 19a and 19b. Replicas of the side surface of the specimen taken after the initial exposure to 800 cycles in air showed that cracks were present when the environment was changed to 60 psi O_2; however, no evidence of the environmental change were seen on the fracture surface. The crack path appeared to be transgrannular for both environments. Any minor changes in crack growth that may occur on going from air to high pressure O_2 were masked by the extensive oxidation of the fracture surface. As in the case for other specimens, the majority of the fracture surface oxide had a rounded appearance due to rubbing of the fracture. Figure 19c is from a small area near the initiation where partial rubbing occurred and shows the oxide in this area has both a crystalline and a rubbed appearance.

Three block atmosphere tests were all run at the same basic low strain, fast rate conditions: 982°C (1800°F), 0.40%, 12.5 CPM, and the block atmospheres were varied to search for effects due to environment in this regime. Specimen 144C was tested for 100 cycles in pressurized oxygen, followed by lab air for the remainder of the test. Its initiation and separation lives were 735 and 1442 cycles, respectively. Specimen 144B was tested at the same conditions except with 500 cycles in oxygen instead of 100. At 848 and 1542 cycles, its lives were very similar to those from the previous test. The last environmental block test was specimen 144A which was run in lab air for 800 cycles, followed by pressurized oxygen for the remainder of the test. Its lives of 806 and 1521 cycles were again similar to those from the previous two specimens.

The completed matrix of test conditions run during the block atmosphere tests is shown in Table IV. Note that in most cases very little effect of the sequencing of the block atmospheres can be observed. The overall conclusion is that there is sufficient oxygen in the laboratory air to saturate the damage processes caused by oxygen. The final environmental specimen tests were run in pure oxygen at various hold times and R=0 conditions run earlier in lab air.

Hold Time Effects

The final five environmental specimen tests explored the effects of tensile hold times and one-way tension cycling in pure oxygen or pure argon.

Specimen 136D was run in oxygen at 871°C (1600°F) using a one minute tensile hold combined with 0.50%, R=-1 cycling at a 10 CPM rate. Its initiation and separation lives were 900 and 5940 cycles. These were directly compared to the results of baseline run at identical conditions: 1328 and 3963 cycles, respectively. Under these conditions, a somewhat lower initiation life under the oxygen atmosphere were seen, but the total life was higher.

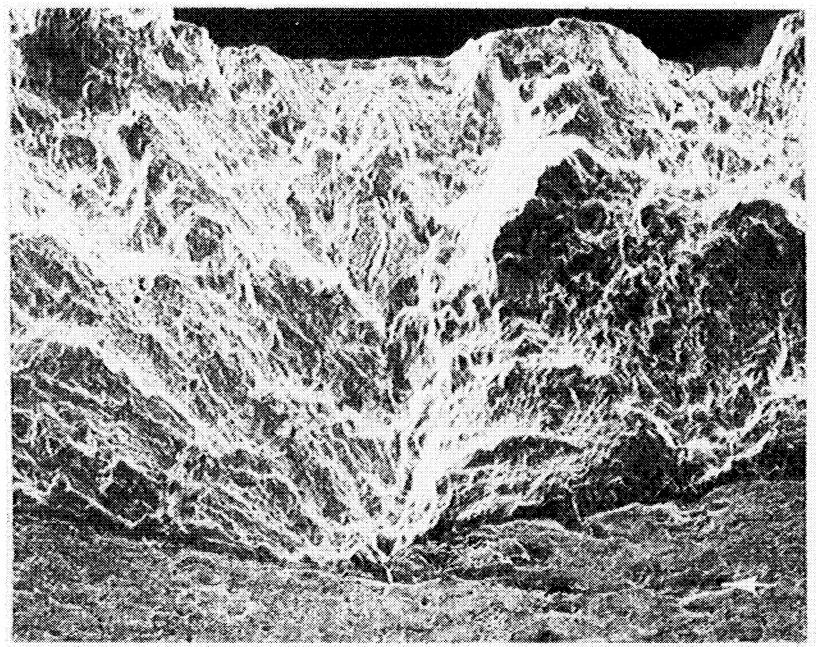

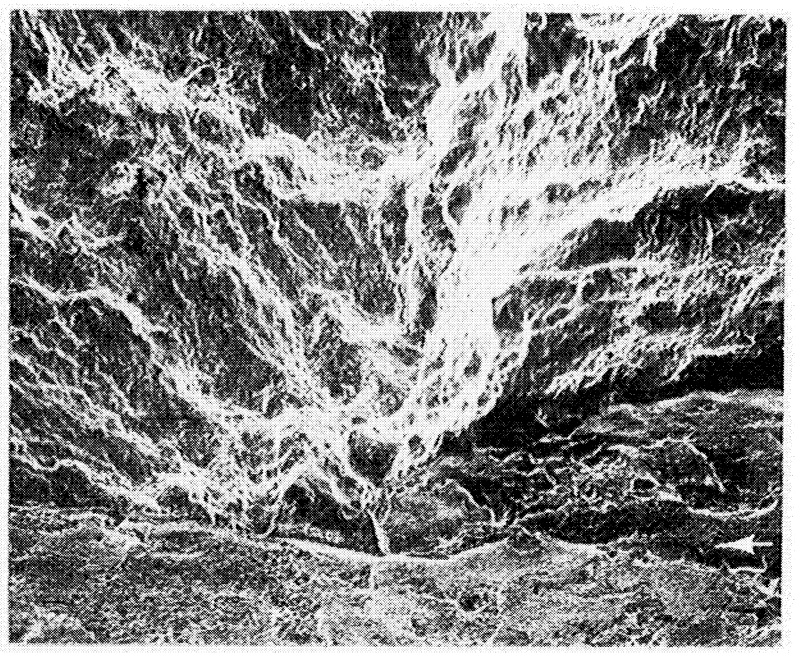

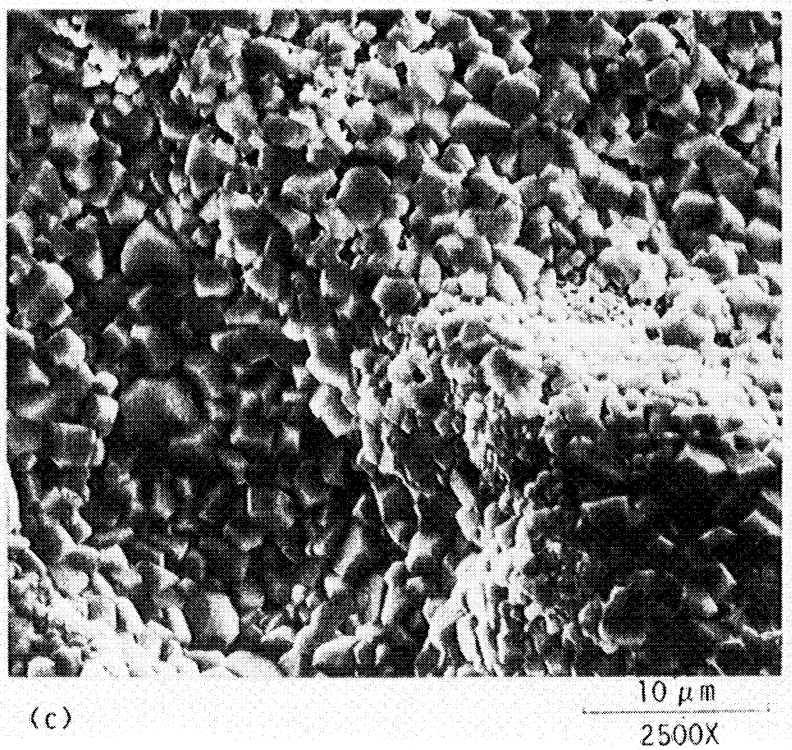

Figure 19.- SEM Micrograghs of Environmental Specimen 139D. [982°C(1800°F), $\Delta\epsilon$= 0.4%, R=-1, 1.25 CPM, 800 cycles in laboratory air, then remainder in 60 psi O_2, 1119 cycles total]

(a) and (b) Primary initiation site, secondary crack at arrow

(c) Fracture surface oxide near initiation site. Some rubbing occurred in this area due to R=-1 loading conditions.

Specimen 139B, was also run in oxygen but at 871°C (1600°F), 0.50%, R=0, and 1 CPM. Its initiation and separation lives were 150 and 1186 cycles, respectively. Median lives from baseline specimens run in lab air at similar conditions but at only 0.5 CPM were 511 and 1525 cycles, respectively. Here again it can be seen that the oxygen caused significant damage during the crack initiation process, but its influence on the total life was much less. In fact, the propagation lives were very nearly the same.

Specimen 143C was run at 982°C (1800°F), 0.40% strain range, R=-1, and 12.5 CPM plus a one minute tensile hold time. The atmosphere was pure oxygen at 60 psig for the entire test. The resulting initiation life was 200 cycles, and the separation life was 1259 cycles. Although this was the first test to be run at these exact conditions, its initiation life was much lower than that of specimens run at the same conditions but without the hold time (average Ni = 510 cycles for 1.25 CPM; similar periods). However, note that its separation life was essentially the same as for other tests (average Nsep = 1108 cycles).

Specimen 143D was run at 982°C (1800°F), 0.40%, R=0, and 1.25 CPM, using pressurized oxygen for the entire test. The initiation life was 280 cycles, and the separation life was 808 cycles. As with specimen 143C, there were no other tests at these identical conditions in lab air, but these results can be compared to the same lives mentioned earlier. Clearly the R=0 cycling in pure oxygen had a very strong influence on initiation life, with this specimen having about half the life of the specimens run at R=-1. However, as before, the separation lives did not show the same difference.

Specimen 143A test was a final attempt to explore the effects of argon as an alternative environment. Various improvements in the sealing of the chamber indicated that a clean argon atmosphere could be maintained during testing. Pretest trials using a dummy specimen showed very little surface degradation using the current setup. Specimen 143A was run at the same conditions used earlier for specimen 137D: 982°C(1800°F), 0.40% strain range, R=-1, and 1.25 CPM. The resulting initiation and separation lives were 487 and 993 cycles, which were nearly double the lives of the earlier test. However, these lives are still about the same as what was seen during tests in pure oxygen at the same conditions; the expected high lives due to the absence of oxygen have never been demonstrated using the current material and experimental setup.

The conclusions of the microstructural observations under this task were as follows:

1. Analysis of the environmental test results showed that even limited exposure to 60 psig O_2 resulted in a significant reduction in fatigue life. Specimens tested in 60 psig O_2 at 871°C(1600°F) and 982°C(1800°F) were found to have transgrannular fractures. Extensive oxidation of the fracture surfaces was observed. In isolated areas of the specimens, the oxide was found to have an angular, crystalline appearance. In most areas the oxide had a rubbed appearance due to the R=-1 loading conditions used for these tests.

2. Fractographic exmaminations of samples tested using block environments did not reveal a change in crack growth mode that might occur with a change in environment. If there is a change, it may be masked by the extensive fracture surface oxidation.

3. The specimens tested in argon showed clear evidence of the contamination of the test environment; this may explain the low lives of these tests.

TASK X - PROTECTIVE COATING MODELS

This task was conducted to develop, evaluate and verify a life prediction system that would account for the effects of protective coatings used on cast superalloys. Specimen testing has been completed and was reported in Nelson et al (1992). During the remainder of the contract, work focused on the development of a methodology to calculate life for coated material, based on results of the testing and from work performed under the companion HOST contract for anisotropic materials under contract NAS3-23939 (Nissley et al, 1992).

TASK XI - CYCLIC MEAN STRESS MODEL

The purpose of this task was to develop a cyclic mean stress failure model having the capability to deal with mean stresses during mechanical cycling and cyclic biaxial stress states. As reported in Nelson et al (1991), five controlled mean stress TMF tests were conducted. The remaining twenty tests were completed on PWA 1455 under isothermal conditions using special mean stress-strain range software available at the University of Rhode Island. These tests were run at 760°C (1400°F), 871°C (1600°F), and 982°C (1800°F). A summary of the results of these tests are given in Table V; details for each test are given in Appendix B.

TABLE V.- MEAN STRESS TESTING - PWA 1455

Spec ID	Temp (°C)	Strain Range (%)	Mean Stress (ksi)	Cyclic Rate (CPM)	Initiation Life (Cycles)	Separation Life (Cycles)	Final Mean Strain (%)
110A	871	0.4	0	12.5	24182e	45626e	0
110C		0.4	0		24470e	46170e	0
123C		0.4	+30		6791	14448	0.84
127B		0.4	+43		2043	5108	0.77
125B		0.4	+57		139	516	1.78
127C		0.5	+30		1053	2847	1.54
125A		0.5	+43		234	780	0.86
125C		0.5	+57		46	209	2.87
135A		0.35	+60		246	819e	1.50
133C		0.35	+45		3800	8207	1.10
134C	982	0.35	+30	12.5	139	604	2.6
126B		0.40	+22		76	380	5.7
135C		0.35	+22		388	1386	4.0
135D		0.40	+13		1692	4833	2.2
127A		0.30	+22		788	2543	4.7
135B		0.30	+13		2313	6252	2.6
134B	760	0.40	+43	12.5	4809	10930	0.3
133D		0.50	+43		3413	8126	0.3
134A		0.50	+60		631	1855	1.6
134D		0.70	+30		584	1770	0.52

Notes: 1. All testing performed at U.R.I.
2. "e" = estimated life; test was discontinued

Cyclic Mean Stress Testing at 760°C (1400°F)

Specimen 134B was run at 0.40% strain range, 12.5 CPM, and a mean stress of +43 KSI. The initiation life was 4809 cycles and the separation life was 10930 cycles, with an accumulated mean strain of only 0.3% at separation. The second test, specimen 133D, was run at 0.50% strain range, 12.5 CPM, and a mean stress of +43 KSI. The initiation life was 343 cycles and the separation life was 8126 cycles, with an accumulated mean strain of 0.3% . Specimen 134A was run at 0.50% strain range, 12.5 CPM, and a mean stress of +60 KSI. The initiation life was 631 cycles and the separation life was 1855 cycles with an accumulated mean strain of 1.6% at the end of the test. Specimen 134D was run at 0.70% strain range, 12.5 CPM, and a mean stress of +30 KSI. The initiation life was 584 cycles and the separation life was 1770 cycles with a final accumulated mean strain of 0.52%.

Cyclic Mean Stess Testing at 871°C (1600°F)

Specimen 110A was run at the baseline conditions of 871°C (1600°F), 0.4% strain range, zero mean stress, and 10 CPM. This test had estimated initiation and separation lives of 24182 cycles and 45626 cycles, respectively. This was the first test run at URI. The data acquisition software functioned very well and temperature control seemed to be adequate.

Specimen 110C was run at the same conditions used for the first URI specimen (110A): 871°C (1600°F), 0.4% strain range, zero mean stress, and 10 CPM. The specimen ran to 14,000 cycles with a stable, fully reversed cycle. At 15,000 cycles, however, the computer data showed that the hysteresis loops had shifted downward in stress and had opened somewhat wider relative to the earlier data. The test was terminated at 15,148 cycles due to apparent load drop and subsequent examination indicated the possibility of a crack outside the extensometer gage section (0.5 in.). Further testing were made by moving the extensometer to include the primary crack within the extensometer gage length. Specimen 110C had estimated initiation and separation lives of 24470 cycles and 46170 cycles, respectively.

Specimen 123C was run at the same strain conditions used for the initial baseline URI specimens, but with a mean stress of +30 KSI. This was the first non-zero mean stress run at URI. The initiation life was 6791 cycles and the separation life was 14,400 cycles, with the mean strain increasing to 0.8% by the end of the test. Since these tests did not show any "load drop" (by definition), the onset of tertiary creep in the mean strain data were used to terminate the test prior to actual specimen separation. This avoided destruction of the extensometer rods when the specimen broke.

Specimen 127B was run at the same strain conditions used for 123C, but with a mean stress of +45 KSI instead of +30 KSI. The specimen separation life was 5,089 cycles, with the mean strain increasing to 0.8% by the end of the test (onset of tertiary creep).

Specimen 125B was run using the same conditions as for 123C and 127B but with a mean stress of +60 KSI. The initiation life was 139 cycles and the separation life was 516 cycles, with the mean strain increasing to 1.78% by the end of the test (onset of tertiary creep). The fourth test was specimen 127C, which was run at 0.5% strain range, 10 CPM, and a mean stress of +30 KSI. Its separation life was 2840 cycles, with the mean strain increasing to 1.54% by the end of the test.

Specimen 125A was run at 0.5% strain range, 10 CPM, and a mean stress of +43 KSI. The initiation life was 234 cycles and the separation life was 780 cycles, with the mean strain increasing to 0.86% by the end of the test (onset of tertiary creep). Specimen 125C was run at 0.5% strain range, 10 CPM, and a mean stress of +57 KSI. Its initiation life was 46 cycles and its separation life was 209 cycles, with the mean strain increasing to 2.87% by the end of the test.

Specimen 135A was run at 0.35% strain range, 12.5 CPM, and a mean stress of +60 KSI. The specimen showed rapid acceleration of the mean strain rate at 300 cycles, with a mean strain of 1.5%. At that point, the test was stopped. The specimen was then sectioned for detailed examination of void growth mechanisms active at that level of mean strain. Based on comparison with similar tests in this series and examination of the fracture surface, the initiation life was determined to be 246 cycles and the separation life was estimated at 819 cycles.

Specimen 133C was run at 0.35% strain range, 12.5 CPM, and a mean stress of +45 KSI. The initiation life was 3800 cycles and separation life was 8207 cycles, with an accumulated mean strain of 1.10% at that time.

Cyclic Mean Stress Testing at 982°C (1800°F)

It was felt that testing at this higher temperature would accelerate the creep interaction due to the imposed mean stress. Specimen 135B was tested at 982°C (1800°F), 0.30% strain range, 12.5 cpm, with a mean stress of +13 ksi. Its initiation and sepration lives were 2313 and 6252 cycles, respectively. At the conclusion of the test, this specimen accumulated a mean strain of 2.6%. Specimen 127A was tested using the same conditions for 135B but with a higher mean stress of +22 ksi. The initiation life was 788 cycles and the separation life was 2543 cycles. This specimen accumulated a mean strain of 4.7%. Specimen 135C was also run at 982°C (1800°F), 12.5 cpm, with a mean stress of +22 ksi but at a higher strain range of 0.35%. Its initiation and separation lives were 388 cycles and 1386 cycles, respectively. This specimen had an accumulated mean strain of 4.0% at the conclusion of the test.

Specimen 134C was run under similar conditions as 135C but using a higher mean stress of +30 ksi. The initiation life was 44 cycles and the separation life was 259 cycles. This test had an unexpectedly low life and no replicas were taken before the test was terminated. Its final mean strain was 2.6%.

Specimen 135D was run at 982°C (1800°F), 0.40% strain range, 12.5 cpm and a mean stress of +13 ksi. Its initiation life was 1692 cycles and its separation life was 4833 cycles. Its final mean strain was 2.2%.

Specimen 126B was run under conditions similar to those of 135D but at a higher mean stress level of +22 ksi. The initiation life was 76 cycles and the separation life was 380 cycles. This specimen had an accumulated mean strain of 5.7%. Only one replica was taken during this test.

TASK XII - FINAL VERIFICATION AND EVALUATION OF THE ALTERNATIVE MATERIAL/PROTECTIVE COATING SYSTEM/COMPONENT COMBINATION

Testing of an alternative alloy, INCO 718, was continued to verify the life prediction models developed under the contract. Initial monotonic and fatigue tests were completed and reported by Nelson et al (1991).

IN 718 Monotonic Tensile Tests

A series of nine INCO 718 monotonic tensile tests were performed using temperatures from room temperature up to 732°C (1350°F). Three different strain rates were used at the higher temperatures to determine rate effects on the monotonic data. Table VI shows the matrix of these tests and the resulting modulus, ultimate tensile strength, and 0.2% yield stress data. Figures 20, 21, and 22 present the stress-strain curves for the standard, slow, and fast strain rates, respectively.

TABLE VI.- MONOTONIC TENSILE TESTS - INCO 718

Temp		Spec.		E	0.2% YS	UTS	Elong	RA
°C	(°F)	ID	(min^{-1})	(psi)	(psi)	(psi)	(%)	(%)
RT	RT	410	.005	33.1E6	160,800	184,100	15.0	24.7
316	600	411	.005	27.9E6	140,900	159,100	20.0	33.9
482	900	412	.005	28.2E6	131,800	154,100	24.0	41.8
649	1200	413	.005	23.5E6	134,600	149,800	17.0	35.4
↓	↓	415	.050	24.7E6	133,400	147,700	18.0	42.3
↓	↓	417	.001	25.3E6	131,500	149,800	13.0	20.1
732	1350	414	.005	22.4E6	116,200	125,000	9.0	14.1
↓	↓	416	.050	22.2E6	115,600	131,600	17.0	15.7
↓	↓	418	.001	24.1E6	116,100	124,400	7.4	10.3

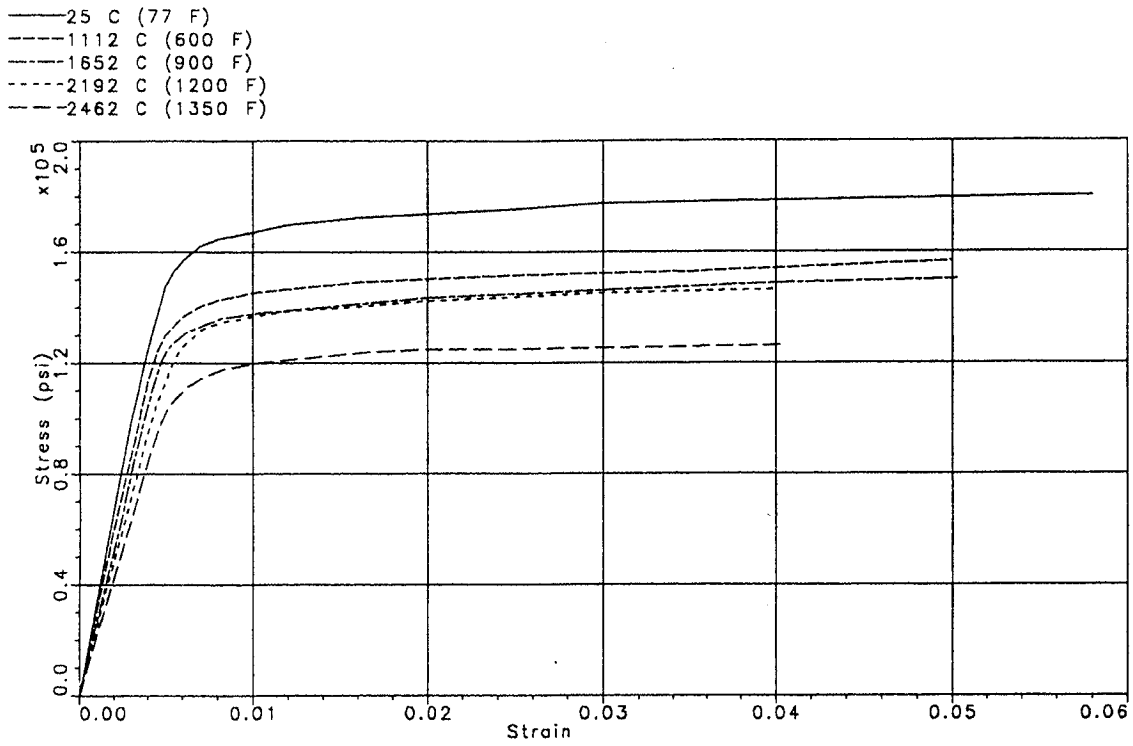

Figure 20.- INCO 718 Tensile Data Standard Rate (0.0005 sec^{-1}).

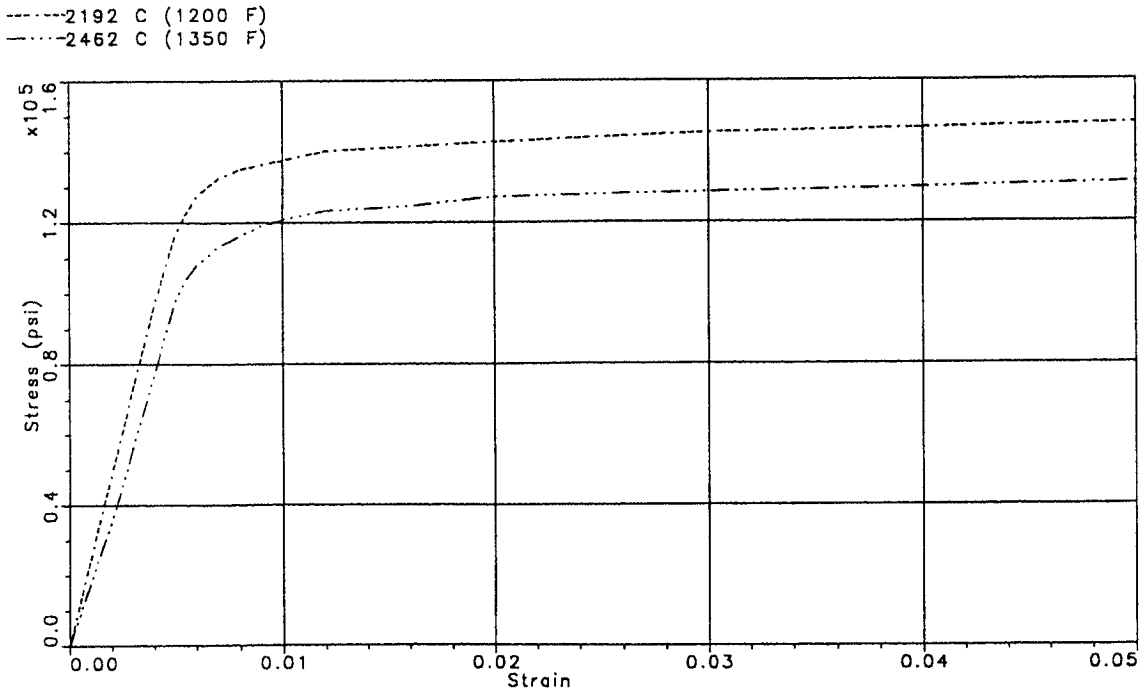

Figure 21.- INCO 718 Tensile Data Slow Rate (0.001 sec^{-1}).

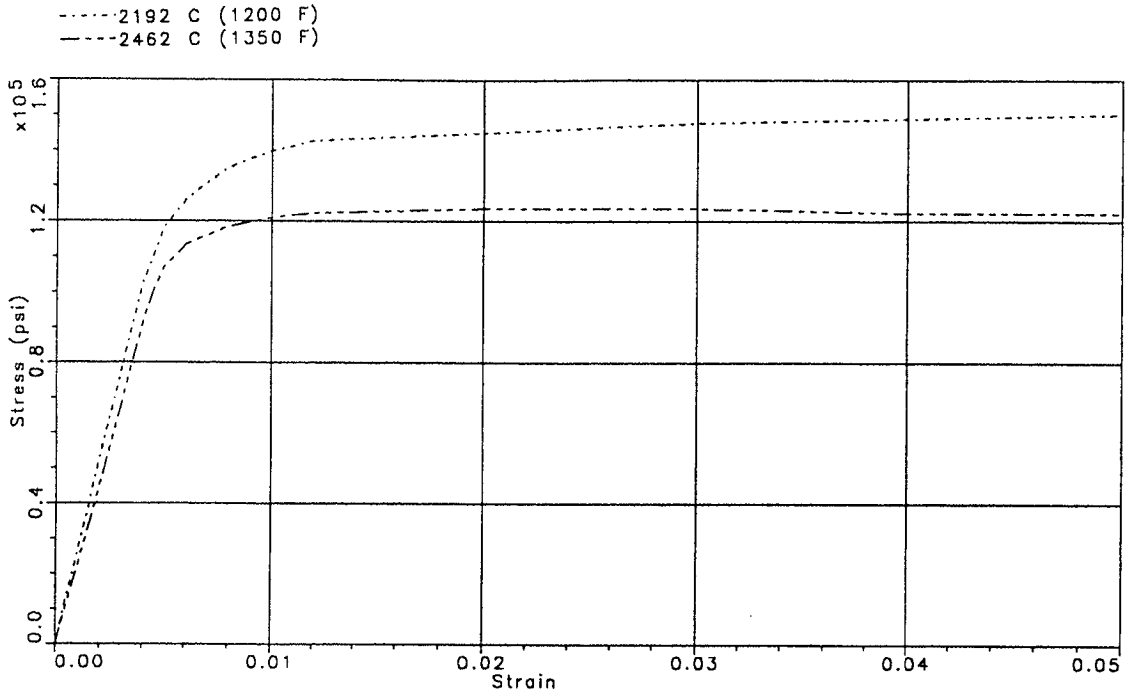

Figure 22.- INCO 718 Tensile Data Fast Rate (0.05 sec^{-1}).

IN 718 Creep Tests

Monotonic isothermal creep testing for the INCO 718 alternate material was performed on of 11 specimens which were run at a broad range of stresses and temperatures. Table VII presents a matrix of the test conditions and the resulting rupture lives. Figures 23-25 show comparisons among the specimens tested in the various life regimes. Of particular interest was the very low primary creep strain seen during most of these tests.

TABLE VII.- INCO 718 CREEP TESTING

Specimen No.	Temp °C	Temp (°F)	Rupture Stress (Ksi)	Secondary Life (Hrs.)	Creep Rate (Sec^{-1})	Reduction Elongation (%)	Reduction of Area (%)
695	593	1100	125	170.7	2.11 E-8	7.3	4.8
696	649	1200	125	4.0	4.13 E-7	5.3	10.8
697	↓	↓	110	24.0	1.49 E-7	8.0	6.4
699			100	41.0	5.40 E-8	3.2	4.8
701			80	1126.0	3.47 E-9	2.6	1.6
698	704	1300	110	1.9	1.69 E-6	8.0	6.4
693	↓	↓	80	32.9	5.46 E-8	8.5	7.8
702				60	376.3	4.46 E-9	1.8
3.1							
700	732	1350	100	1.4	3.97 E-6	8.8	8.0
694	↓	↓	60	109.0	4.14 E-8	7.6	9.4
703			40	497.6	4.73 E-9	12.0	9.3

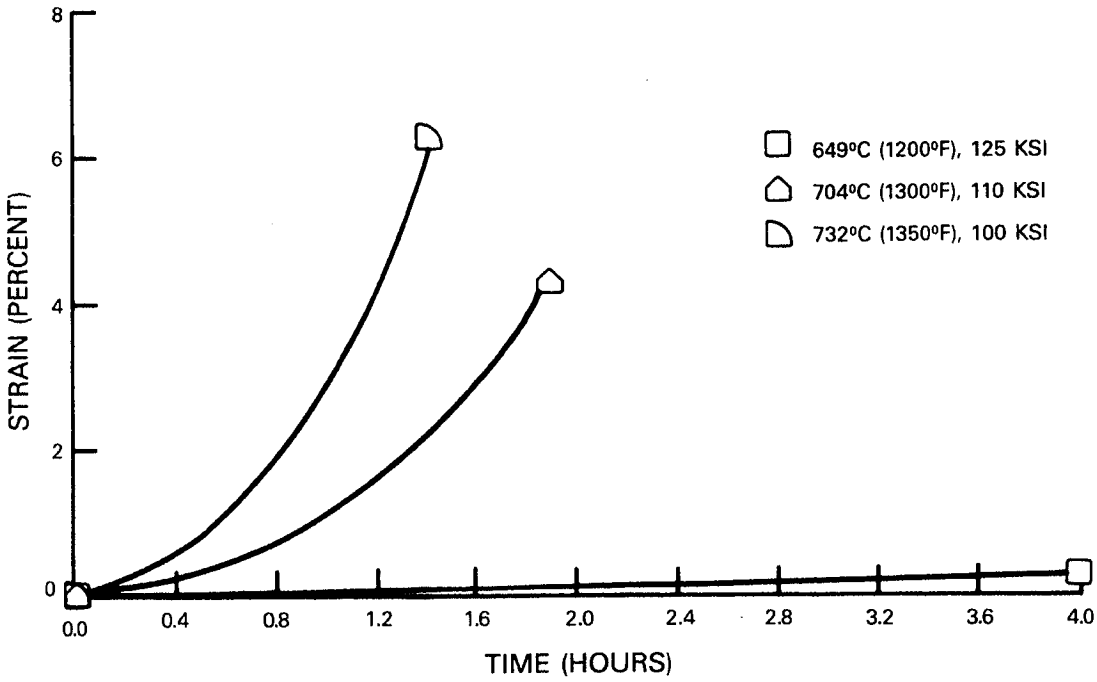

Figure 23.- INCO 718 Testing - High Stress Tests.

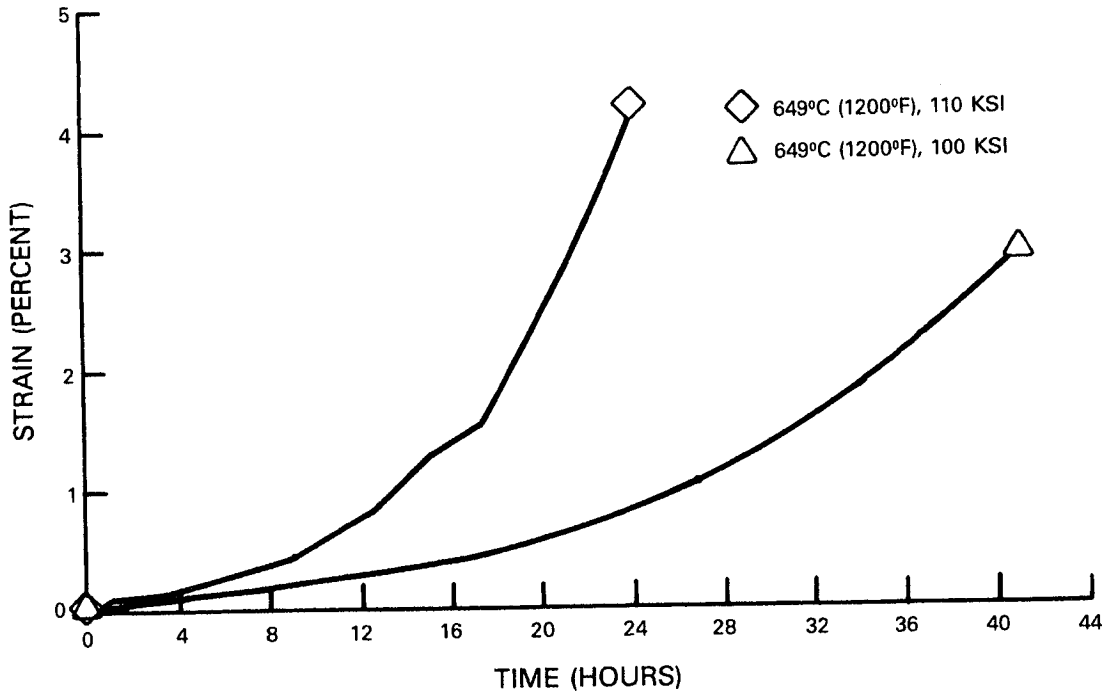

Figure 24.- INCO 718 Testing - Moderate Stress Tests.

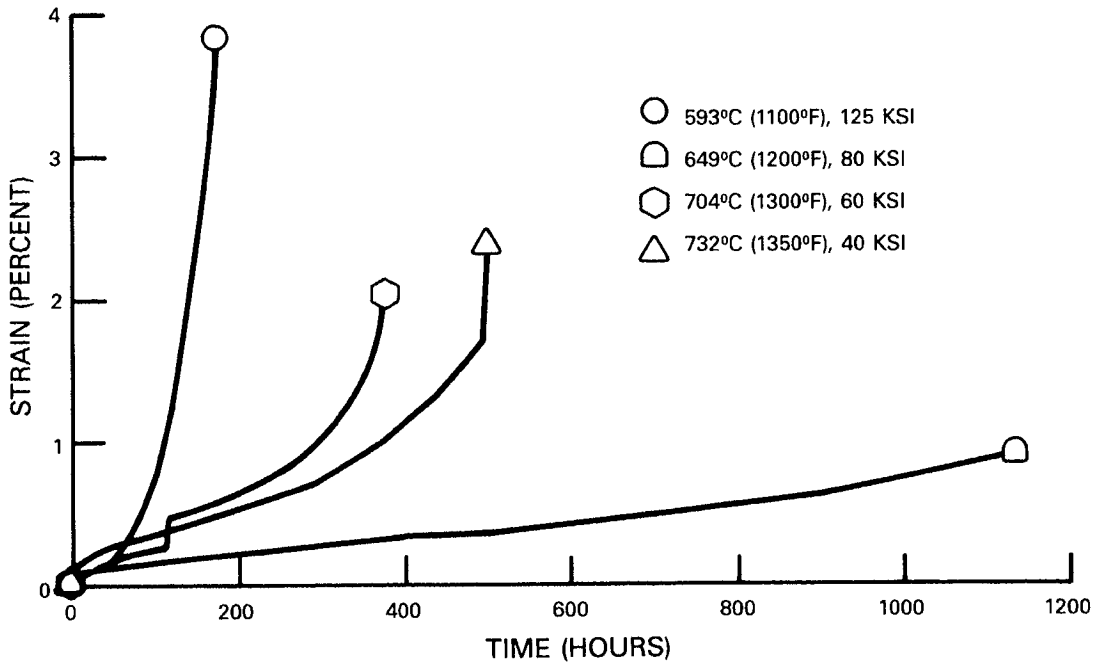

Figure 25.- INCO 718 Testing - Long Life Tests.

IN 718 Cyclic Mean Stress Testing

As part of the testing to be completed under this task, a series of 20 isothermal strain range - mean stress experiments was performed on INCO 718 specimens at the University of Rhode Island (URI) labs. The conditions for these tests were chosen to complement the isothermal test matrix completed at the P&W lab, including several tests at 732°C (1350°F). These high temperature tests were necessary to obtain creep-fatigue interaction data, since this particular heat of INCO 718 showed excellent creep resistance. Also, although this alloy is not normally used at temperatures in excess of 649°C (1200°F) due to its metastable microstructure, understanding the alloy behavior at higher temperatures for certain applications was desired. Specimen 583 was run at 732°C (1350°F), 0.68% strain range, 300 cpm, and zero mean stress as a check of the experimental set-up at URI relative to the P&W lab set-up. Its separation life was 6400 cycles, which compares well with the fully reversed tests completed earlier at P&W under strain control. Tests at 649°C (1200°F) and 732°C (1350°F) showed significant interaction between creep and fatigue. A summary of the results for this series of tests are shown in Table VIII; detailed test data may be found in Appendix F.

IN 718 Thermal-Mechanical Cycling

Various thermal-mechanical test cycles (out-of-phase, in-phase, clockwise, counter clockwise, and bow-tie) were run on IN718 at temperature ranges of 316-649°C (600-1200°F) and 316-732°C (600-1350°F). Details of the test conditions and specimen lives are given in Appendix D. The overall test matrix is shown in Table IX, and the individual tests are discussed below.

TABLE VIII.- MEAN STRESS TESTING - INCO 718

Spec ID	Temp °C	Temp (°F)	Strain Range (%)	Mean Stress (Ksi)	Cyclic Rate (CPM)	Initiation Life (Cycles)	Separation Life (Cycles)	Final Mean Strain (%)
582	732	1350	0.55	+20	30	20,786	26,995	0.23
579				+30		15,086	19,592	0.45
576				0		86,447	101,702	0.0
590				+40		4512	6446	0.84
592				+20	12.5	12,178	16,237	0.25
587				+30	12.5	3854	5586	0.55
554			0.55	0	30	81,312	96,800	0.0
583			0.68	0		4550	6500	0.0
589			0.65	+20		3112	4576	0.33
573			0.65	+30		1924	2915	0.46
558			0.80	+20		610	1017	0.87
566			0.80	+30		308	541	2.08
559			1.00	+20		179	332	3.38
588	649	1200	0.55	+60	30	16,077	20,879	0.81
578			0.55	+30		63,388	78,257	0.22
551			0.65	+30		6397	8645	0.36
567			0.65	+50		3884	5321	1.21
563			0.65	+60		3590	4986	2.30
570			0.80	+50		719	1058	6.54
575			0.80	+30		1663	2375	1.04

TABLE IX.- INCO 718 TMF TEST MATRIX

Temp °C	Range (°F)	σ/ϵ Limits (Ksi/%)	$\Delta\epsilon$ (%)	R_ϵ	CYCLE TYPE Out-of-Phase Spec. ID	Ni	In Phase Spec ID	Ni	CW Spec ID	Ni	CCW Spec ID	Ni
316 – 649												
(600 – 1200)		±.325	.65	-1	1T	12311e	3T	15641	8T	16614e	7T	11435
↓		±.400	.80	-1	2T	3008	4T	4186				
–		±.500	1.00	-1	9T	1704	10T	518				
		-60,+90	.65	n.a.			19T	3084				
316 – 732												
(600 – 1350)		±.275	.55	-1	11T	7969	12T	18939				
↓		±.325	.65	-1	5T	1251	6T	2946	17T	6022	18T	19296e
–		0,+.65	.65	0	15T	3349						
		-.65,0	.65	-∞	16T	2450						
		±.400	.80	-1	13T	2196	14T	558				
		-65,+65	.55	n.a.			20T	8229				

IN 718 TMF Testing at 316-649°C (600-1200°F)

Cycle I (Out-of-Phase)

Specimen 718-1T was tested using a strain range of 0.65%, R = -1. It failed at the button head after 10.964 cycles. Its initiation life was estimated by replica data to be 12,311 cycles. Specimen 718-2T was tested using the same conditions but with a higher strain range of 0.80%, R = -1. Its initiation and separation lives were 3008 and 4487 cycles, respectively. Specimen 718-9T was tested at a strain range of 1.0%, R = -1. Its initiation and separation lives were 1704 and 2434 cycles, respectively.

Cycle II (In-Phase)

Specimen 3T was run at 316-640°C (600-1200°F), 0.65% strain range, 1 CPM, with in-phase strain-temperature cycling; the resulting initiation and separation lives were 15641 and 17001 cycles, respectively. Specimen 4T was run at the same conditions except with a strain range of 0.80%. Its lives were 4186 and 4983 cycles, respectively.

Specimen 10T was run using a strain range of 1.00%. Its initiation and separation lives were 518 and 740 cycles, respectively. These lives are considerably lower than those of specimen 9T which was tested using the same conditions but having a cycle I loading path. This difference in fatigue lives for in-phase and out-of-phase cycle types is in agreement with published observations and data from other researchers. Apparently this behavior occurs only at higher strain ranges.

Specimen 19T was tested using cycle II but under load control from -60 ksi to +90 ksi, giving a strain range of approximately 0.65%. Its initiation life was 3084 cycles.

Clockwise (CW) Cycle

Specimen 8T was tested using a clockwise cycle and a strain range of 0.65%. This specimen failed from a crack in the buttonhead fillet radius at 12,158 cycles, but surface replicas enabled estimation of the initiation and separation lives at 16,614 and 18,476 cycles, respectively.

Counter Clockwise (CCW) Cycle

Specimen 7T was run using the same conditions as for specimen 8T but with a counter clockwise cycle as opposed to a clockwise cycle. Its initiation and separation lives were 11,435 and 13,297 cycles, respectively.

Discussion of 316-649°C (600-1200°F) TMF Results

All four tests conducted at the low strain range have essentially the same life (total scatter less than 1.5X). The trends with cycle type observed during the PWA 1455 baseline testing was not seen for IN718 when tested under these conditions. This suggested that different mechanisms were responsible for the damage; likely this regime was dominated purely by transgrannular fatigue. It was expected that at higher temperatures, the cycle path dependence would be much greater.

IN 718 TMF Testing at 316-732°C (600-1350°F)

Cycle I (Out-of-Phase)

Specimen 11T was run at 316-732°C (600-1350°F), 0.55% strain range, R = -1, 1 CPM, and out-of-phase cycling. Its initiation and separation lives were 7969 and 9601 cycles, respectively. The intent of this test was to provide data at long life, high temperature conditions.

Specimen 5T was run using the same conditions as specimen 11T but at a higher strain range of 0.65%. Its initiation and separation lives were 1251 and 2779 cycles, respectively.

Specimen 13T was run at 316-732°C (600-1350°F), 0.80% strain range, R = -1, and 1 CPM, with out-of-phase strain-temperature cycling. Its initiation and separation lives were 2196 and 2852 cycles, respectively. Note that the lives of -13T are considerably higher than those of -5T, which was tested at the same conditions except at a lower strain range (0.65%).

Specimen 15T was run at 316-732°C (600-1350°F), 0.65% strain range, R=0, and 1 CPM, with out-of-phase strain-temperature cycling. Its initiation and separation lives were 3349 and 4084 cycles, respectively. Specimen 16T was run at the same conditions, except with R=-infinity cycling. Its intiation and separation lives were 2450 and 4152 cycles, respectively. Comparison of these results with those from -11T and -13T suggest that the R=-1 initiation life at 0.65% should in fact be much higher than the 1251 cycles seen from specimen -5T.

Cycle II (In-Phase)

Specimen 12T was run at 316-732°C (600-1350°F), 0.55% strain range, R=-1, 1 CPM, with in-phase, strain-temperature cycling. The resulting initiation life was 18,939 cycles, and the test was discontinued at 20,586 cycles due to a crack in the buttonhead fillet radius. Note that this intiation life is more than double what was seen using out-of-phase cycling.

Specimen 6T was tested at a strain range of 0.65%, R=-1 and had an initiation life of 2946 cycles. The test was terminated because of failure from an I.D. initiated crack.

Specimen 14T was run using a strain range of 0.80%, R=-1 and had initiation and separation lives of 558 and 744 cycles, respectively.

Specimen 20T was run under load control from -65 to +65 ksi which resulted in a strain range of approximately 0.55%. Its initiation life was 8229 cycles.

Clockwise (CW) Cycle

Specimen -17T was run at 316-732°C (600-1350°F), 0.65% strain range, R=-1, and 1 CPM, with clockwise elliptical strain-temperature cycling. Its initiation and separation lives were 6022 and 7821 cycles, respectively.

Counter Clockwise (CCW) Cycle

Specimen -18T was run at the same conditions as specimen 17T , except with counter clockwise strain-temperature cycling. It was cycled for 18,554 cycles, at which time the IRCON infrared pyrometer was accidentally bumped, resulting in the specimen melting. Based on the available replica data before this incident, the initiation and separation lives was estimated as 19,296 and 26,060 cycles, respectively.

Discussion of 316-732°C (600-1350°F) TMF Results

Comparison of the results for the various cycles at a strain range of 0.65% showed that there was a significant difference in lives for the various cycle types at this higher temperature range. In particular, CCW cycling resulted in a significant life increase. These effects were not observed in the 316-649°C (600-1200°F) temperature range, indicating that cycle path effects are strongly dependent on the mechanisms active under these conditions.

Bowtie Cycle

Two TMF experiments were designed to produce constitutive behavior data regarding the effects of temperature rates of opposite signs on a constant positive strain rate. This was achieved using the strain-temperature cycle shown in Figure 26, which has come to be known as a "bow tie" cycle. Two and a half rapid cycles were used at both the minimum and the maximum temperature levels in the cycle to reset the specimen equilibrium stress and to leave the specimen in compression to begin the slow strain rate excursion in the positive direction. A cycle period of 3 minutes was used for all strain ranges, giving one minute for each of the slow positive ramps and twelve seconds for each rapid cycle. Specimen -21T was run using this cycle at 316-649°C (600-1200°F) at various strain ranges from 0.3%-0.8%, all at R=-1. Figure 27 shows the results of this experiment at the 0.8% strain range. It appeared that reversing the sign of the temperature rate had very little effect on the material behavior; the greatest effect was clearly temperature level, not temperature rate. Specimen -22T was run at the same conditions except using 316-732°C (600-1350°F). Figure 28 shows these results, which are similar to those from -21T. Both of these tests were terminated after about 40 cycles were accumulated, since no meaningful life results could be expected. These data can be used to guide constitutive model development for this alloy.

Isothermal Fatigue Testing

Thirty specimens were tested; details of the tests are provided in Appendix C. The overall test matrix for the isothermal INCO 718 testing is shown in Table X, and the details of each of the tests are discussed below.

Isothermal Tests at 649°C (1200°F)

Two isothermal uniaxial specimen tests were conducted at 649°C (1200°F), using a cyclic rate of 30 cpm. Specimen 718-11 was tested at a strain range of 0.65%, R=-1, and its initiation and separation lives were 9633 and 13762 cycles, respectively. Specimen 718-12 was tested at a strain range of 0.80%, R=-1, with resulting initiation and separation lives of 2702 and 4323 cycles, respectively. These lives were very similar to those from other tests conducted at 1 CPM, indicating that rate dependence is not important for this material at 1200°F until very long cycle times are used.

Specimen 718-22 was tested at 649°C (1200°F) and 1 cpm but with a total strain range of 1.0% (R=-1) to provide data in the low life, high inelastic strain regime.

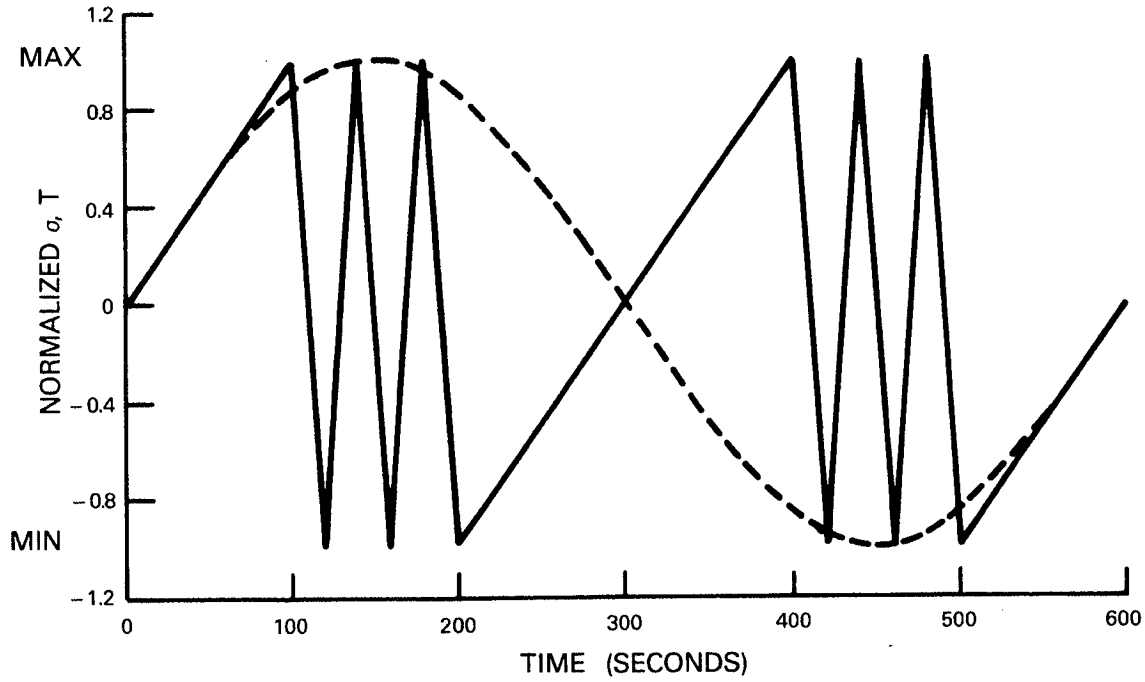

Figure 26.- Strain-Temperature-Time Cycles for INCO 718 TMF Constitutive Tests ("Bow Tie").

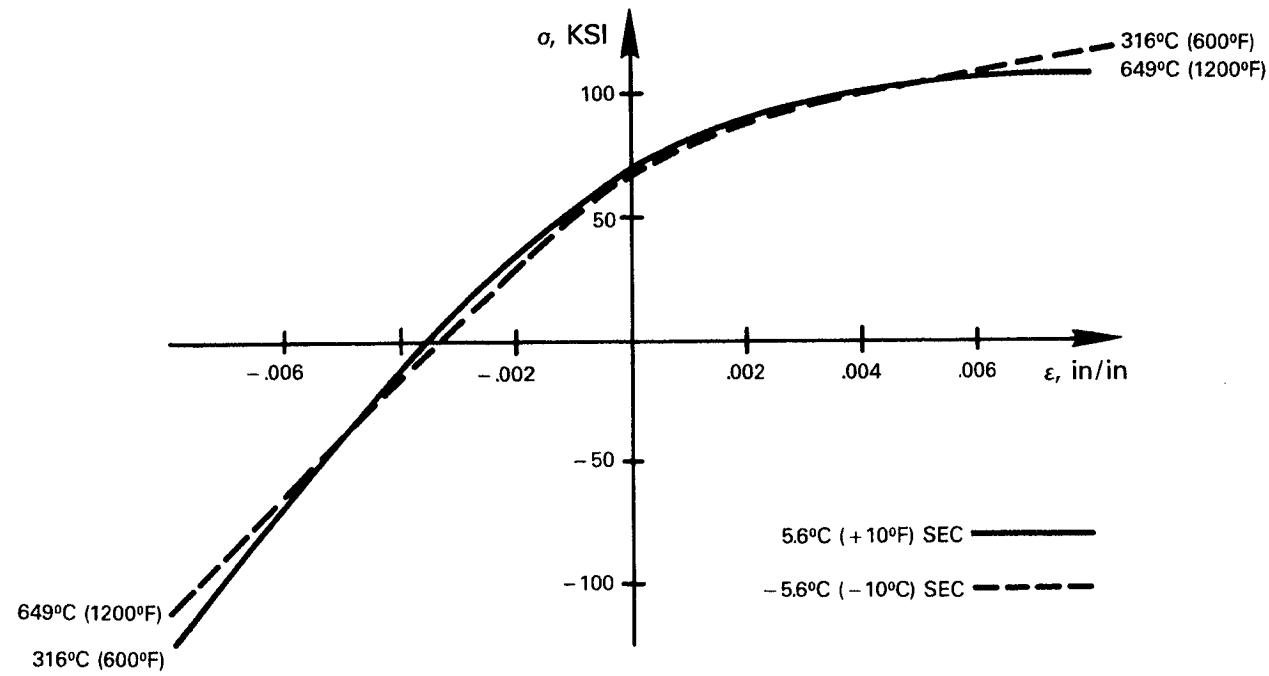

Figure 27.- INCO 718 Constitutive Response During "Bow Tie" TMF Test - 316-649°C (600-1200°F), $\dot{\epsilon} = 2.7 \times 10^{-4}$ sec^{-1}.

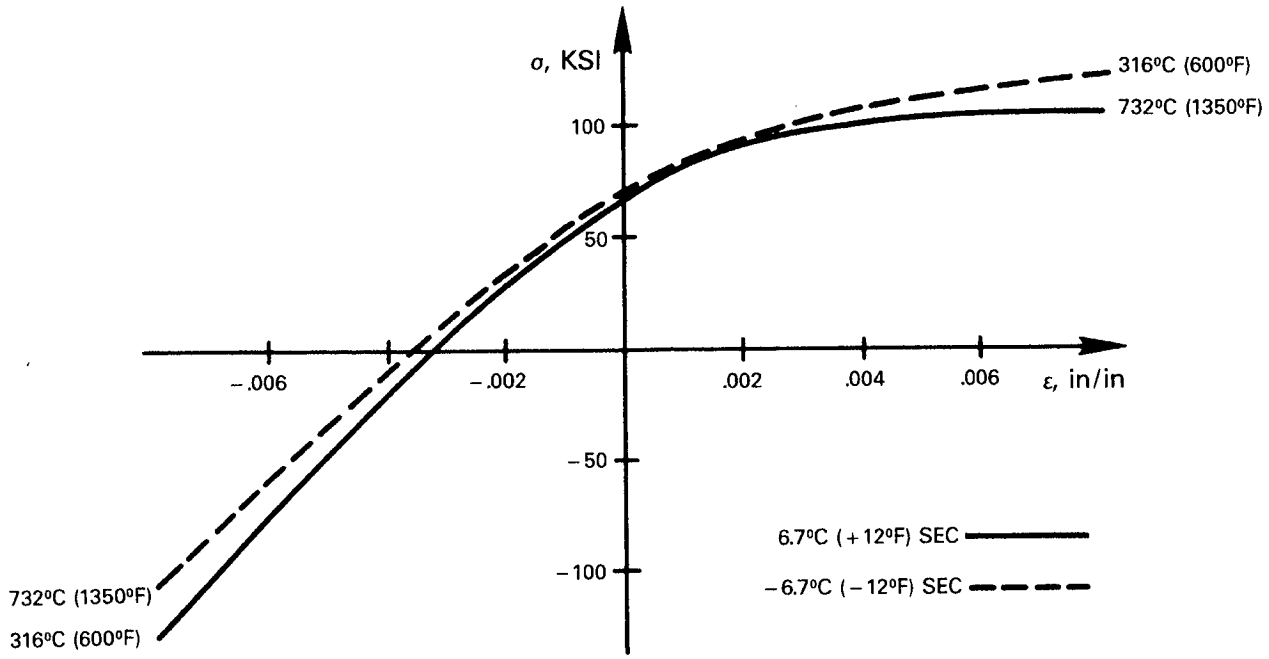

Figure 28.- INCO 718 Constitutive Response During "Bow Tie" TMF Test - 316-732°C (600-1350°F), $\dot{\epsilon} = 2.7 \times 10^{-4}$ sec^{-1}.

TABLE X.- MATRIX FOR INCO 718 ISOTHERMAL TESTING

Temp-$\Delta\epsilon$	Continuous Cycles (freq.- R-ratio)						Hold Time Cycles (minutes-Tens/Comp)			
	←30 CPM→			← 1CPM →						
(°C - %)	0	-1	-∞	0	-1	-∞	1-T	1-C	15-T	15-C
316-0.65	30	15								
-0.80		16								
-1.00		17								
482-0.65		13								
-1.00		14								
649-0.65	27	11	28		4		5,31[2]			
-0.80		12			3				8	9
-1.00		18			22					
732-0.55		25								
-0.65		19		26	2	10	6	7		
-0.80		20,29[1]				1				
-1.00		21			23					

Notes: 1. Specimen #29 was run at 732°C, 0.40%, R=0, with one minute tension hold for 1194 cycles before being run to completion at the conditions shown.

2. Specimen #31 was run at R=0 instead of R=-1.

Isothermal Tests at 732°C (1350°F)

Specimen 718-26 was tested at 732°C (1350°F), 0.65% strain range, R=0, and 1 CPM. Its initiation and separation lives were 3526 and 4521 cycles, respectively, which are about 70% of the lives seen under the same conditions but with R=-1 (specimen 718-2).

To investigate low strain range, high temperature behavior, specimen 718-25 was run at 732°C (1350°F), 0.55% strain range, R=-1, and 30 CPM. The resulting initiation life was 169,670 cycles. The test was discontinued at this point because of the extremely slow crack growth rate. This represented slightly more than 94 hours of test time, so microstructural changes may have been occurring during this test.

Two specimens were tested at 732°C (1350°F), 1.00% strain range, R=-1, to provide data in the low life, high inelastic strain regime at the higher temperature. Specimen 718-21 was tested at 732°C (1350°F) and 30 CPM to provide baseline pure fatigue data; its initiation and separation lives were 636 and 1115 cycles, respectively. Specimen 718-23 was run at 732°C (1350°F) and 1 CPM, and its initiation and separation lives were 437 and 590 cycles.

Isothermal Test at 649°C (1200°F) With Hold Times

Specimen 718-5 was tested at 640°C (1200°F), 0.65% strain range, R=-1, with a one minute hold in tension at +0.325%. The cyclic portion of the strain cycle was run in 6 seconds (10 CPM rate). The initiation and separation lives were 10593 and 13668 cycles, respectively. This indicated that the effect of the hold was minimal, since these lives were essentially the same as those from a specimen run at the same conditions, except at 1 cpm continuous cycling.

Specimen 718-8 was tested at 649°C (1200°F), 0.80% strain range, R=-1, with a 15 minute hold in tension at +0.40%. The cyclic portion of the strain cycle was run in 6 seconds (10 CPM rate). The initiation and separation lives were 572 and 689 cycles, respectively. This suggested that the effect of this long hold is pronounced at this temperature, since these lives are approximately 4X lower than those from the specimen run at the same conditions, except at 1 CPM continuous cycling (specimen 718-3).

Specimen 718-9 was tested using the same conditions as 718-8, although in this case, a compression hold was used. This test had initiation and separation lives of 1115 and 1751 cycles, respectively.

Isothermal Tests at 732°C (1350°C) With Hold Times

Specimen 718-6 was tested at 732°C (1350°F), 0.65% strain range, R=-1, with a one minute hold in tension at +0.325%. The cyclic portion of the strain cycle was run in 6 seconds (10 CPM rate). The initiation and separation lives were 1531 and 2219 cycles, respectively. This suggested that the effect of the hold is quite pronounced at this temperature, since these lives are roughly one-third of those from the specimen run at the same conditions, except at 1 CPM continuous cycling (specimen 718-2). Note that the total time per cycle is nearly the same for these two tests.

The second specimen test, specimen 718-7, was conducted at the same conditions used for 718-6, except that the hold was in compression (-0.325%) instead of tension. The initiation and separation lives were 1318 and 3012 cycles, respectively, which are very similar to those from the previous test.

Specimen 718-29 was meant to be run at 732°C (1350°F), 0.8% strain range, R=-1, with a one minute hold in tension; however, it was inadvertently started at 0.4%, R=0. This oversight was discovered at 1194 cycles, and it was decided at that point to switch to 0.8%, R=-1, without the one minute tension hold. Another 3240 cycles were then completed under these conditions before separation occurred, with a 0.030-in. crack being observed at the 2000 cycle mark. The earlier experiment at these final conditions was specimen 718-20, which had initiation and separation lives of 2312 and 3612 cycles, respectively. This indicated a much smaller cumulative damage effect due to the prior cycling than was expected; the creep damage resulting from the prior tension hold cycling was calculated to be very large (normalized value of about 1.2).

Microstructural Evaluations

In order to evaluate the effects of exposure to 732°C (1350°F), microhardness measurements were made on IN 718 (alternative material) in the as-received condition and on four samples after fatigue testing, specimen 718-1 732°C (1350°F), ϵ_{min} = -0.4%, ϵ_{max} = 0.4%, 1 cpm, 2939 cycles), specimen 718-2 732°C (1350°F), ϵ_{min} = -0.325%, ϵ_{max} = 0.325%, 1 cpm, 6506 cycles), specimen 718-3 649°C (1200°F), ϵ_{min} = -0.4%, ϵ_{max} = 0.4%, 1 cpm, 2868 cycles), and specimen 718-4 649°C (1200°F), ϵ_{min} = -0.325%, ϵ_{max} = 0.325%, 1 cpm, 13332 cycles). Four hardness measurements were made on each condition and the results are shown in Figure 29. It can be seen that increasing the fatigue test temperature decreases the hardness. Also, for a given temperature, longer exposure times also decrease the hardness but to a lesser extent as compared to the effect of increasing temperature. The change in the hardness of the material from the as-received condition was suspected to be the result of coarsening of the γ' and/or γ'' particles. Comparison of the hardness values for the as-received condition and the 649°C (1200°F) specimens (718-3 and 718-4) indicated that little or no change occurred in the microstructure as a result of the 649°C (1200°F) exposure. A more definite change in hardness was found between the as-received condition and the 732°C (1350°F) specimens (718-1 and 718-2), indicating that changes do occur in the microstructure as a result of the 732°C (1350°F) exposure. Based on these results, the IN 718 alternative material in the as-received and post-test conditions was also examined by TEM. The post-test sample chosen for examination was 718-2.

The strength of IN 718 is derived from the fine, disk shaped precipitate γ''. Due to the small size of these precipitates and coherency strain contrast effects, it was necessary to use dark field TEM techniques to image the γ''. The typical appearance of the γ'' precipitates in the as-received condition is shown in the dark field micrograph of Figure 30. The precipitates are $\sim$15 nm long by $\sim$4 nm thick. The typical appearance of the post-test material taken from specimen 718-2 is shown in Figure 31. The precipitates have become markedly larger, now measuring 130 nm long by 20 nm thick.

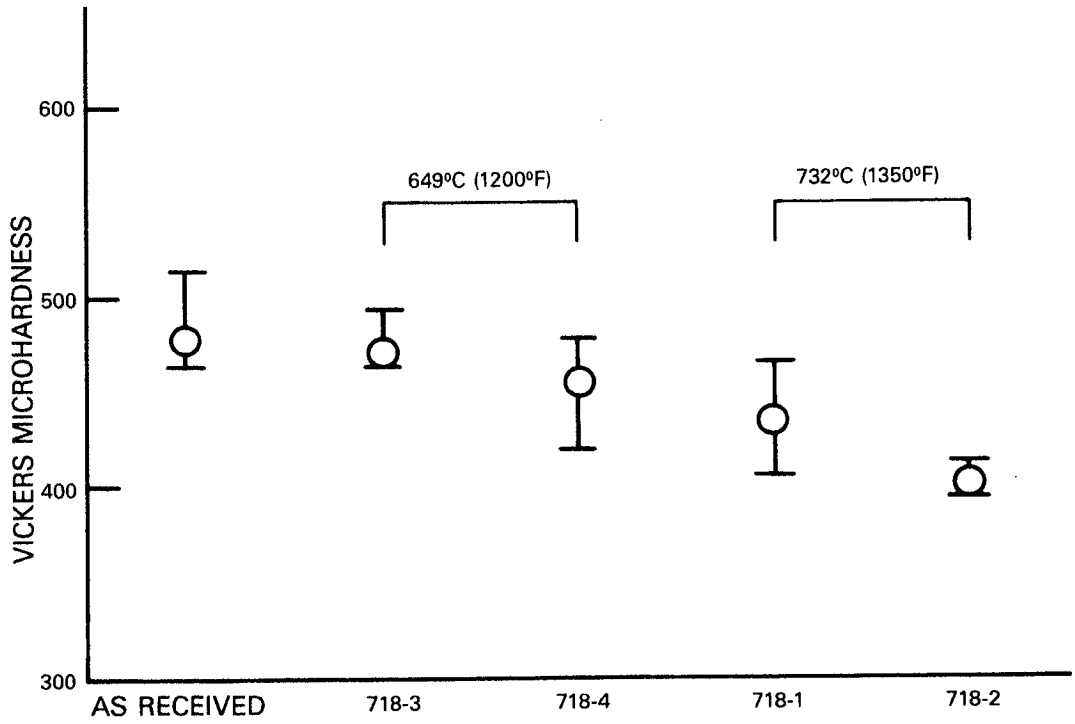

718-1 732°C (1350°F), ε_{MIN} = −0.4%, ε_{MAX} = 0.4%, 1 CPM, 2939 CYCLES
718-2 732°C (1350°F), ε_{MIN} = −0.325%, ε_{MAX} = 0.325%, 1 CPM, 6506 CYCLES
718-3 649°C (1200°F), ε_{MIN} = −0.4% ε_{MAX} = 0.4%, 1 CPM, 2868 CYCLES
718-4 649°C (1200°F), ε_{MIN} = −0.325%, ε_{MAX} = 0.325%, 1 CPM, 13332 CYCLES

Figure 29.- Vickers Microhardness Results for the IN 718 Material in the As-Received and Post-Test Conditions.

The increases in γ'' size observed after exposure to 732°C (1350°F) was consistent with the observations of a decrease in the post-test microhardness of specimen 718-2 as compared to the as-received condition (~475 Vickers as-received vs. ~425 Vickers post-test). These observations indicated that a loss of strength occurred in this material when tested for extended times at 732°C (1350°F).

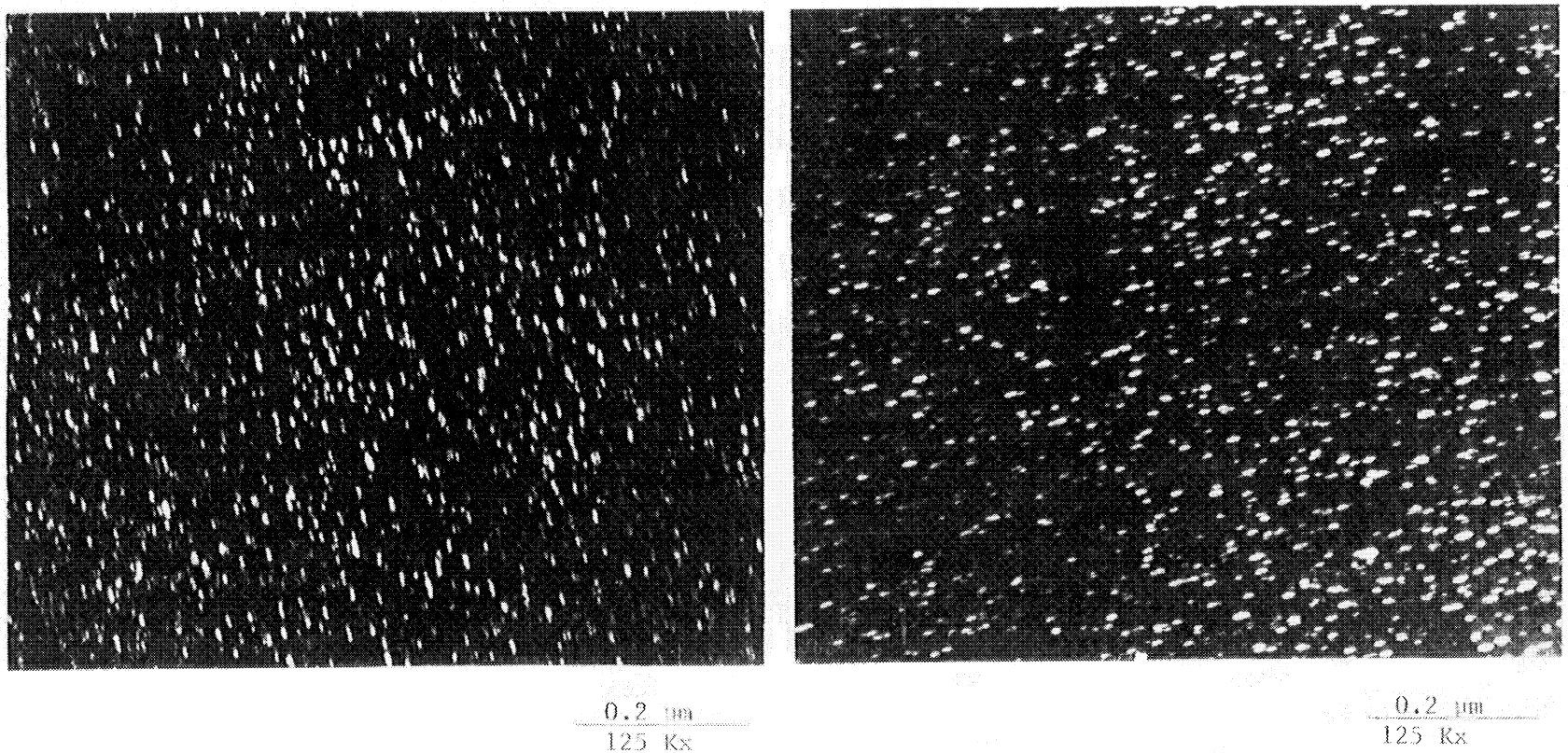

Figure 30.- Dark Field TEM Micrographs of γ'' Precipitates in IN718 in the As-Received Condition. Precipitates are ~15nm long by ~4nm thick. The two different orientations of γ'' shown here result from the use of different diffracted spots to form the images.

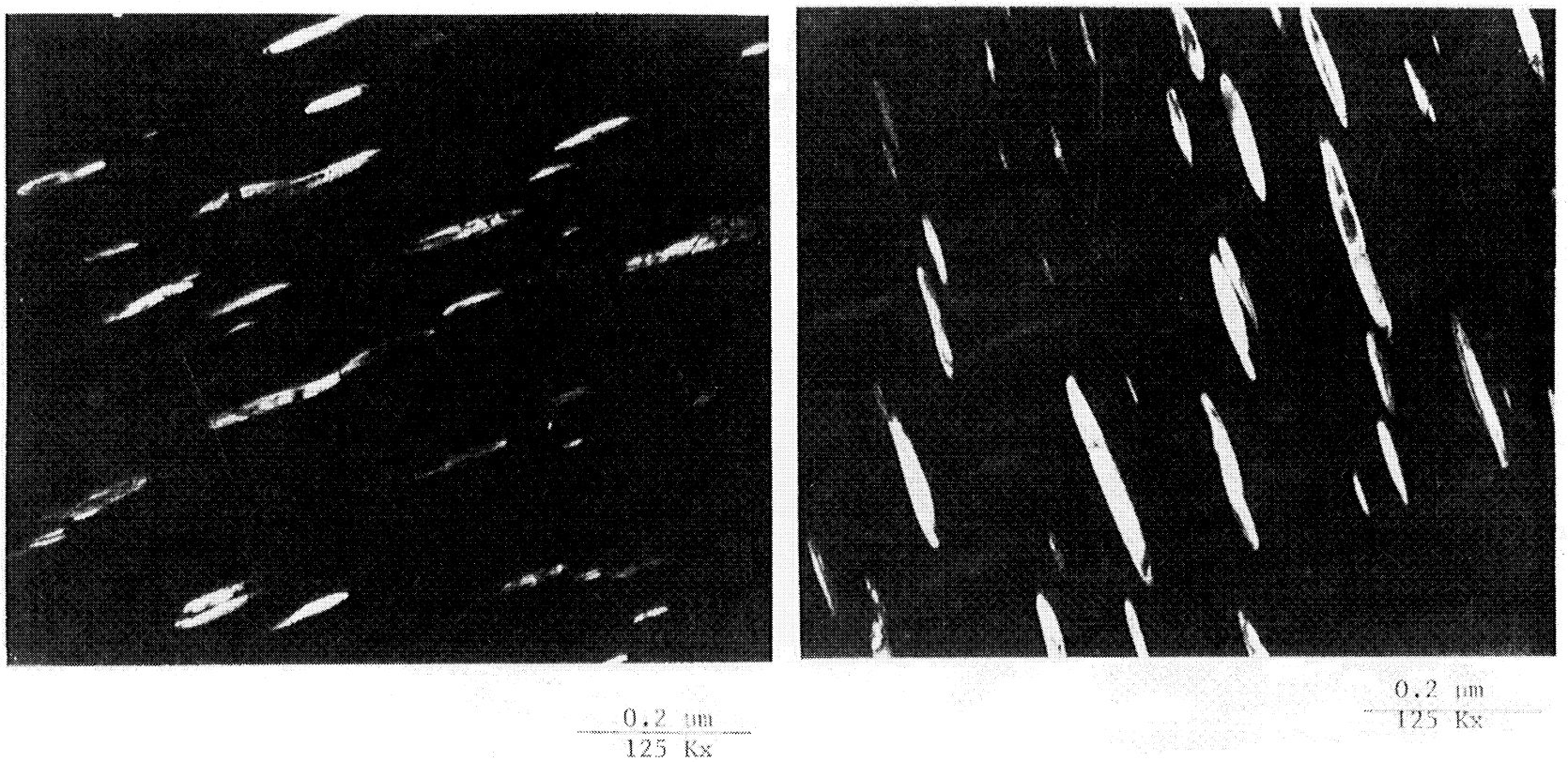

Figure 31.- Dark Field TEM Micrographs of " Precipitates in IN718-2 After Testing at 732°C(1350°F), $\Delta\epsilon$ = 0.65, R=-1, 1 cpm for 6506 Cycles. Precipitates are ~130nm long by ~20nm thick. The two different orientations of γ" shown here result from the use of different diffracted spots to form the images.

IN 718 Multiaxial Stress Testing

Table XI summarizes the test matrix and results for the 15 multiaxial specimen tests completed at the University of Connecticut under the direction of Prof. Eric Jordan. Figure 32 displays the Type I and Type II multiaxial waveforms as reported in Table XII. Detailed test data are given in Appendix E. During the multiaxial testing of the IN 718, a review of strip chart data of the load drop history revealed that the initially stated initiation lives required re-evaluation. The process of determining the revised initiation lives involved a finite element model of the test specimen with varying crack sizes. The results of the finite element analyses are for elastic conditions; however, during the stable load portion of these tests, only the local crack tip region experienced any significant plasticity. Therefore, for small cracks it was assumed that the local plasticity effects have a negligible effect on the total load drop. The analyses showed that a 1% drop in tensile load results from a crack size of 170 mils, whereas, an initiation crack of 30 mils represents a .035% load drop (which, of course, is too small to be measured directly). Replica data supported the finite element results for small cracks (less than 50 mils).

TABLE XI.- INCONEL 718 MULTIAXIAL TEST MATRIX

Conditions		Tension		Torsion		In Phase		Out-of-Phase		Type I		Type II	
$\Delta\epsilon_1$ (%)	Freq (CPM)	Spec ID	Ni (cycles)	Spec ID	Ni (cycles	Spec ID	Ni (cycles)	Spec ID	Ni (cycles)	Spec ID	Ni (cycles)	Spec ID	Ni (cyles)
0.325	30									309	8890	314	10000
0.400	30									313	4700	312	5206
0.400	1									311	4563	315	5000
0.650	30	307	5344	303	3975	301	3865	302	1700				
0.800	30			310	2220	308	3404	305	1682				
0.800	1					306	2069	304	484				

Notes: 1. Specimens 301-305 and 310 were run at 693°C (1280°F); all others were run at 649°C(1200°F).
2. All tests were run at $R_\epsilon = -1$
3. Tension-torsion tests were run at (torsion/tension), or γ_1, of 1.5.

A finite element model of the B1900+Hf test specimen revealed similar information to that of the INCONEL 718 model. It showed that circumferential crack lengths of 30 mils do not produce a measurable elastic tensile load drop. It was observed that the B1900+HF specimen load drop grew at a more appreciable rate than that of the INCONEL 718 specimen. However, the finite element results only considered elastic load drop and thus ignored the importance of plastic load relaxation.

A computer program was written to determine crack initiation based on load drop data from the multiaxial test rig. Using the strip chart data, several data points were recorded prior to and during the onset of measurable tensile load drop. The algorithm then splined this data and interpolated them to predict load drop as a function of number of cycles. The intent was to find the location of .05% load drop and define this point as the initiation life.

However, the algorithm proved to be incapable of reliably calculating this life, and consequently, manual measurement was adopted as a substitute method of measurement.

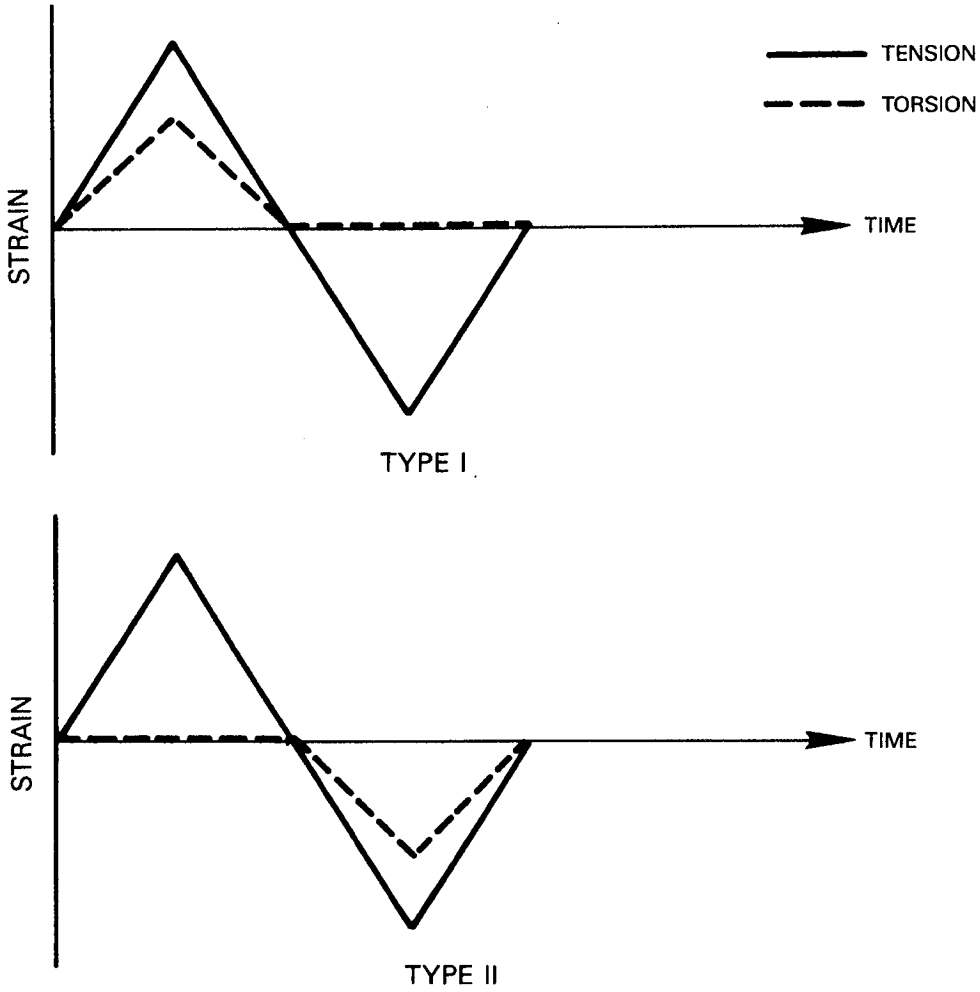

Figure 32.- Type I and II Waveforms.

After completion of the multiaxial testing, an error was discovered in the test setup for some of the UCONN multiaxial specimens; specimens 309, 311, 312, 313, 314, and 315. The problem occurred with the special 'TYPE I' and 'TYPE II' tests which were intended to show the effect of tension with torsion versus compression with torsion. However, these multiaxial tests were run opposite to the format intended. The 'TYPE I' test was actually run with a fully reversed cyclic axial load with torsion applied only when the specimen was in tension. The 'TYPE II' test was similar with the exception of the torsion applied only during the compression part of the axial cycle. The torsion waveform was triangular for one-half period and flat zero for the remaining one-half period. Figure 32 shows the wave forms as tested.

It was planned to conduct multiaxial fatigue testing at 649°C (1200°F). However, part way through this series of tests, recalibration of the temperature sensor, an infrared IRCON unit, using both an optical 'hot wire' pyrometer and thermocouples revealed that the first seven of fifteen tests were actually conducted at approximately 693°C (1280°F) rather than the proposed 649°C (1200°F). Rigorous calibration of the extensometer and load cells showed there were no loading discrepancies. Final correlation of the life data from these tests accounted for this temperature variation.

The first of seven specimens tested at 693°C (1280°F) specimen was tested under proportional biaxial conditions using ±.245% axial strain, ±.368 torsional strain, in-phase, and 30 CPM. Its initiation life was approximately 4100 cycles, and the separation life was 7006 cycles. The second specimen was tested with non-proportional biaxial loading at ±.325% axial strain, ±.488 torsional strain, 90° phase angle, and 30 CPM. Its initiation life was approximately 2000 cycles, and the separation life was 3650 cycles. The third specimen was tested in pure torsion using ±.650 torsional strain at a 30 CPM rate. Its initiation life was approximately 4600 cycles, and the separation life was 5362 cycles.

Tests on the fourth and fifth specimens were conducted using non-proportional biaxial conditions at a higher maximum normal strain than was used for the second test. The fourth specimen was tested at ±.400% axial strain, ±.600 torsional strain, 90° phase angle, and 1 CPM. Its initiation life was approximately 600 cycles, and the separation life was 831 cycles. The fifth specimen was tested at the same conditions, except at a rate of 30 CPM; its initiation life was approximately 1800 cycles, and the separation life was 1863 cycles. These results compared favorably to those of the second test, in that the lives followed expected trends of decreasing life with decreasing cyclic rate or increasing maximum normal strain.

The sixth specimen was tested in pure torsion using ±.800 torsional strain and 30 CPM. Its initiation life was approximately 3400 cycles, and the separation life was 3691 cycles. The third specimen was tested with similar conditions but at a lower maximum normal strain. For direct comparison with baseline axial test data, the seventh specimen was tested using only ±.325% axial strain at a rate of 30 CPM. Its initiation life was approximately 6300 cycles, and the separation life was 8900 cycles.

These multiaxial stress tests conducted on seven specimens at 693°C (1280°F) yielded results which were generally lower than expected based upon the results of previous uniaxial INCO 718 high temperature specimen tests. Although there were no strong reasons to discount the validity of these tests, microstructural studies were conducted. One area of particular concern was the effect of the black paint used for temperature measurement on the local stress/strain conditions and the surface finish.

It is believed that the high emissivity paint used on the gage sections of the specimens caused an effective tensile mean stress beneath the paint spot due to the temperature difference between the black painted spot and the shiny surface of the specimens. A temperature difference of 19°C (35°F) was measured with thermocouples. This effective mean stress caused by the paint may essentially creep away for high strain tests, but the lower strain tests of 0.65% maximum normal strain showed no frequency effects at 649°C (1200°F) for in-house testing, and hence the mean stress would likely remain at this lower strain range. Specimens 1, 2, 3 and 7 all propagated cracks through the painted area, while specimens 4 through 6 did not. Optical examination of specimen 1 showed that initiation began in the paint.

The eighth specimen was tested at conditions similar to the first specimen with the only difference being in maximum strain range. Problems encountered with temperature measurement during the initial IN 718 multiaxial testing were corrected and this and subsequent tests were run at 649°C (1200°F). Specimen 8 was run with $\pm$.302% axial strain and $\pm$.453% torsional strain. The approximate initiation of 4680 cycles was higher than that of the first specimen; however, this test was run at a temperature of about 42°C (75°F) lower. In addition, it was felt that at the lower strain range the temperature difference between the black paint spot and the surrounding metal caused an effective mean stress which lowered the life of the specimen.

The ninth specimen was tested at conditions similar to the specimen 8 with the only difference being in frequency. Specimen 9 was run at 1 cpm and showed about a 2X reduction in life due to creep effects. The initiation life was approximately 2400 cycles. The results of these tests compared well to the results of in-house INCO 718 specimen data.

Fifteen INCONEL multiaxial specimens were analyzed to determine the plane in which the maximum normal strain resides through the use of an algorithm which reads data from DASH to calculate pertinent physical loading parameters. The results revealed that the maximum normal strain range changes significantly as the phase difference between the two strain cycles changes. In particular, the 90° out-of-phase tests were run at significantly higher maximum normal strain ranges than the corresponding in-phase tests. Although review of the data is not yet complete, the results of the INCO 718 tests now appear to be plausible when plotted against maximum normal strain range. Also, both UCONN and P&W data for INCONEL 718 showed that at 649°C (1200°F) for tests with increasing amounts of plasticity, the damaging effects of lower frequency become more and more significant. At maximum strain ranges of 0.65%, frequency effects are negligible, whereas for 0.8% and 1.2%, the life debits caused by a 1 CPM versus a 30 CPM test were 2:1 and 3:1, respectively.

Multiaxial as well as uniaxial specimen data can be analyzed using a computer program to calculate the orientation of the plane with the highest shear strain amplitude. The Inconel 718 multiaxial specimens at the University of Connecticut were analyzed using this program for maximum shear strain amplitude. In order to provide accurate initiation life data, detailed measurements of the primary crack orientation were made for specimens 312, 314, and 315.

The crack of specimen 312 ran at an angle of 15° off the horizontal axis. Similarly, the specimen 315 crack grew at an angle of 16°. However, the crack of specimen 314 ran parallel to the horizontal direction; thus, both the axial and torsional loads showed negligible changes until crack lengths reached significant dimensions. For example, a crack length of .880 inch was recorded at 22963 cycles yet no measurable load drop was observed.

Revised 5%, 10% and 50% load drop data for specimens 301 to 304 and 306 to 308 were measured using strip charts of tensile and torsion load. Specimen 305 was accidentally overloaded when the test was restarted after taking a replica; thus, no load drop measurements were possible.

Fractography of Isothermal and TMF Tests on IN 718

SEM examinations were made of several IN718 fatigue specimens tested under isothermal and thermal mechanical fatigue (TMF) conditions. The purpose of this study was to determine if any major differences in crack growth mode existed between the various conditions tested. A summary of the test conditions and dominant crack propagation modes is presented in Tables XII and XIII.

TABLE XII.- ISOTHERMAL LCF TESTS

Specimen ID	Temperature °C	Temperature (°F)	Test Conditions (%)	R	Freq. cpm	Hold	Initiation Life	Separation Life	Dominant Crack Growth Mode
718-4	649	1200	0.65	-1	1	None	11,066	13,332	Transgranular
718-27	649	1200	0.65	0	30	None	7,608	10,011	Transgranular
718-2	732	1350	0.65	-1	1	None	4,719	6,506	Transgranular
718-26	732	1350	0.65	0	1	None	3,526	4,521	Transgranular
718-6	732	1350	0.65	-1	10	1 min	1,531	2,219	Transgranular
718-7	732	1350	0.65	-1	10	1 min	1,318	3,012	Transgranular

TABLE XIII.- THERMOMECHANICAL FATIGUE TESTS

Specimen ID	Temperature Range C°	Temperature Range (°F)	Test Conditions	R	Cycle	Initiation Life	Dominant Crack Growth Mode
718-3T	316-649	600-1200	0.65	-1	II	15,641	Transgranular
718-10T	316-649	600-1200	1.0	-1	II	518	Mixed, Predom. Trans.
718-6T	316-732	600-1350	0.65	-1	II	2,946	Transgranular
718-14T			0.80	-1	II	558	Mixed, Trans/Inter.
718-5T			0.65	-1	I	1,251	Transgranular
718-17T			0.65	-1	CW	6,022	Transgranular

Isothermal Tests at 649°C (1200°F)

Specimen 718-4 was tested at 649°C (1200°F), $\Delta\epsilon = 0.65$, R = -1, 1 cpm, initiation life = 11066 cycles, separation life = 13332 cycles. Optical examinations indicated that this sample had one major initiation site. A SEM micrograph showing the overall fracture surface appearance in this area is shown in Figure 33a. In the immediate vicinity of the initiation the fracture surface was relatively flat and featureless as shown in Figure 33b which is a more detailed view of the initiation site. Away from the initiation site the fracture surface became rougher and had a more faceted appearance. The morphology of the initiation area indicated transgranular growth. The typical appearance of the fracture in an area away from the initiation site is shown in Figure 33c. These areas showed cleavage facet formation as well as faint striations and appeared to be predominantly transgranular. There may be a limited amount of intergranular crack growth as well, the fracture surface oxide made it difficult to be certain. This oxide may also obscure the striations. The dominant crack growth mode was transgranular. Slip lines as well as a secondary crack were visible on the side surface of the specimen.

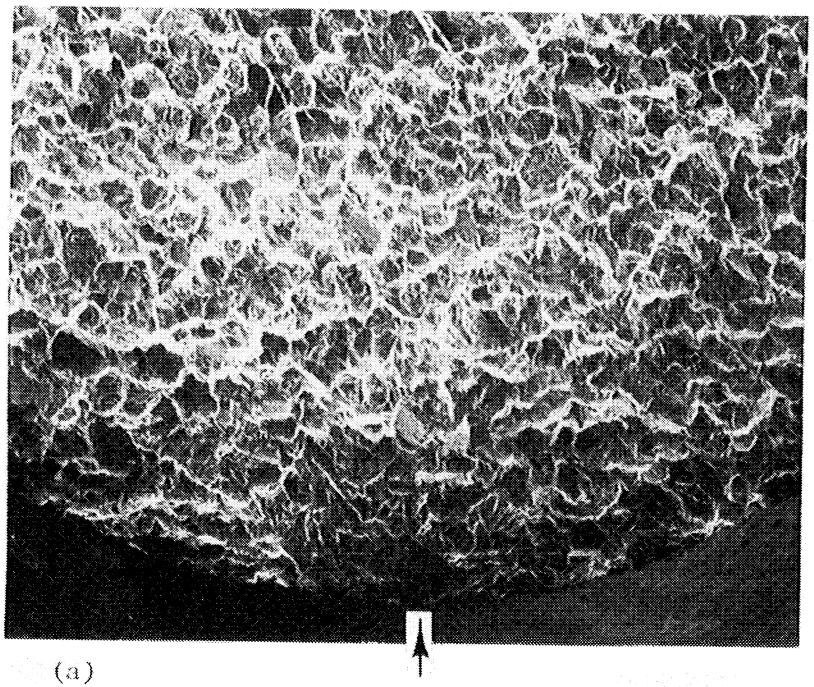

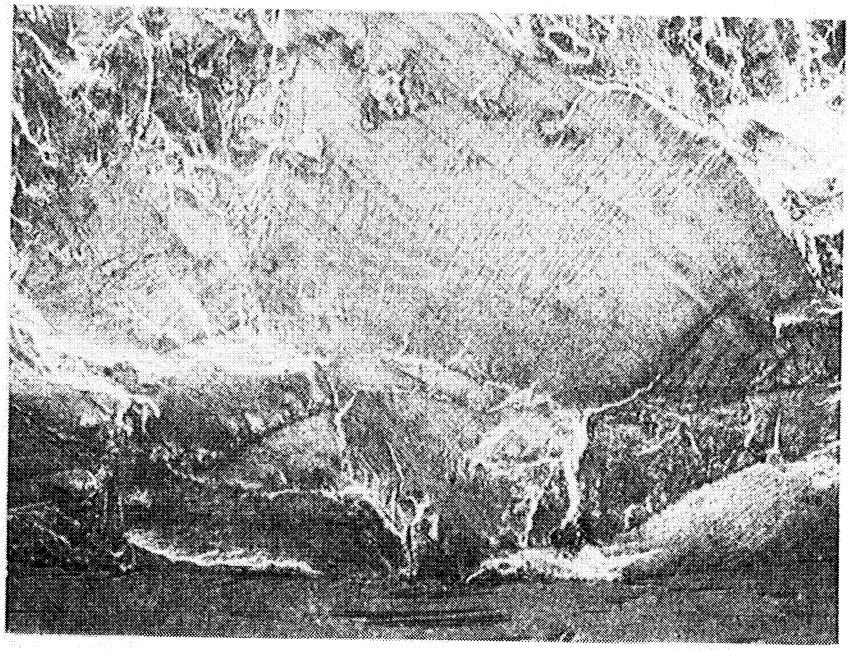

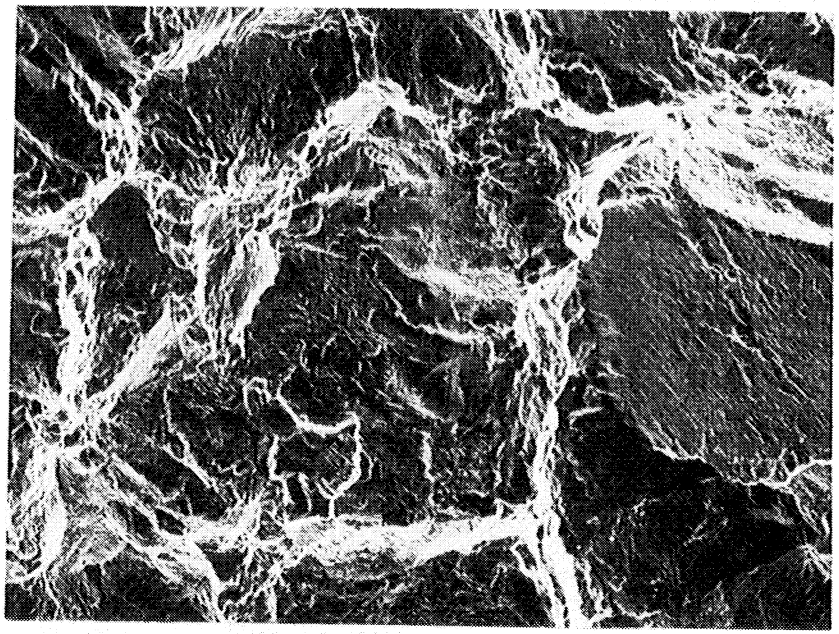

Figure 33.- Specimen 718-4. [649°C(1200°F), $\Delta\epsilon$ = 0.65, R=-1, 1 cpm, initiation life = 11066 cycles, separation life = 13332 cycles]

(a) General fracture surface appearance. Initiation site is indicated by arrow.
(b) Higher magnification of initiation site.
(c) Appearance of fracture in an area away from the initiation site.

Specimen 718-27 was tested at 649°C (1200°F), $\Delta\epsilon$ = 0.65, R = 0, 30 cpm, initiation life = 7608 cycles, separation life = 10011 cycles. The general fracture surface appearance of this specimen is shown in Figure 34a. Cleavage facets were evident on this specimen. The initiation area is shown in Figure 34b, and numerous striations can be seen. The crack growth mode in this area was transgranular. Figure 34c is from an area away from the initiation site and numerous, well defined striations are visible in this area. The dominant mode of fracture was transgranular. The amount of faceting on this sample was somewhat less than that of specimen 718-4.

Isothermal Tests at 732°C (1350°F)

Specimen 718-2 was tested at 732°C (1350°F), $\Delta\epsilon$= 0.65, R = -1, 1 cpm, initiation life = 4719 cycles, separation life = 6506 cycles. Optical examinations showed that the sample had one major and several minor initiation sites. A SEM micrograph of the overall fracture is shown in Figure 35a which shows that the immediate vicinity of the major initiation site is relatively flat as compared to the more faceted appearance of the rest of the fracture. A detailed view of the initiation area is shown in Figure 35b. Crack growth was transgranular in this region. Crack growth in regions away from the initiation, such as that shown in Figure 35c, appeared to be a mixture of transgranular and intergranular modes with the transgranular mode predominating. Striations were observed in various areas of the specimen but were always faint and ill defined, apparently a result of fracture surface oxidation. Slip lines were observed on the side surface of the specimen below the initiation site.

Specimen 718-26 was tested at 732°C (1350°F), $\Delta\epsilon$ = 0.65, R = 0, 1 cpm, initiation life = 3526 cycles, separation life = 4521 cycles. Numerous cleavage facets were visible on the fracture as shown in Figure 36a. The SEM micrograph of the primary initiation shown in Figure 36b revealed that a transgranular crack growth mode is operative in this region. An area of the fracture away from the initiation is shown in Figure 36c. It appeared from Figure 36c and Figure 36a that the predominant crack growth mode was transgranular with a few indications of intergranular growth in isolated areas. No striations were observed on the specimen, possibly due to the oxidation of the fracture surface. Slip lines were visible on the side surface of the specimen below the initiation site.

732°C (1350°F) Holdtime Tests

Specimen 718-6 was tested at 732°C (1350°F), $\Delta\epsilon$= 0.65, R = -1, 10 cpm, 1 minute tension hold, initiation life = 1531 cycles, separation life = 2219 cycles. Optical examinations showed that this sample had one primary initiation site. The fracture surface had a faceted appearance overall as shown in Figure 37a. The initiation site is shown in Figure 37b. This area had a faceted appearance and the crack growth mode was transgranular. As shown in Figure 37c, the appearance of the fracture in a region away from the initiation area showed that the crack growth mode appeared to be predominantly transgranular with some isolated areas of intergranular growth. Some faint striations were observed and others may have been hidden by the fracture surface oxide. Slip lines and a secondary crack were observed on the side surface of the sample below the initiation site.

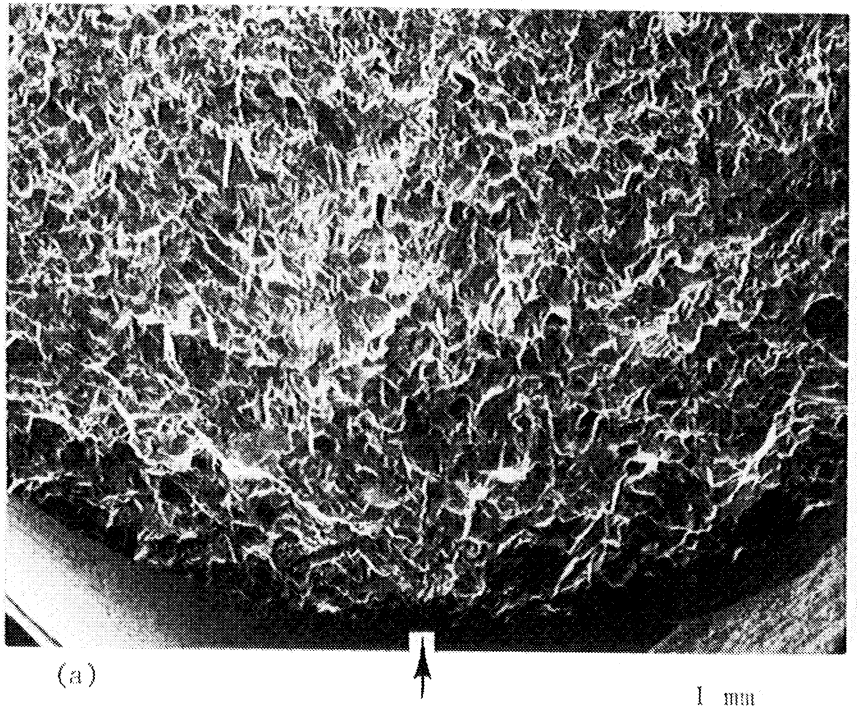

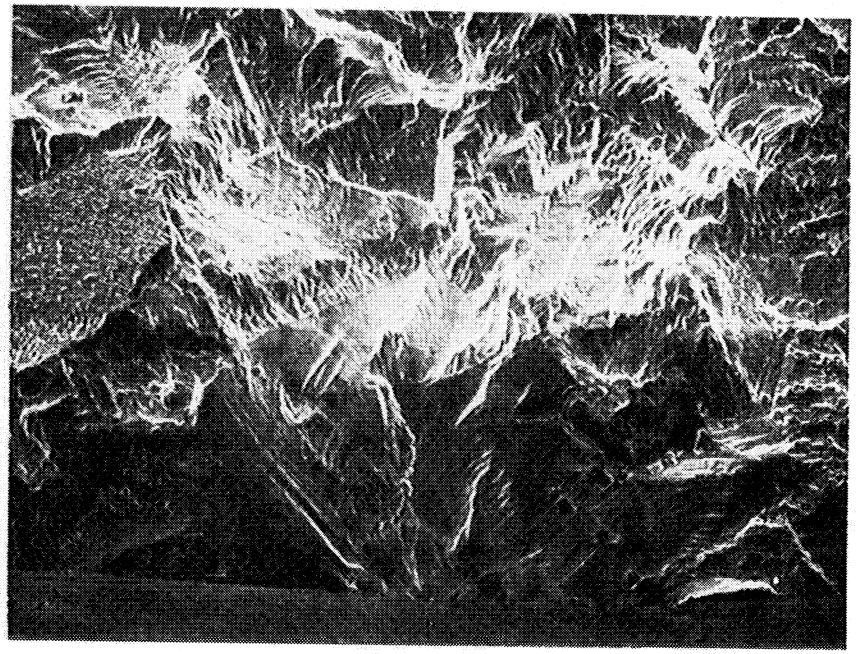

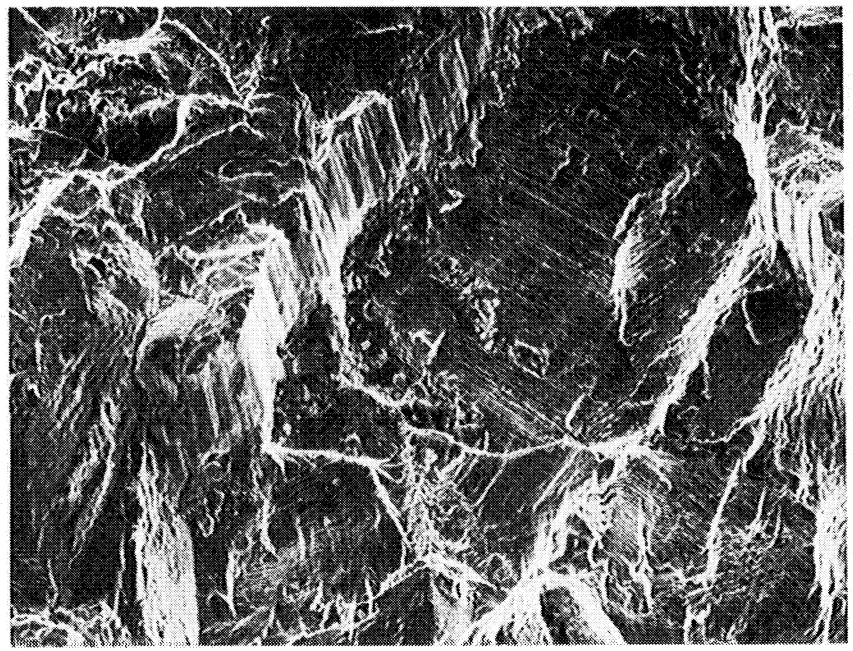

Figure 34.- Specimen 718-27 [649°C(1200°F), $\Delta\epsilon$ = 0.65, R=0, 30 cpm, initiation life = 7608 cycles, separation life = 10011 cycles].

(a) General fracture surface appearance. Initiation site is indicated by arrow.
(b) Higher magnification of initation site.
(c) Appearance of fracture away from initiation site. Numerous striations are visible in this area.

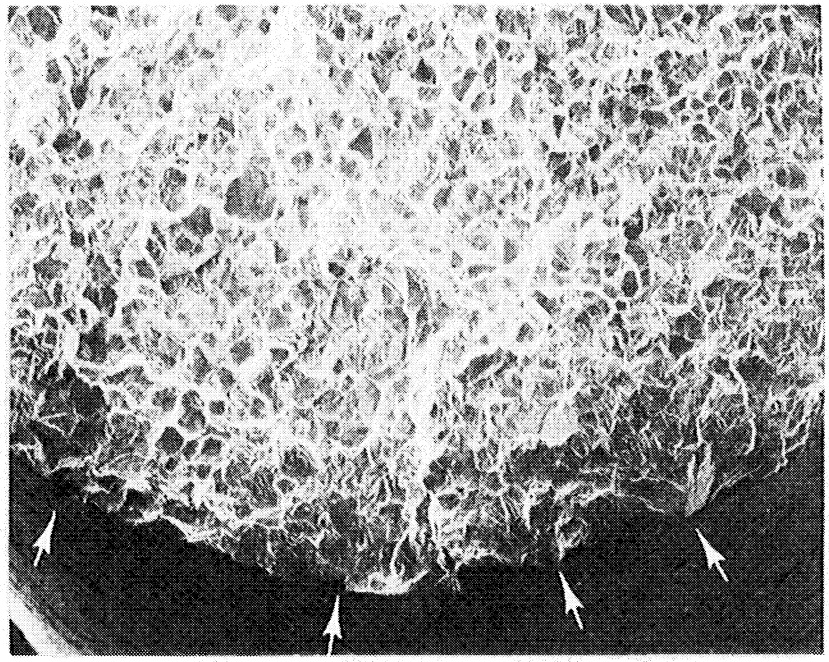

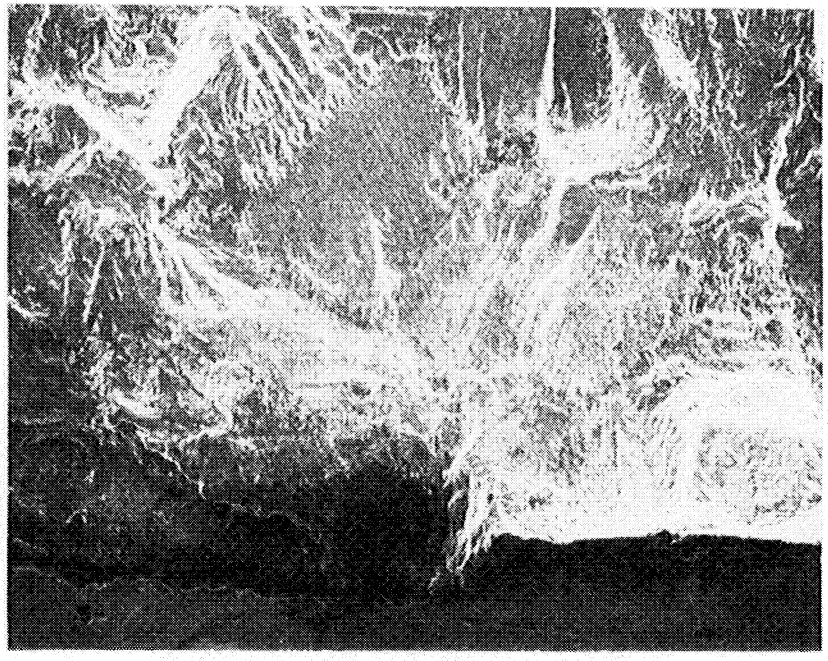

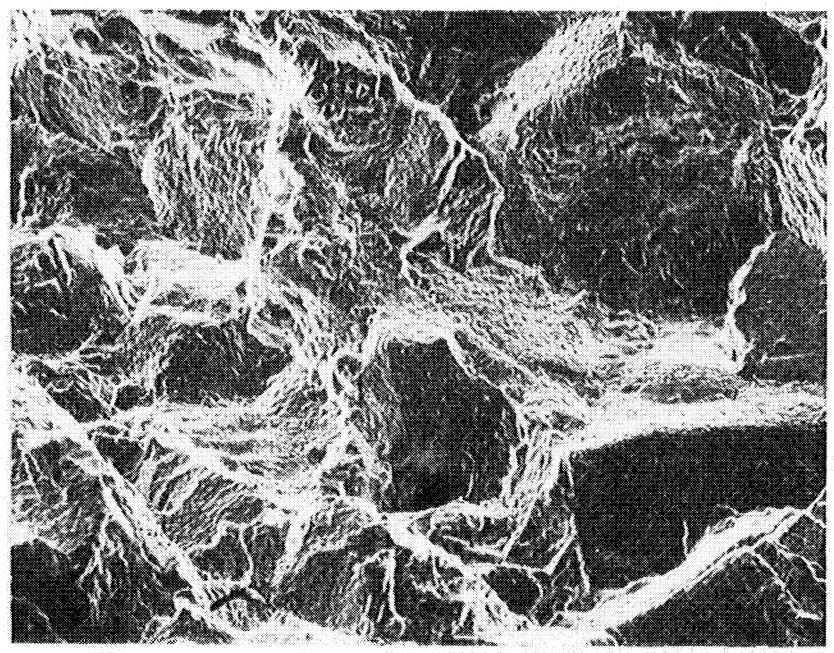

Figure 35.- Specimen 718-2 [732°C(1350°F), $\Delta\epsilon$ = 0.65, R=-1, 1 cpm, initiation life = 4719 cycles, separation life = 6506 cycles].

(a) SEM micrograph of overall fracture surface showing multiple initiation sites as indicated by arrow.
(b) Detailed view of primary initiation site.
(c) Fracture surface appearance in an area away from initiation.

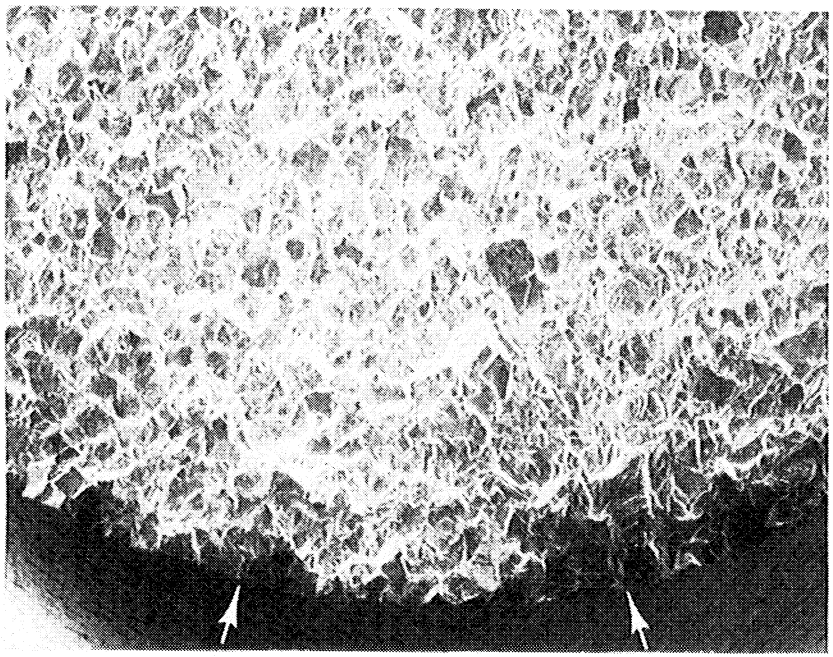

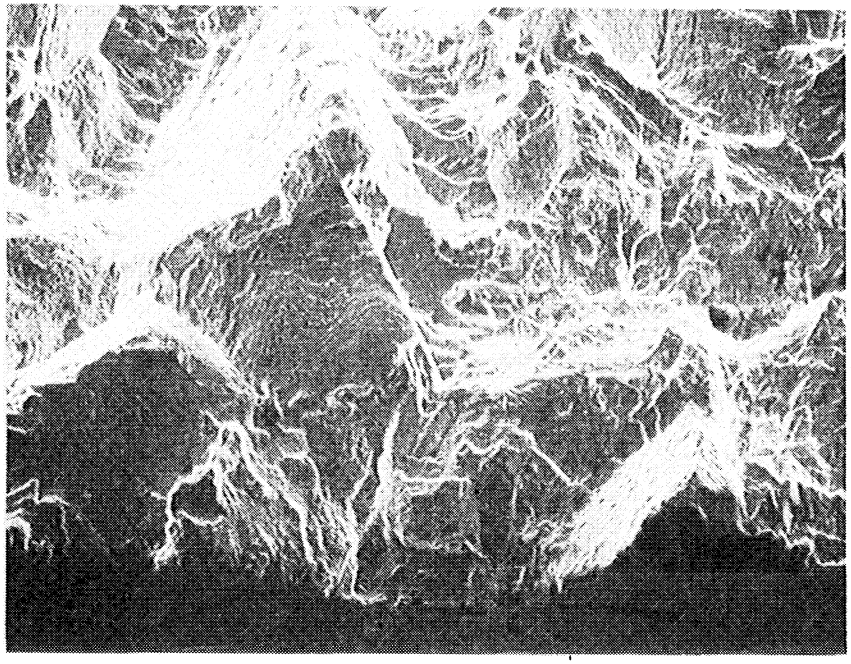

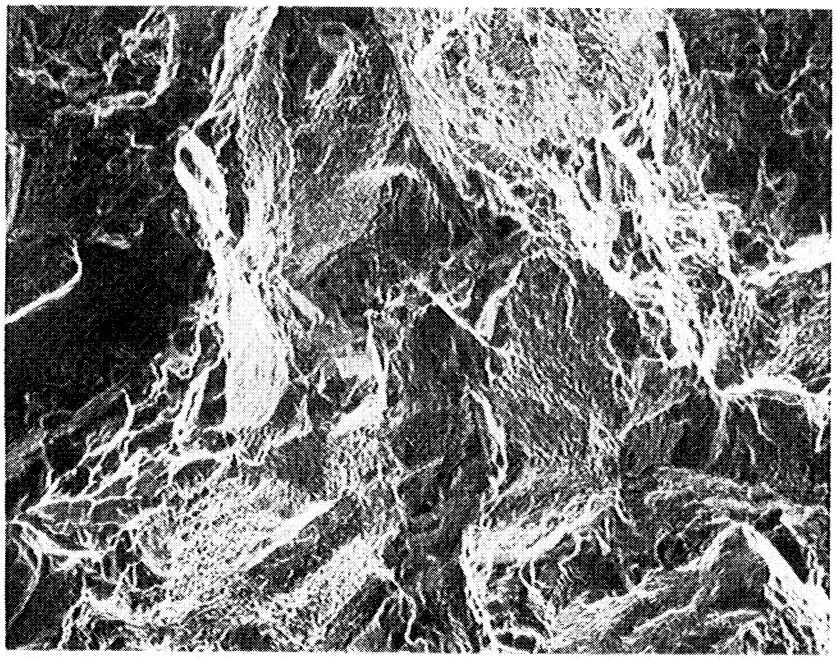

Figure 36.- Specimen 718-26 [732°C(1350°F), $\Delta\epsilon$ = 0.65, R=0, 1 cpm, initiation life = 3526 cycles, separation life = 4521 cycles].

(a) General fracture surface appearance. Initiation sites are indicated by arrows.
(b) Primary initiation site.
(c) Fracture surface appearance in an area away from initiation.

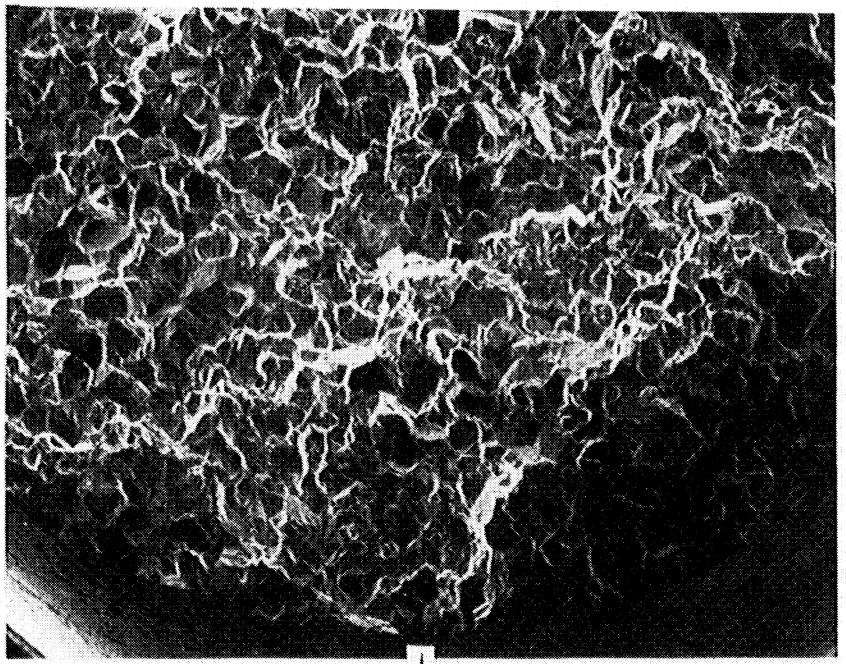

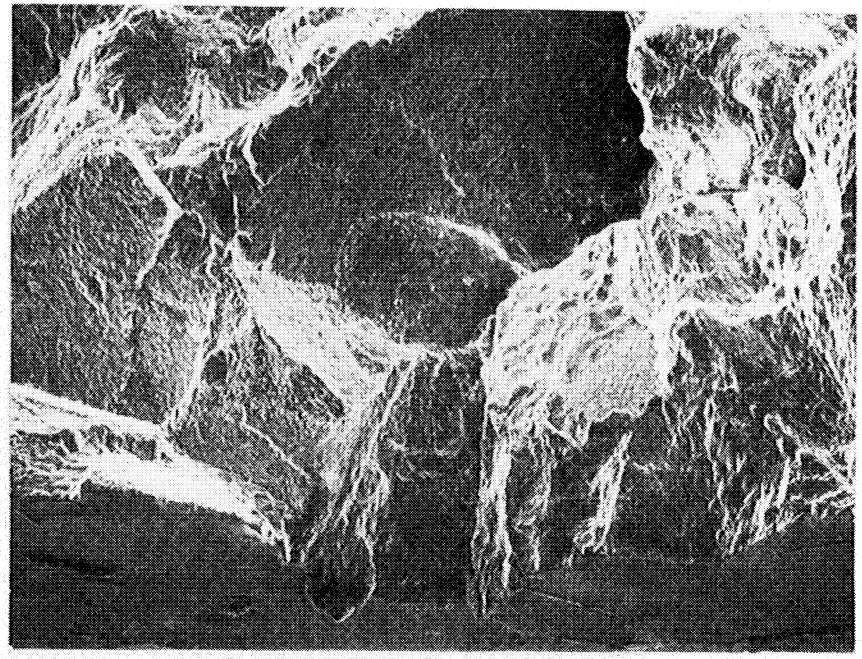

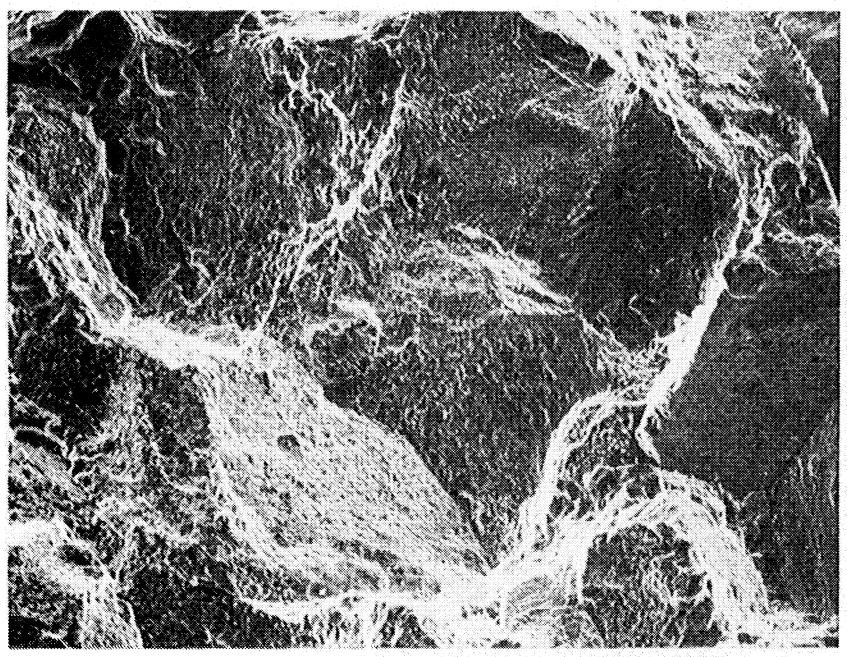

Figure 37.- Specimen 718-6 [732°C(1350°F), $\Delta\epsilon$ = 0.65, R=-1, 10 cpm, 1 minute tension hold, initiation life = 1531 cycles, separation life = 2219 cycles].

(a) General fracture surface appearance. Initiation site is indicated by arrow.
(b) Primary initiation site.
(c) Fracture surface appearance in an area away from initiation.

Specimen 718-7 was tested at 732°C (1350°F), $\Delta\epsilon$ = 0.65, R = -1, 10 cpm, 1 minute compression hold, initiation life = 1318 cycles, separation life = 3012 cycles. As shown in Figure 38a the fracture surface had a somewhat faceted appearance but the facets were fewer and not as well defined as for specimen 718-6, which had a tension hold as opposed to a compression hold. Specimen 718-7 had one primary initiation site and this is shown in Figure 38b. The crack growth mode in this area was transgranular. The appearance of the fracture away from the initiation is shown in Figure 38c. The crack growth mode in this region was predominantly transgranular. No striations were observed, possibly due to fracture surface oxidation. Slip lines were observed on the side surface of the specimen below the initiation site.

TMF Tests

Specimen 718-3T was tested at 316-649°C (600-1200°F), $\Delta\epsilon$ = 0.65, R = -1, Cycle II, for 15641 cycles. The initiation area is shown in Figure 39a. A large cleavage facet was evident and the crack growth mode in this region was predominantly transgranular. An area away from the initiation site is shown in Figure 39b. Cleavage facets formed in these regions and the predominant growth mode was transgranular but there was some intergranular growth as indicated by the locations of the secondary cracks. Striations were observed in various areas of this specimen.

Specimen 718-10T was tested at 316-649°C (600-1200°F), $\Delta\epsilon$ = 1.0, R = -1, Cycle II, for 518 cycles. An overall view of the fatigue fracture area on this specimen is shown in Figure 40a. The fracture mode appeared to be mixed with the transgranular mode predominating. As shown in Figure 40b the crack growth mode was transgranular in the vicinity of the initiation site. No striations were observed on this specimen, possibly due to fracture surface oxidation. Slip lines were observed on the side surface of the specimen below the initiation site.

Specimen 718-6T was tested at 316-732°C (600-1350°F), $\Delta\epsilon$ = 0.65, R = -1, Cycle II, for 2946 cycles. The overall fatigue fracture area is shown in Figure 41. Cleavage facets were evident throughout the fracture. The initiation site is shown in Figure 42a and the fracture surface away from the initiation site is shown in Figure 42b. In both locations the crack growth mode was predominantly transgranular. No striations were detected, possibly due to fracture surface oxidation. Slip lines were visible on the side surface of the specimen below the initiation site.

Specimen 718-14T was tested at 316-732°C (600-1350°F), $\Delta\epsilon$ = 0.8, R = -1, Cycle II, for 558 cycles. An overall view of the fracture is shown in Figure 43a. The area of the initiation site is shown in Figure 43b. The crack growth mode in this region was transgranular, as indicated by the faceting. Away from the initiation area the crack growth mode was found to be a mixture of transgranular and intergranular. An area that was predominantly intergranular is shown in Figure 43c. In general the crack growth mode in this specimen was roughly an equal mixture of transgranular and intergranular fracture. No striations were observed on this specimen, possibly due to fracture surface oxidation. Slip lines were observed on the side surface of the specimen below the initiation site.

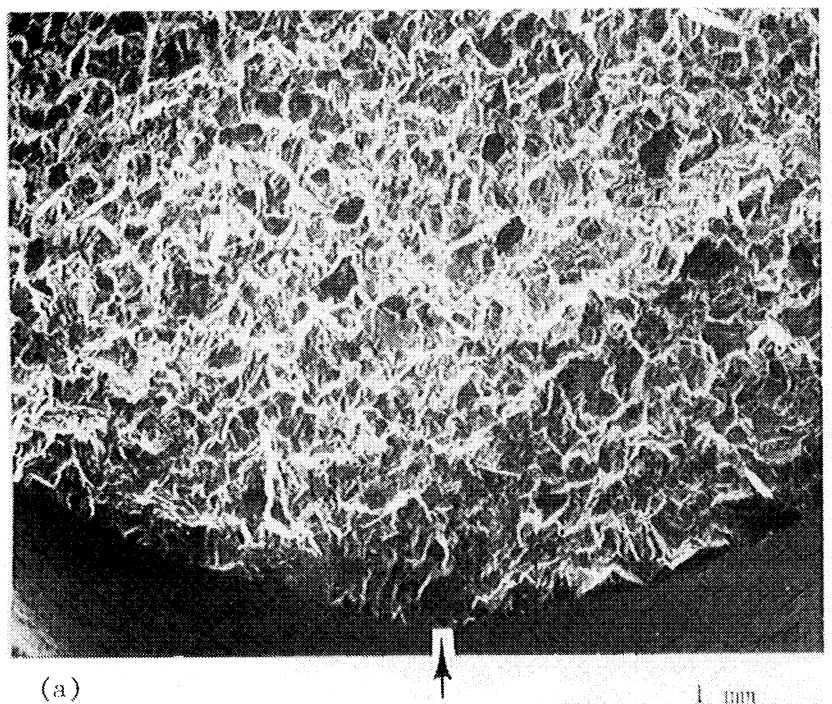

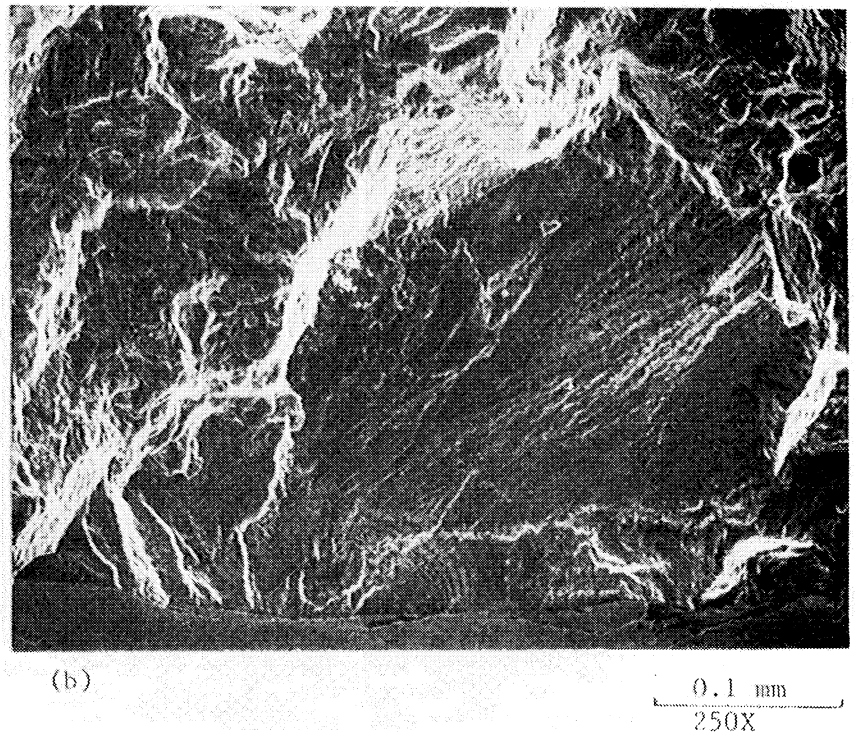

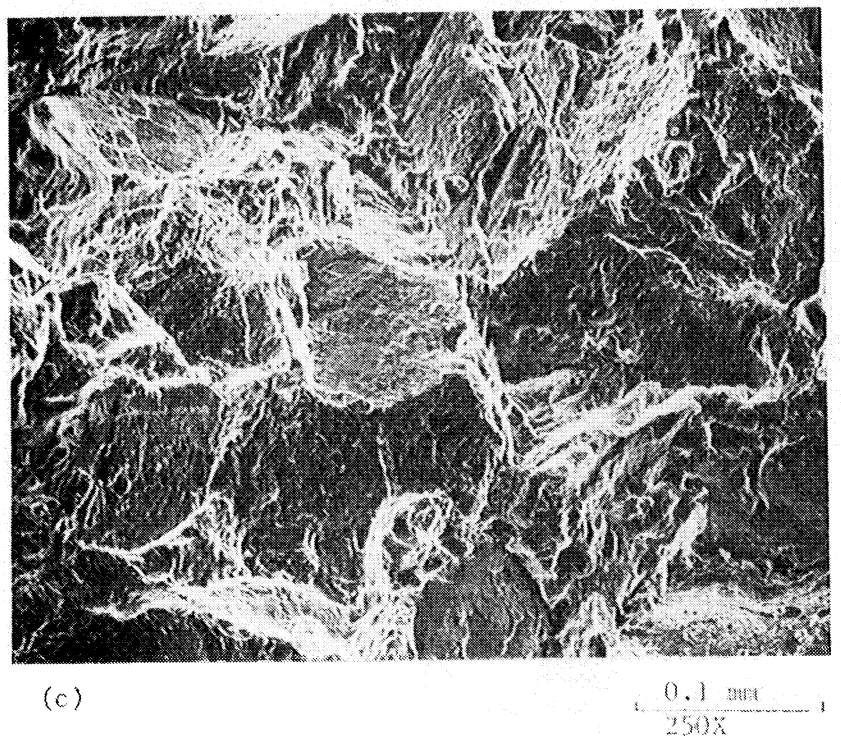

Figure 38.- Specimen 718-7 [732°C(1350°F), $\Delta\epsilon$ = 0.65, R=-1, 10 cpm, 1 minute compression hold, initiation life = 1318 cycles, separation life = 3012 cycles].

(a) General fracture surface appearance. Initiation site is indicated by arrow.
(b) Detailed view of initiation site.
(c) Fracture surface appearance in an area away from initiation.

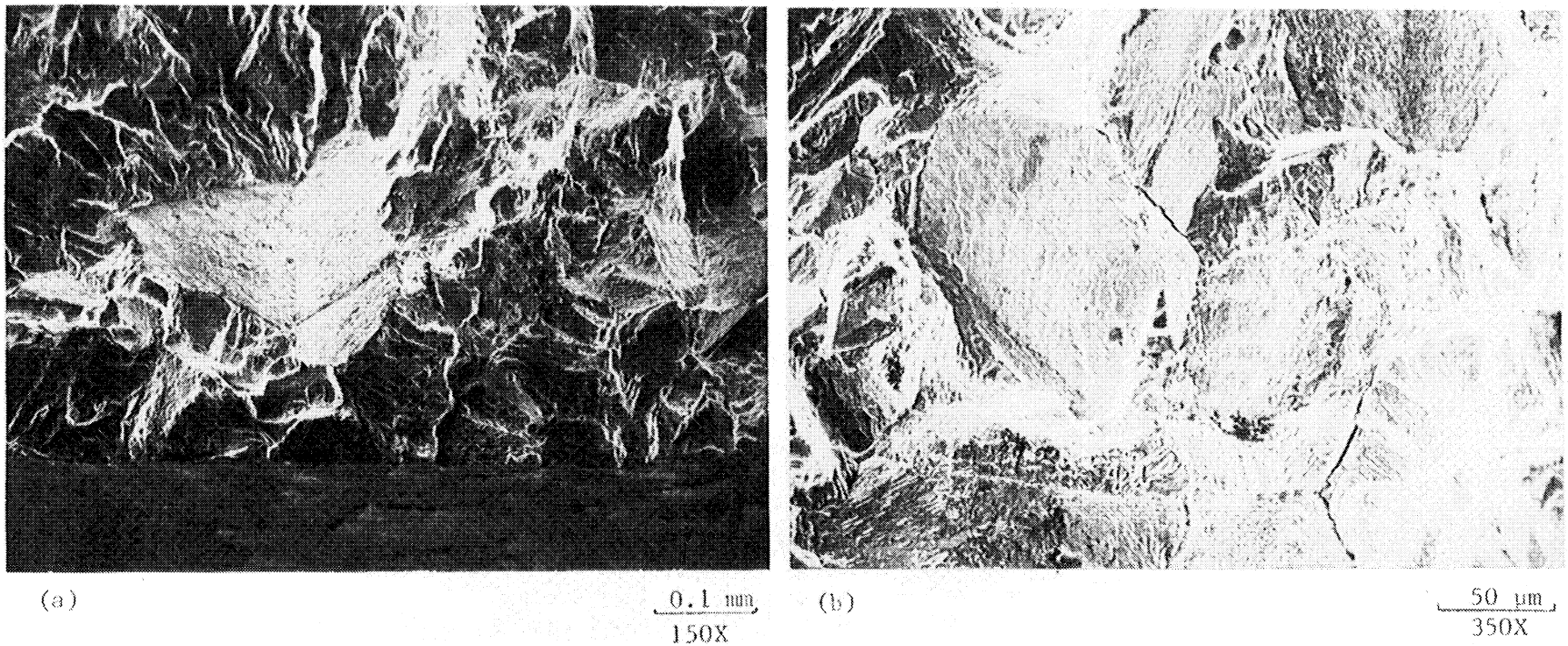

Figure 39.- Specimen 718-3T [316 - 649°C(600 - 1200°F), $\Delta\epsilon$ = 0.65, R=-1, Cycle II, 15641 cycles].

(a) Primary initiation area.
(b) Fracture surface appearance in an area away from initiation.

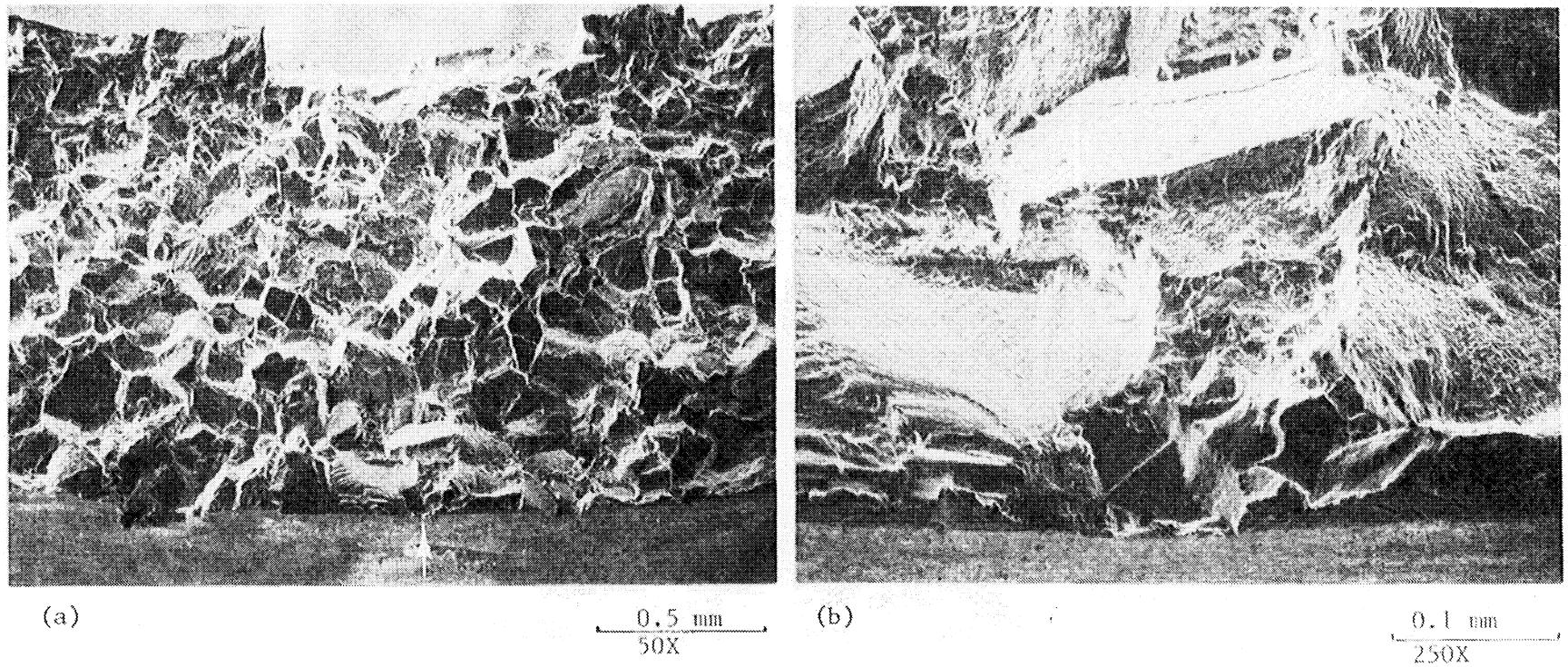

Figure 40.- Specimen 718-10T [316 - 649°C(600 - 1200°F), $\Delta\epsilon$ = 1.0, R=-1, Cycle II, 518 cycles].

(a) General fracture surface appearance. Initiation site is indicated by arrow.
(b) Detailed view of initiation site.

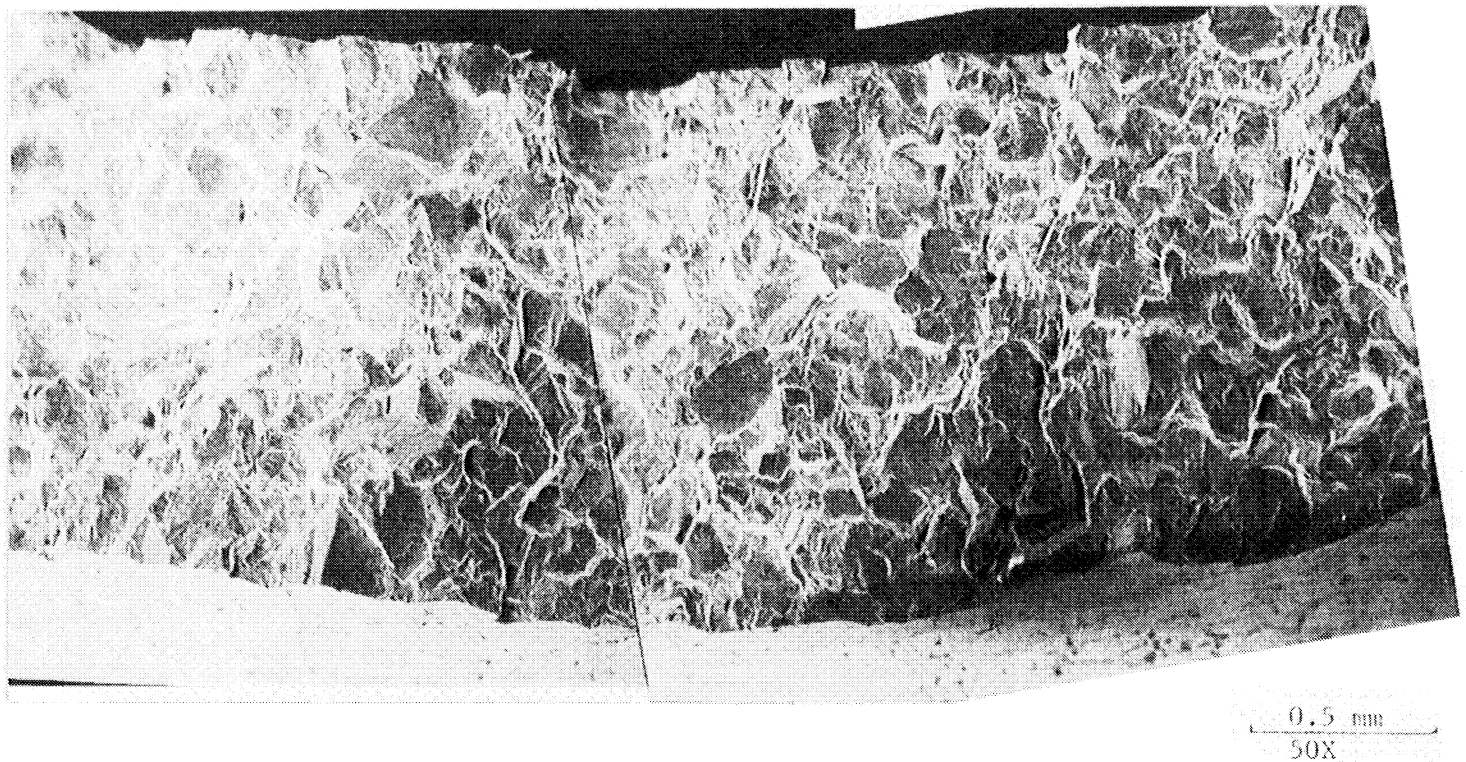

Figure 41.- Specimen 718-6T [316 - 649°C(600 - 1200°F), $\Delta\epsilon$ = 0.65, R=-1, Cycle II, 2946 cycles]. General view of fracture surface.

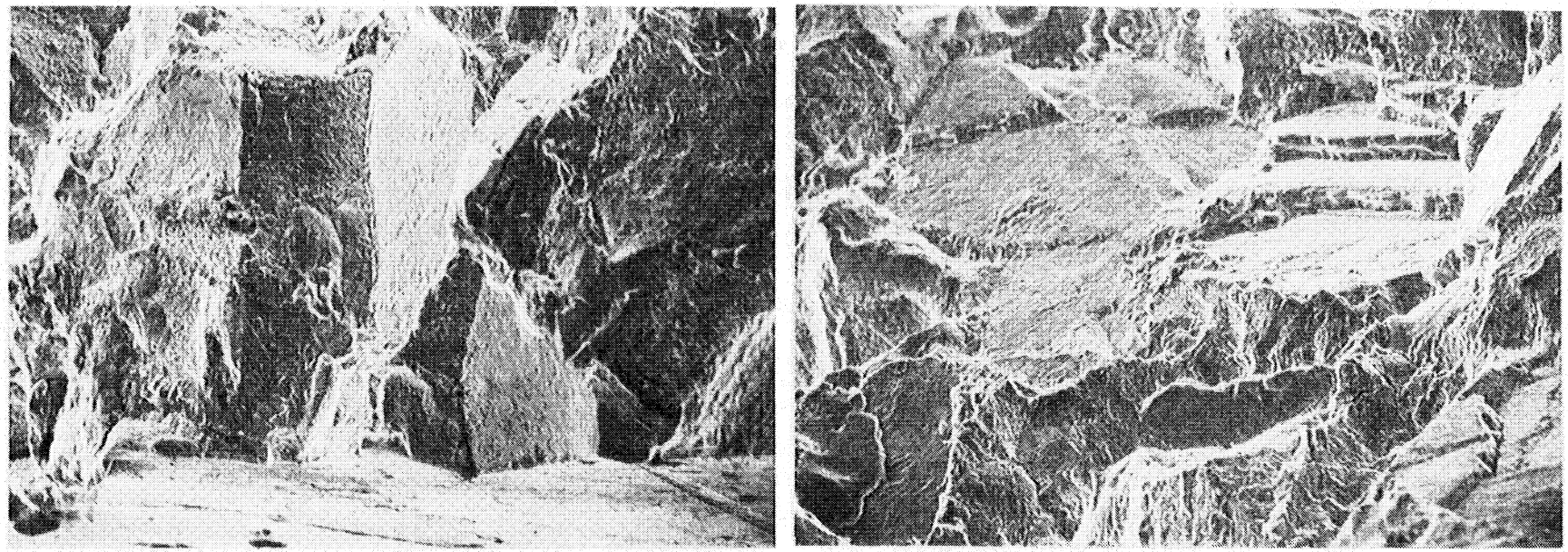

Figure 42.- Specimen 718-6T [316 - 649°C(600 - 1200°F), $\Delta\epsilon$ = 0.65, R=-1, Cycle II, 2946 cycles].

(a) Primary initiation site.
(b) Fracture surface appearance in an area away from initiation.

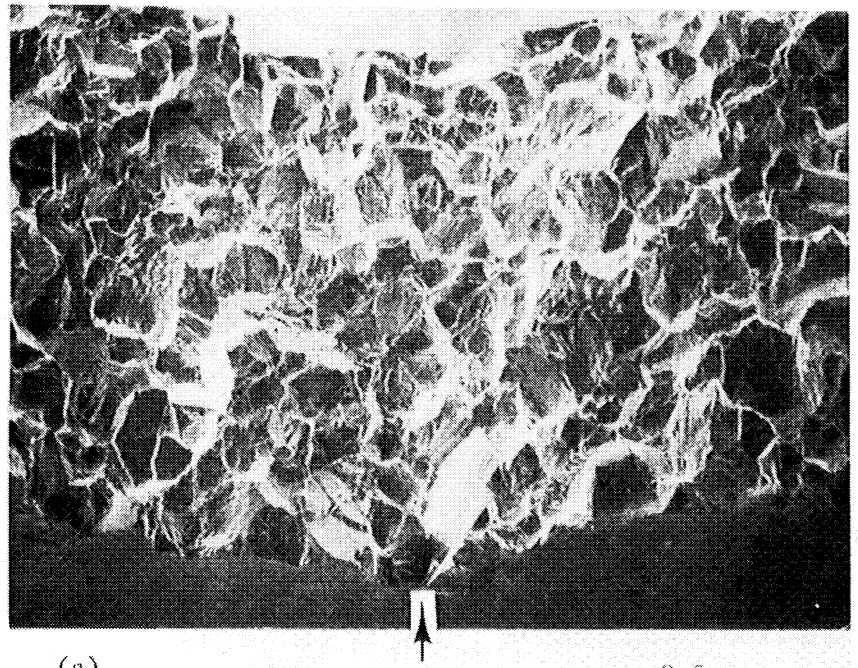

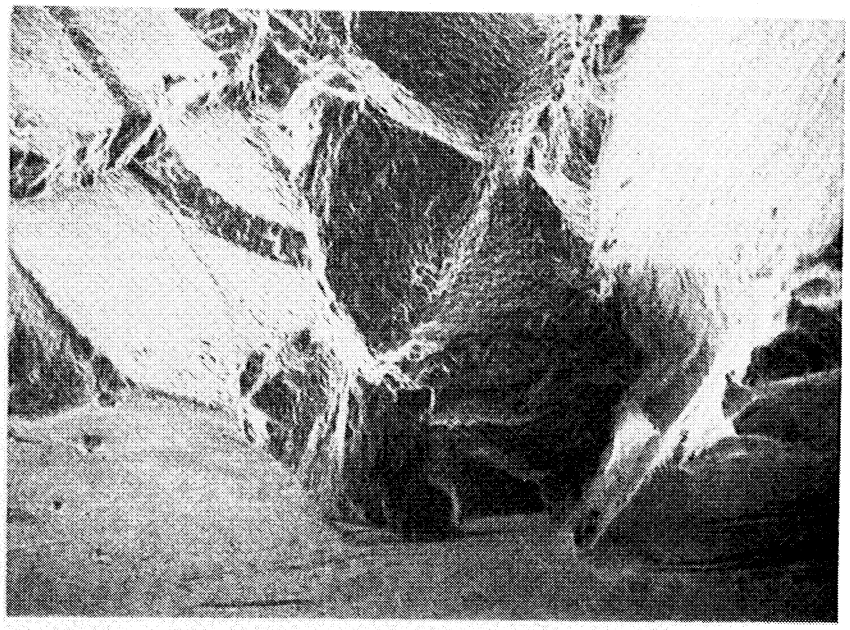

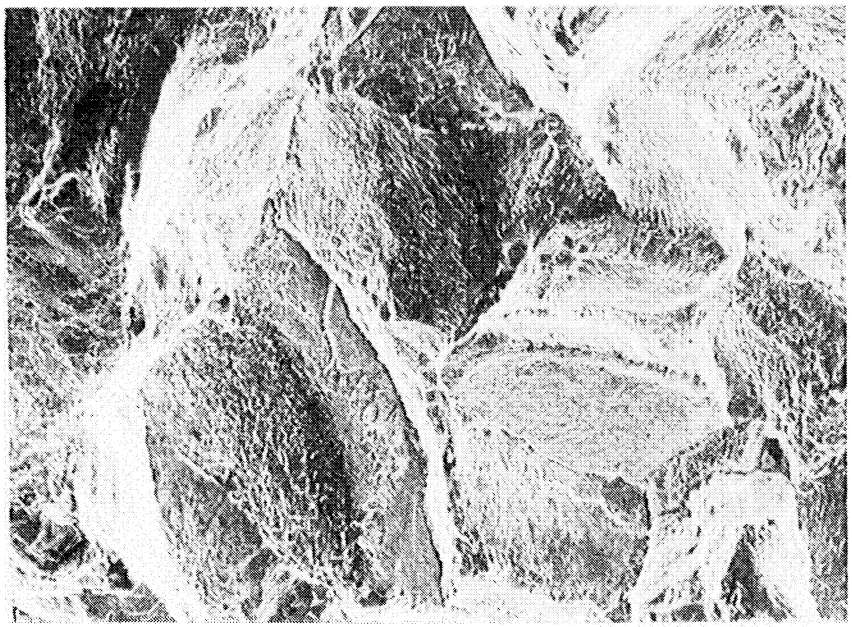

Figure 43.- Specimen 718-14T [316 - 732°C (600-1350°F), $\Delta\epsilon$ =0.8, R=-1, Cycle II, 558 cycles).

(a) General fracture surface appearance. Initiation site is shown by arrow.
(b) Higher magnification of initiation site.
(c) Area of predominately intergranular fracture in a region away from the origin.

Specimen 718-5T was tested at 316-732°C (600-1350°F), $\Delta\epsilon$= 0.65, R = -1, Cycle I, for 1251 cycles. This specimen had one major initiation site. An overall view of the fracture is shown in Figure 44a. There was very little faceting on this fracture and it had a much smoother appearance as compared to the TMF specimens discussed above. The initiation area of this sample is shown in Figure 44b. The crack growth mode in this area was transgranular and striations were observed quite close to the initiation site. The fracture surface approximately midwall in the specimen is shown in Figure 44c. An abundant amount of striations are seen in this area as well as others. The overall crack growth mode in this specimen is transgranular. Slip lines are visible on the side surface of the specimen below the fracture.

Specimen 718-17T was TMF tested at 316-732°C (600-1350°F), $\Delta\epsilon$ = 0.65, R = -1, CW cycle, for 6022 cycles. This specimen had three initiation sites, an overall view of the primary initiation site is shown in Figure 45a. This fracture appeared similar to 718-5T in that there was minimal faceting and the fracture had a smoother overall appearance as compared to the other TMF specimens, although it had more facets than 718-5T. A large cleavage facet was present at the initiation site as shown in Figure 45b, and the crack growth mode in this region was transgranular. The fracture surface at the midwall of the specimen is shown in Figure 45c. Here the fracture had a generally smooth appearance with numerous striations present as well as a few secondary cracks. The crack growth mode was predominantly transgranular.

SUMMARY

All the isothermal test specimens had transgranular crack growth as the dominant mode. Specimens 718-2 and 718-6 both showed a greater than average amount of intergranular growth but in both cases the dominant mode was still transgranular. In general transgranular growth was also the dominant mode of growth for most of the TMF specimens. Specimens 718-5T and 718-17T had the smoothest fractures overall and the most striations observed of the group, which indicated that the Cycle I and CW cycles examined here particularly favor transgranular growth. However, for both temperature ranges significant amounts of intergranular growth were seen for Cycle II loading at higher strain ranges (Specimens 718-10T and 718-14T). It appeared that of the test conditions discussed above, Cycle II loading has the greatest propensity for intergranular growth.

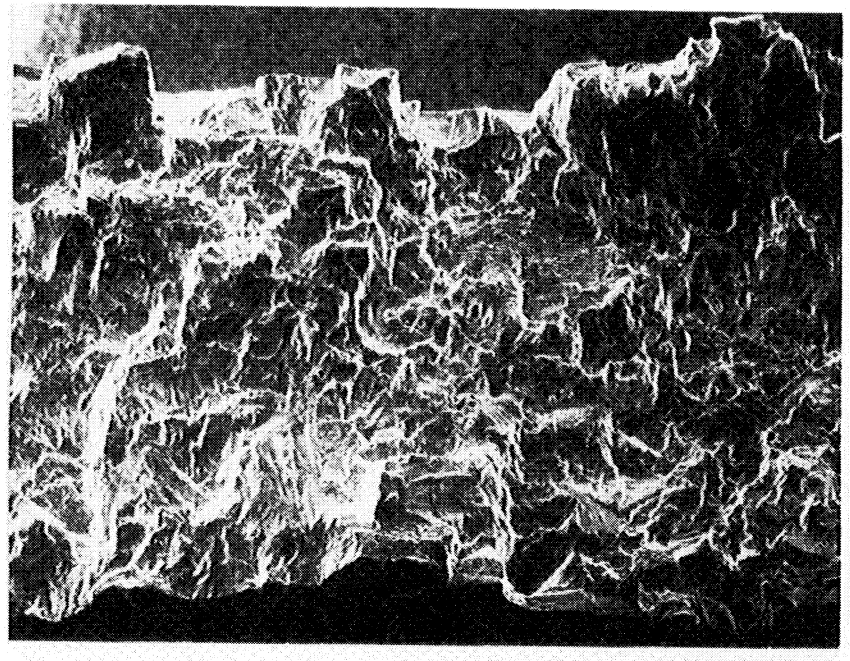

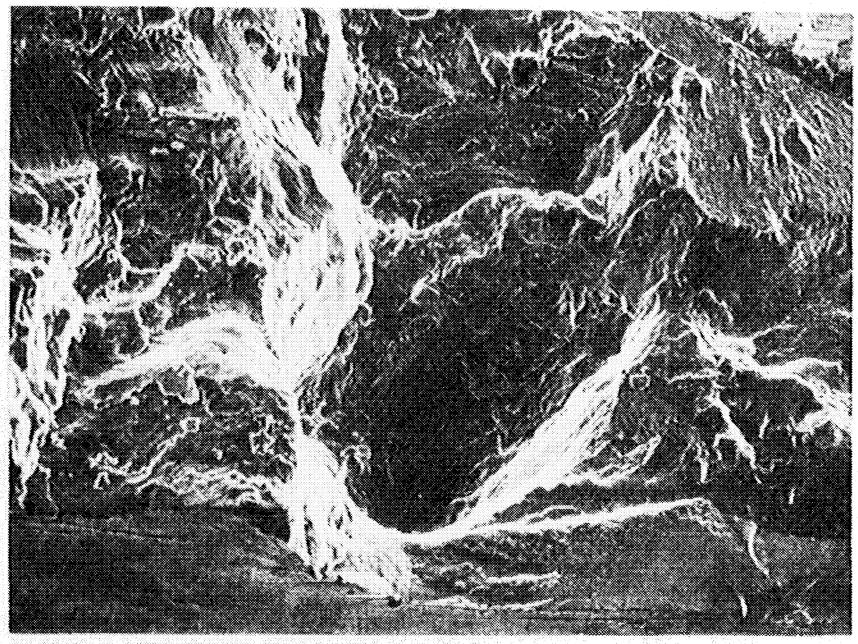

Figure 44.- Specimen 718-5T [316 - 732°C (600-1350°F, $\Delta\epsilon$ =0.65, R=-1, Cycle I, 1251 cycles].

(a) General fracture surface appearance.
(b) Detailed view of initiation site.
(c) Fracture surface appearance at approximately midwall in the specimen.

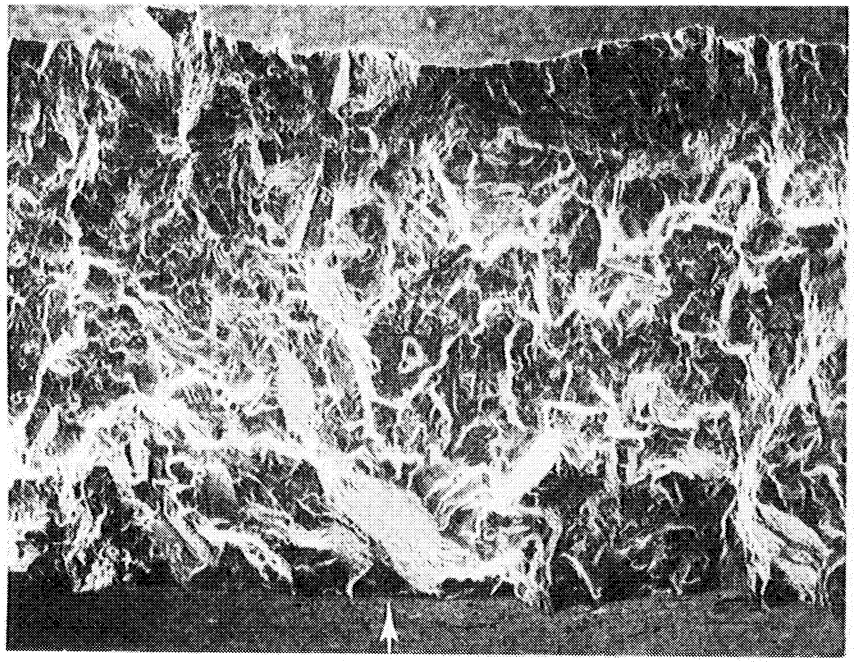

(a)

0.5 mm
50X

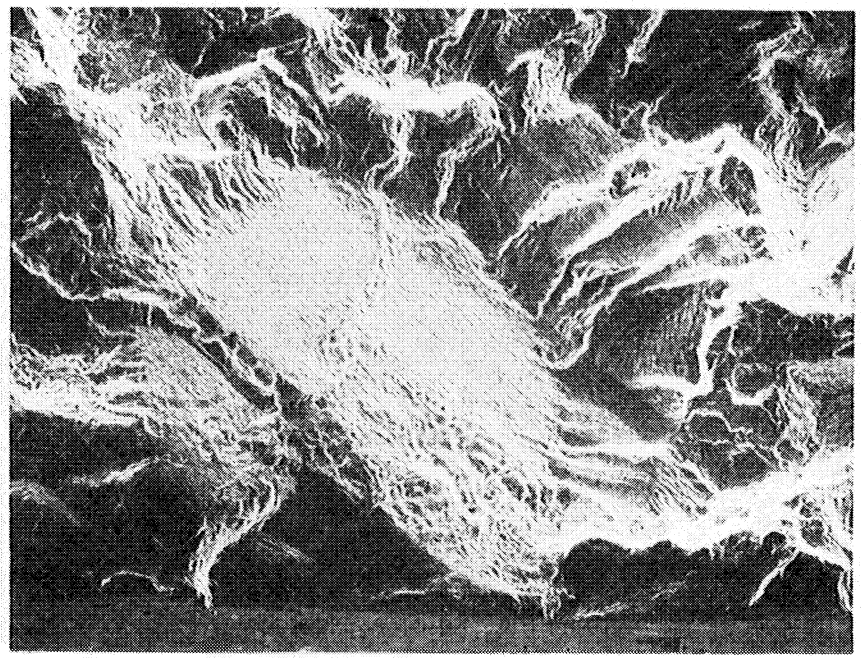

(b)

0.1 mm
200X

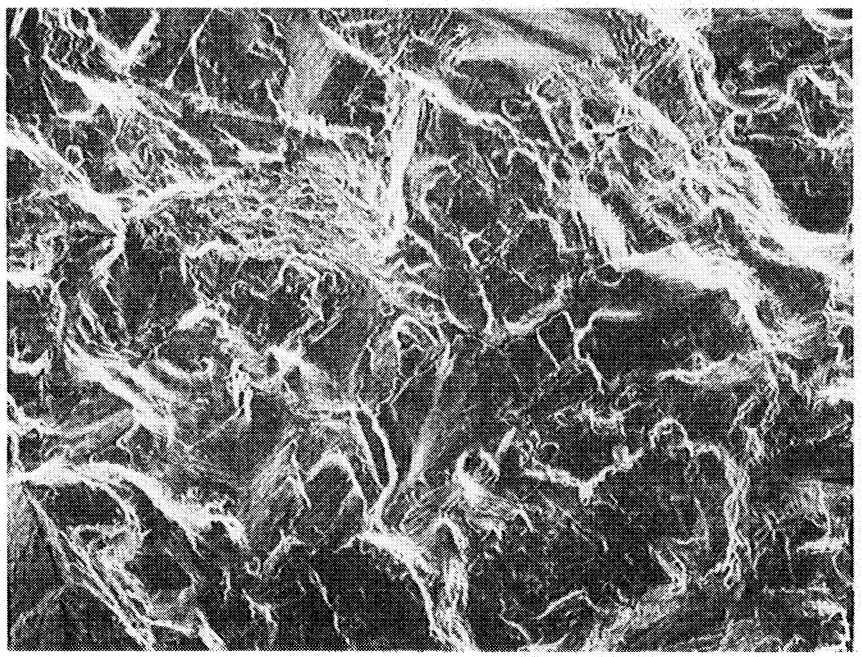

(c)

0.1 mm
250X

Figure 45.- Specimen 718-17T [316 - 732°C (600-1350°F), $\Delta\epsilon$ =0.65, R=-1, CW Cycle, 6022 cycles].

(a) General fracture surface appearance in area of primary initiation site. Initation site is indicated by arrows.
(b) Detailed view of primary initiation site.
(c) Fracture surface appearance at approximately midwall in the specimen.

SECTION 4.0
DISCUSSION OF RESULTS

The most important result from the tests conducted under this contract is the database showing the effects of creep fatigue under the full spectrum of loading encountered by modern gas turbines. In most cases, the interaction was non-linear and not accurately predicted by simple rules. In some of the experiments, the creep fatigue interaction was less than anticipated. The likely explanation in all these cases is that different mechanisms are responsible for the damage occurring during the test. A successful life prediction model must therefore be able to account for different damage mechanisms and allow them to interact mathematically in accord with the physical processes involved. The Cyclic Damage Accumulation (CDA) life prediction model is designed to do just that. The damage state is a vector, the components of which represent either direct mechanisms or interactions as required by the material being analyzed. Both the CDA system (in FORTRAN 77) and an extensive set of specimen data files (in CDA input format; includes all INCO 718 tests and many B1900+Hf tests) will be available through COSMIC (Janitor and Nelson, 1989).

All the life results from the various tasks were compared to the predictions made using the CDA life prediction model. Figure 46 shows the predictions made for the controlled mean stress-strain range tests conducted under Task XI on B1900+Hf. Although none of these data were used to obtain the constants for the CDA model, the predictions look reasonable, with most being within a factor of 3.

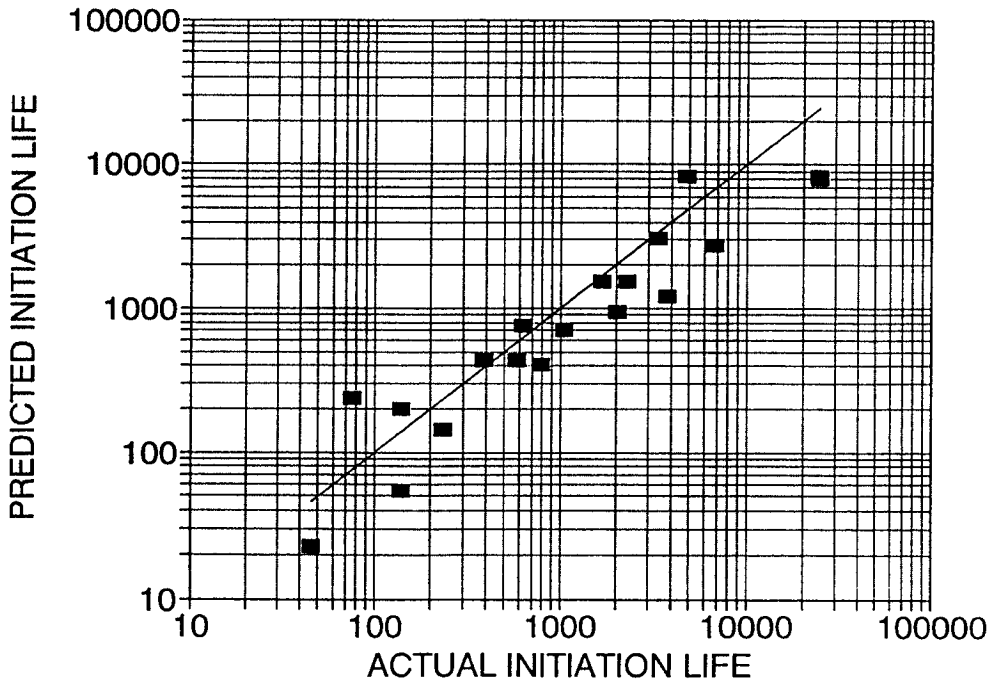

Figure 46.- B1900+Hf CDA Predictions - Mean Stress-Strain Range Tests.

CDA life model correlations for the alternative alloy, INCO 718, proved to be somewhat more difficult than for B1900+Hf. The strong dependence of fatigue life on the primary creep strain level which was seen on B1900+Hf was not as strong for INCO 718. The CDA constants controlling this effect were detuned for INCO 718, although they were still needed to predict the R-ratio data. Figure 47 shows the correlation of the CDA model for INCO 718 isothermal data. The low strain range, high life result at 732°(1350°F) was not well predicted, but the constants were determined to yield a conservative prediction in this regime. Also, the two low strain range, one-way cycled specimens at 732°C(1350°F) generated large predicted creep damage components, but the data showed only small effects. These results were therefore conservatively predicted by the CDA model. Otherwise, the data are fairly well predicted. Figure 48 shows the CDA predictions for the INCO 718 TMF data, and once again, for the complexity of the conditions represented in the data, the correlation is good.

Figure 49 shows the CDA life model correlation for the INCO 718 multiaxial data. The Socie parameter is used within the CDA model to provide equivalent values of the uniaxial-based model constants. It is clear that additional work will be needed to capture fully the effects seen in the figure. Figure 50 shows the predictions for the mean stress-strain range tests, and here the trend is to underpredict the lives relative to the actual data. In both of these loadings, more work would be needed to extend the model to cover new mechanisms or interactions not currently included.

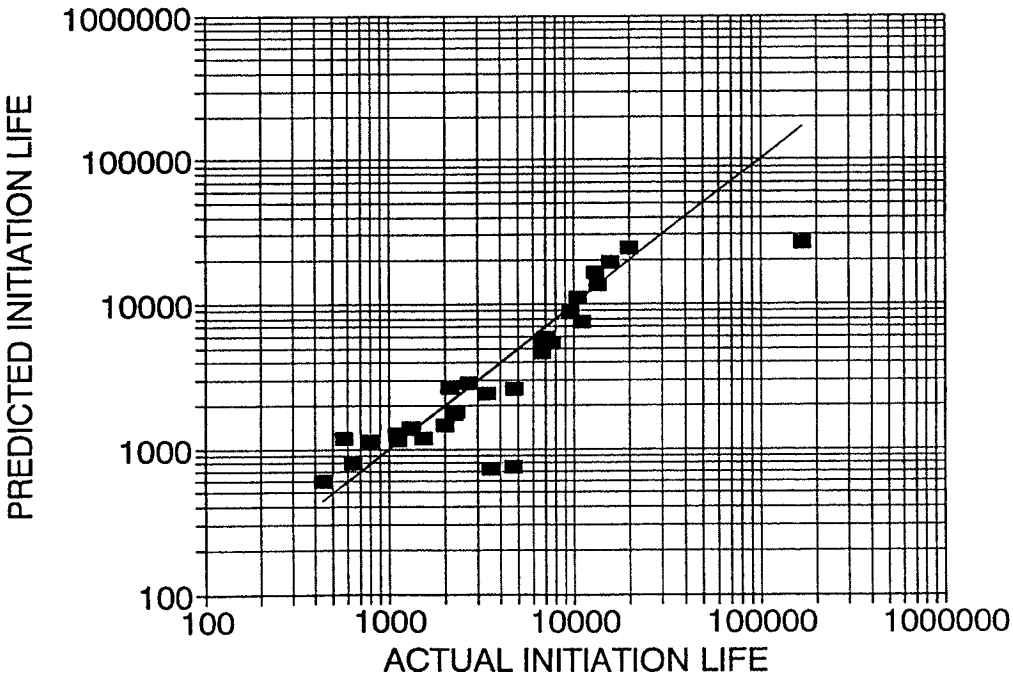

Figure 47.- INCO 718 CDA Predictions - Isothermal Tests.

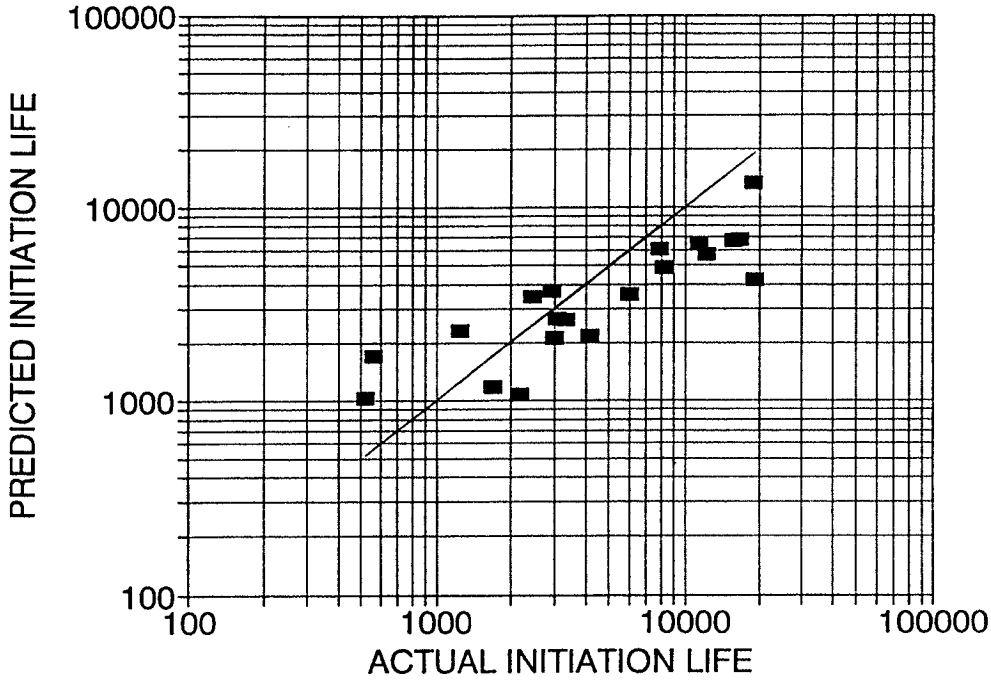

Figure 48.- INCO 718 CDA Predictions - Thermomechanical Fatigue Tests.

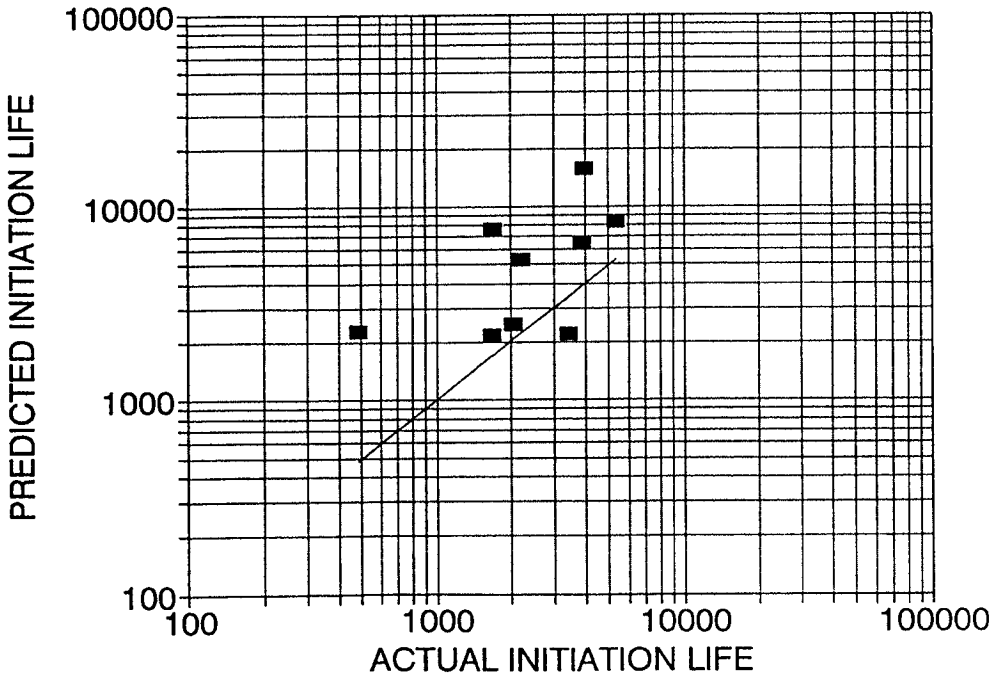

Figure 49.- INCO 718 CDA Predictions - Multiaxial Tests.

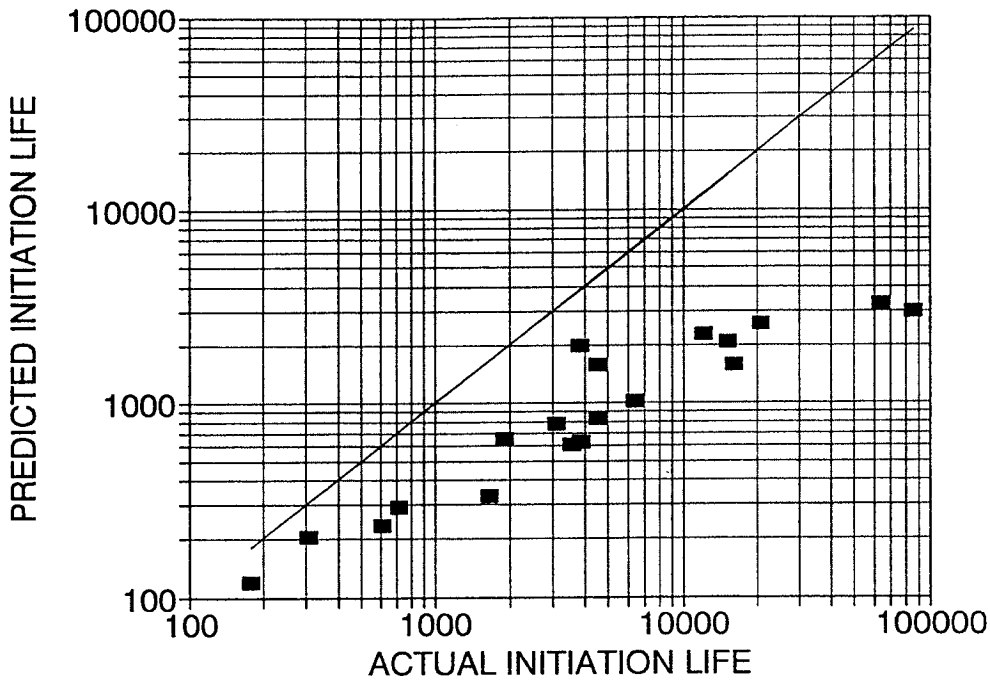

Figure 50.- INCO 718 CDA Predictions - Mean Stress-Strain Range Tests.

SECTION 5.0
CONCLUSIONS

The major conclusions of this program are as follows:

1. The extensive database generated under this contract covers a broad range of conditions experienced by hot section components.

2. Strain range and cycling history (stress/strain/temperature vs. time) were consistently shown to be major parameters in deteriming creep fatigue life.

3. For multiaxial life predictions, maximum principal strain range was the best correlating parameter for B1900+Hf, and the Socie parameter was the best for INCO 718.

4. The CDA life prediction model and its associated computer program provide a practical means of making life predictions under these conditions.

5. New theories and additional damage mechanism models can be easily tested and calibrated using these data and the modular structure of the CDA program.

6. Strain range and cycle type were both shown to be significant factors in determining coated TMF life. As with the uncoated TMF tests, the phase angle between strain and temperature for elliptical cycle tests (clockwise vs. counterclockwise) was also very important, especially at low strain ranges.

7. For the conditions used in this task, the presence of the coatings in general increased the specimen lives by 2-5X. This is in contrast to most actual service conditions, in which the coating will crack prematurely when exposed to high local strains. This was confirmed by judicious selection of a cycle type which resulted in high coating strains and hence lower life than an uncoated specimen.

8. Fracture surface examinations of specimens tested showed that for both coating systems, frequent initiations on the uncoated I.D. as well as the coated O.D occurred. Major fatigue crack initiations occurring at the uncoated I.D. surface may influence test results and interpretation.

9. No recrystallization resulting from the post coating heat treatment was observed at the worked surfaces of two PWA 286 coated specimens.

APPENDIX A-1

PWA 1455 ENVIRONMENTAL TESTING

LAB AIR / SHOP AIR ATMOSPHERES

Specimen Identification	123B	124B	124D	137A	123A
Type of Specimen	MERL 75	MERL 75	MERL 75	MERL 73C	MERL 75
Test Conditions:					
Environment	LAB AIR	LAB AIR	LAB AIR	LAB AIR	SHOP AIR
Temperature (°C)	982.	982.	871.	982.	871.
" (°F)	1800.	1800.	1600.	1800.	1600.
Strain Range	0.004070	0.003993	0.005150	0.003990	0.005130
Strain R-Ratio (min/max)	-0.983	-1.000	-0.977	-0.983	-0.963
Strain Rate (1/sec)	1.70E-04	1.66E-03	1.70E-04	1.10E-04	1.70E-04
Frequency (cyc/min)	1.248	12.500	1.000	0.800	0.996
Tension Hold (sec)	0.000	0.000	0.000	0.000	0.000
Compression Hold (sec)	0.000	0.000	0.000	0.000	0.000
Stress-Strain Response:					
Stress Range, Init (Mpa)	452.9	487.9	676.0	408.2	688.5
" " " (psi)	65690.4	70758.0	98044.2	59198.5	99852.9
Stress Range, Nf/2 (Mpa)	442.9	485.1	647.9	377.8	659.7
" " " (psi)	64236.3	70360.0	93965.7	54798.3	95678.4
Mean Stress, Init (Mpa)	-8.7	-8.2	-13.2	1.3	-10.8
" " " (psi)	-1261.3	-1187.0	-1911.8	186.4	-1560.2
Mean Stress, Nf/2 (Mpa)	2.9	-0.2	-19.3	8.2	-0.6
" " " (psi)	427.2	-30.0	-2796.3	1190.9	-91.2
Inel Stn Rng, Init	0.000654	0.000386	0.000192	0.000736	0.000280
Inel Stn Rng, Nf/2	0.000759	0.000404	0.000355	0.000879	0.000458
Life Results:					
Initiation (cycles)	1320.	1560.	1350.	989.	560.[1]
5% Load Drop (cycles)	2395.	4173.	4847.	1829.	1342.[1]
10% Load Drop (cycles)	2444.	4254.	5199.	1958.	1380.[1]
50% Load Drop (cycles)	2493.	4464.	5632.	2105.	1443.[1]

Note: 1. Life apparently reduced by foreign substances in air supply.

APPENDIX A-2

PWA 1455 ENVIRONMENTAL TESTING

PURIFIED ARGON ATMOSPHERE

Specimen Identification		137C	137D	143A
Type of Specimen		MERL 75	MERL 75	MERL 73C
Test Conditions:				
Environment		ARGON	ARGON	ARGON
Temperature	(°C)	871.	982.	982.
"	(°F)	1600.	1800.	1800.
Strain Range		0.005230	0.004170	0.004000
Strain R-Ratio (min/max)		-0.998	-1.010	-1.019
Strain Rate	(1/sec)	1.70E-04	1.70E-04	1.70E-04
Frequency	(cyc/min)	0.996	1.244	1.250
Tension Hold	(sec)	0.000	0.000	0.000
Compression Hold	(sec)	0.000	0.000	0.000
Stress-Strain Response:				
Stress Range, Init	(Mpa)	749.1	458.9	482.3
" " "	(psi)	108643.0	66554.2	69951.1
Stress Range, Nf/2	(Mpa)	705.6	441.1	463.1
" " "	(psi)	102339.0	63980.4	67162.1
Mean Stress, Init	(Mpa)	-3.9	-2.9	-8.3
" " "	(psi)	-570.2	-414.7	-1210.8
Mean Stress, Nf/2	(Mpa)	10.8	3.8	2.3
" " "	(psi)	1573.3	547.1	331.4
Inel Stn Rng, Init		0.000480	0.001085	0.000719
Inel Stn Rng, Nf/2		0.000675	0.001175	0.000789
Life Results:				
Initiation	(cycles)	521.	256.	487.
5% Load Drop	(cycles)	886.	471.	873.
10% Load Drop	(cycles)	1133.	491.	918.
50% Load Drop	(cycles)	1544.	522.	993.

APPENDIX A-3

PWA 1455 ENVIRONMENTAL TESTING

75 PSIA OXYGEN ATMOSPHERE

Specimen Identification	111C	139B	136D	111D	112A	112C	143D	143C
Type of Specimen	MERL 75	MERL 75	MERL 75	MERL 75	MERL 75	MERL 75	MERL 73C	MERL 73C
Test Conditions:								
Environment	OXYGEN	OXYGEN	OXYGEN	OXYGEN	OXYGEN	OXYGEN	OXYGEN	OXYGEN
Temperature (°C)	871.	871.	871.	982.	982.	982.	982.	982.
" (°F)	1600.	1600.	1600.	1800.	1800.	1800.	1800.	1800.
Strain Range	0.005130	0.005010	0.004948	0.004030	0.004070	0.003943	0.004010	0.004020
Strain R-Ratio (min/max)	-0.961	-0.001	-0.963	-1.002	-0.974	-0.984	0.000	-0.988
Strain Rate (1/sec)	1.70E-04	1.70E-04	1.50E-04	1.70E-04	1.70E-04	1.64E-03	1.70E-04	1.24E-04
Frequency (cyc/min)	0.996	1.000	0.909	1.260	1.248	12.500	1.250	0.926
Tension Hold (sec)	0.000	0.000	60.000	0.000	0.000	0.000	0.000	60.000
Compression Hold (sec)	0.000	0.000	0.000	0.000	0.000	0.000	0.000	0.000
Stress-Strain Response:								
Stress Range, Init (Mpa)	695.4	647.2	647.0	477.1	470.1	505.2	428.1	491.0
" " " (psi)	100858.0	93870.6	93835.9	69191.1	68184.7	73272.0	62083.7	71210.0
Stress Range, Nf/2 (Mpa)	748.2	661.9	680.7	428.4	456.9	547.0	428.6	452.9
" " " (psi)	108518.0	96002.0	98722.4	62137.6	66264.9	79326.0	62165.7	65685.0
Mean Stress, Init (Mpa)	-10.6	173.2	-12.7	-9.6	-8.8	-6.2	49.3	-24.9
" " " (psi)	-1542.9	25113.4	-1840.1	-1392.1	-1282.7	-895.0	7154.1	-3609.5
Mean Stress, Nf/2 (Mpa)	-18.1	27.6	-104.4	-24.2	-6.2	5.1	0.7	-60.7
" " " (psi)	-2629.0	4008.3	-15143.0	-3505.8	-893.0	737.0	102.6	-8804.2
Inel Stn Rng, Init	0.000150	0.000655	0.000269	0.000941	0.000716	0.000582	0.001016	0.000969
Inel Stn Rng, Nf/2	0.000487	0.000576	0.000643	0.001204	0.000939	0.000682	0.001081	0.001104
Life Results:								
Initiation (cycles)	674.	150.	900.	559.	460.	924.	280.	200.
5% Load Drop (cycles)	1869.	1028.	5282.	1143.	904.	2483.[1]	697.	457.
10% Load Drop (cycles)	2080.	1119.	5816.	1167.	951.	2562.[1]	729.	1039.
50% Load Drop (cycles)	2245.	1186.	5940.	1216.	1000.	2641.[1]	808.	1259.

Note: 1. Specimen 112C failed at 958 cycles under the extensometer rods; load drop lives estimated.

APPENDIX A-4

PWA 1455 ENVIRONMENTAL TESTING

BLOCK ATMOSPHERES: 75 PSIA OXYGEN FIRST; LAB AIR REMAINDER

Specimen Identification	140A	136B	138B	142A	144C	144B	143B	138C
Type of Specimen	MERL 75	MERL 75	MERL 75	MERL 75	MERL 73C	MERL 73C	MERL 73C	MERL 73C
Test Conditions:								
Environment	O2 / AIR	O2 / AIR	O2 / AIR	O2 / AIR	O2 / AIR	O2 / AIR	O2 / AIR	O2 / AIR
Block 1 Length (cycles)	1800.	363.[1]	80.	300.	100.	500.	50.	260.
Temperature (°C)	871.	871.	871.	871.	982.	982.	982.	982.
" (°F)	1600.	1600.	1600.	1600.	1800.	1800.	1800.	1800.
Strain Range	0.004170	0.005218	0.005030	0.005250	0.004006	0.004011	0.004010	0.004000
Strain R-Ratio (min/max)	-0.987	-0.977	-0.971	-0.977	-1.008	-1.022	-0.999	-0.997
Strain Rate (1/sec)	1.74E-03	1.74E-03	1.70E-04	1.80E-04	1.67E-03	1.67E-03	1.70E-04	1.70E-04
Frequency (cyc/min)	12.500	10.000[1]	1.000	1.000	12.500	12.500	1.250	1.248
Tension Hold (sec)	0.000	0.000	0.000	0.000	0.000	0.000	0.000	0.000
Compression Hold (sec)	0.000	0.000	0.000	0.000	0.000	0.000	0.000	0.000
Stress-Strain Response:								
Stress Range, Init (Mpa)	567.1	714.2	683.0	737.8	512.3	512.1	448.6	439.7
" " " (psi)	82242.6	103579.0	99055.6	107002.0	74299.4	74276.1	65054.6	63763.8
Stress Range, Nf/2 (Mpa)	567.9	718.3	653.2	703.1	498.4	488.4	436.3	411.8
" " " (psi)	82361.7	104171.0	94731.9	101975.0	72279.9	70835.2	63279.0	59723.2
Mean Stress, Init (Mpa)	7.7	-6.3	7.2	-14.0	-19.5	-15.1	-10.6	-5.0
" " " (psi)	1123.1	-913.2	1040.1	-2030.2	-2833.4	-2193.6	-1533.0	-726.0
Mean Stress, Nf/2 (Mpa)	20.5	-20.1	3.5	-4.4	-5.7	-4.0	6.0	3.9
" " " (psi)	2978.6	-2910.5	501.4	-631.9	-831.8	-582.3	867.8	564.8
Inel Stn Rng, Init	0.000150	0.000354	0.000318	0.000236	0.000546	0.000637	0.000803	0.000856
Inel Stn Rng, Nf/2	0.000081	0.000306	0.000499	0.000443	0.000703	0.000703	0.000866	0.000918
Life Results:								
Initiation (cycles)	14017.	2019.	837.	427.	735.	848.	716.	624.
5% Load Drop (cycles)	26536.	5469.	2105.	1707.	1262.	1443.	1178.	1182.
10% Load Drop (cycles)	26777.	5634.	2156.	1824.	1315.	1479.	1223.	1231.
50% Load Drop (cycles)	27218.	5963.	2263.	2033.	1442.	1542.	1301.	1301.

Note: 1. Specimen 136B intially ran at 1 CPM for the first 63 cycles.

APPENDIX A-5

PWA 1455 ENVIRONMENTAL TESTING

BLOCK ATMOSPHERES: LAB AIR FIRST; 75 PSIA OXYGEN REMAINDER

Specimen Identification	140B	142B	142C	144A	139D
Type of Specimen	MERL 75	MERL 75	MERL 75	MERL 73C	MERL 73C
Test Conditions:					
Environment	AIR / 02	AIR / 02	AIR / 02	AIR / 02	AIR / 02
Block 1 Length (cycles)	1800.	300.	600.	800.	800.
Temperature (°C)	871.	871.	871.	982.	982.
" (°F)	1600.	1600.	1600.	1800.	1800.
Strain Range	0.004001	0.005250	0.005030	0.004006	0.004010
Strain R-Ratio (min/max)	-1.031	-0.964	-0.994	-1.014	-0.976
Strain Rate (1/sec)	1.67E-03	1.70E-04	1.70E-04	1.67E-03	2.30E-04
Frequency (cyc/min)	12.500	1.000	1.000	12.500	1.700
Tension Hold (sec)	0.000	0.000	0.000	0.000	0.000
Compression Hold (sec)	0.000	0.000	0.000	0.000	0.000
Stress-Strain Response:					
Stress Range, Init (Mpa)	561.4	680.0	670.8	499.0	435.2
" " " (psi)	81425.2	98621.9	97291.6	72371.7	63123.3
Stress Range, Nf/2 (Mpa)	545.9	646.3	630.1	484.8	436.3
" " " (psi)	79174.9	93738.6	91387.2	70309.1	63278.1
Mean Stress, Init (Mpa)	-6.3	5.8	-2.0	-14.0	-13.7
" " " (psi)	-910.2	846.6	-285.1	-2033.6	-1979.9
Mean Stress, Nf/2 (Mpa)	-3.4	-11.4	5.0	-0.8	1.3
" " " (psi)	-492.1	-1651.7	724.4	-111.3	188.0
Inel Stn Rng, Init	0.000083	0.000217	0.000241	0.000697	0.000911
Inel Stn Rng, Nf/2	0.000082	0.000514	0.000486	0.000740	0.000889
Life Results:					
Initiation (cycles)	18833.	597.	901.	806.	470.
5% Load Drop (cycles)	32025.	2050.	2370.	1207.	819.
10% Load Drop (cycles)	32424.	2065.	3085.	1327.	883.
50% Load Drop (cycles)	32753.	2093.	3278.	1521.	1119.

APPENDIX B-1

PWA 1455 MEAN STRESS TESTING

871°C (1600°F) BASELINE (ZERO MEAN)

Specimen Identification		110A	110C
Type of Specimen		MERL 75	MERL 75
Test Conditions:			
Temperature	(°C)	871.	871.
"	(°F)	1600.	1600.
Strain Range		0.003920	0.003920
Strain R-Ratio	(min/max)	-1.016	-1.014
Strain Rate	(1/sec)	1.63E-03	1.63E-03
Frequency	(cyc/min)	12.500	12.500
Tension Hold	(sec)	0.000	0.000
Compression Hold	(sec)	0.000	0.000
Stress-Strain Response:			
Stress Range, Init	(Mpa)	536.5	555.9
" " "	(psi)	77805.6	80617.1
Stress Range, Nf/2	(Mpa)	521.5	539.8
" " "	(psi)	75635.7	78291.3
Mean Stress, Init	(Mpa)	-15.5	-14.3
" " "	(psi)	-2253.0	-2081.0
Mean Stress, Nf/2	(Mpa)	-3.1	-1.3
" " "	(psi)	-449.7	-189.4
Inel Stn Rng, Init		0.000048	0.000065
Inel Stn Rng, Nf/2		0.000066	0.000062
Final Mean Strain		0.000000	0.000000
Life Results:			
Initiation	(cycles)	24182.[1]	24470.[2]
5% Load Drop	(cycles)	41520.[1]	42015.[2]
10% Load Drop	(cycles)	42888.[1]	43400.[2]
50% Load Drop	(cycles)	45626.[1]	46170.[2]

Notes: 1. Specimen 110A was discontinued at 19,000 cycles; the lives shown were estimated based on the available inspection results.

2. Specimen 110C was discontinued at 15,148 cycles; the lives shown were estimated based on the available inspection results.

APPENDIX B-2

PWA 1455 MEAN STRESS TESTING

871°C (1600°F) ISOTHERMAL

Specimen Identification	133C	135A	123C	127B	125B	127C	125A	125C
Type of Specimen	MERL 75	MERL 75	MERL 75	MERL 75	MERL 75	MERL 75	MERL 75	MERL 75
Test Conditions:								
Temperature (°C)	871.	871.	871.	871.	871.	871.	871.	871.
" (°F)	1600.	1600.	1600.	1600.	1600.	1600.	1600.	1600.
Strain Range	0.003450	0.003450	0.003880	0.003890	0.003900	0.004870	0.004850	0.005030
Strain R-Ratio (min/max)	0.637	0.791	0.250	0.381	0.582	0.424	0.267	0.715
Strain Rate (1/sec)	1.44E-03	1.44E-03	1.62E-03	1.62E-03	1.63E-03	2.06E-03	2.02E-03	2.10E-03
Frequency (cyc/min)	12.500	12.512	12.500	12.500	12.500	12.686	12.500	12.500
Tension Hold (sec)	0.000	0.000	0.000	0.000	0.000	0.000	0.000	0.000
Compression Hold (sec)	0.000	0.000	0.000	0.000	0.000	0.000	0.000	0.000
Stress-Strain Response:								
Stress Range, Init (Mpa)	444.8	462.6	533.0	467.7	520.3	688.7	661.1	678.6
" " " (psi)	64511.9	67090.0	77307.0	67825.0	75454.7	99886.9	95879.6	98422.8
Stress Range, Nf/2 (Mpa)	432.1	401.4	533.3	461.6	501.8	673.2	666.7	646.3
" " " (psi)	62668.7	58222.7	77348.6	66943.6	72774.5	97637.4	96699.0	93739.4
Mean Stress, Init (Mpa)	243.7	414.4	188.4	242.3	296.8	169.5	253.5	319.6
" " " (psi)	35338.8	60095.0	27322.5	35146.3	43044.2	24586.7	36763.4	46358.9
Mean Stress, Nf/2 (Mpa)	300.0	490.7	212.3	300.4	420.2	212.4	296.8	389.6
" " " (psi)	43510.4	71166.0	30795.3	43573.5	60944.7	30798.0	43048.5	56502.9
Inel Stn Rng, Init	0.000125	0.000141	0.000123	0.000109	0.000234	0.000291	0.000396	0.000455
Inel Stn Rng, Nf/2	0.000082	0.001229	0.000129	0.000107	0.000137	0.000253	0.000245	0.000316
Final Mean Strain	0.0110	0.0150	0.0084	0.0077	0.0178	0.0154	0.0086	0.0287
Life Results:								
Initiation (cycles)	3800.	246.	6791.	2043.	139.	1053.	234.	46.
5% Load Drop (cycles)	7658.	745.[1]	13784.	4648.	470.	2446.	700.	200.
10% Load Drop (cycles)	7886.	770.[1]	14095.	4822.	485.	2527.	734.	205.
50% Load Drop (cycles)	8207.	819.[1]	14448.	5108.	516.	2847.	780.	213.

Note: 1. Specimen 135A was discontinued at 301 cycles for SEM investigation of the crack morphology. The load drop lives shown were estimated based on the available inspection results.

APPENDIX B-3

PWA 1455 MEAN STRESS TESTING

760°C (1400°F) ISOTHERMAL

Specimen Identification	134B	133D	134A	134D
Type of Specimen	MERL 75	MERL 75	MERL 75	MERL 75
Test Conditions:				
Temperature (°C)	760.	760.	760.	760.
" (°F)	1400.	1400.	1400.	1400.
Strain Range	0.003870	0.004860	0.004950	0.006830
Strain R-Ratio (min/max)	0.251	0.111	0.662	-0.021
Strain Rate (1/sec)	1.61E-03	2.03E-03	2.06E-03	2.85E-03
Frequency (cyc/min)	12.500	12.500	12.500	12.500
Tension Hold (sec)	0.000	0.000	0.000	0.000
Compression Hold (sec)	0.000	0.000	0.000	0.000
Stress-Strain Response:				
Stress Range, Init (Mpa)	648.3	679.7	752.0	973.0
" " " (psi)	94030.6	98574.3	109060.0	141122.0
Stress Range, Nf/2 (Mpa)	592.7	672.8	732.5	964.4
" " " (psi)	85957.4	97580.4	106233.0	139866.0
Mean Stress, Init (Mpa)	294.4	205.9	132.6	156.5
" " " (psi)	42698.7	29865.7	19230.5	22696.7
Mean Stress, Nf/2 (Mpa)	299.7	301.6	429.6	215.9
" " " (psi)	43467.8	43741.2	62313.3	31316.1
Inel Stn Rng, Init	0.000045	0.000113	0.000048	0.000052
Inel Stn Rng, Nf/2	0.000005	0.000034	0.000093	0.000083
Final Mean Strain	0.0030	0.0030	0.0160	0.0052
Life Results:				
Initiation (cycles)	4809.	3413.	631.	584.
5% Load Drop (cycles)	9500.	7700.	1700.	1682.
10% Load Drop (cycles)	10000.	7850.	1750.	1717.
50% Load Drop (cycles)	10930.	8126.	1855.	1770.

APPENDIX B-4

PWA 1455 MEAN STRESS TESTING

982°C (1800°F) ISOTHERMAL

Specimen Identification	135B	127A	135C	134C	135D	126B
Type of Specimen	MERL 75	MERL 75	MERL 75	MERL 75	MERL 75	MERL 75
Test Conditions:						
Temperature (°C)	982.	982.	982.	982.	982.	982.
" (°F)	1800.	1800.	1800.	1800.	1800.	1800.
Strain Range	0.002860	0.002940	0.003430	0.003451	0.003830	0.004040
Strain R-Ratio (min/max)	0.592	0.731	0.686	0.899	0.307	0.725
Strain Rate (1/sec)	1.19E-03	1.22E-03	1.43E-03	1.44E-03	1.59E-03	1.68E-03
Frequency (cyc/min)	12.500	12.500	12.500	12.500	12.500	12.500
Tension Hold (sec)	0.000	0.000	0.000	0.000	0.000	0.000
Compression Hold (sec)	0.000	0.000	0.000	0.000	0.000	0.000
Stress-Strain Response:						
Stress Range, Init (Mpa)	409.7	395.9	403.9	404.9	422.5	458.1
" " " (psi)	59425.5	57418.7	58576.7	58728.2	61274.6	66439.9
Stress Range, Nf/2 (Mpa)	396.8	374.2	385.1	406.7	404.5	440.8
" " " (psi)	57547.3	54264.1	55852.1	58986.2	58659.3	63930.1
Mean Stress, Init (Mpa)	59.3	108.1	67.5	71.2	56.6	78.6
" " " (psi)	8593.7	15683.9	9788.0	10327.6	8208.7	11406.7
Mean Stress, Nf/2 (Mpa)	95.3	157.7	154.4	178.6	94.7	171.8
" " " (psi)	13818.2	22873.1	22395.0	25901.4	13735.1	24912.1
Inel Stn Rng, Init	0.000297	0.000221	0.000398	0.000393	0.000139	0.000692
Inel Stn Rng, Nf/2	0.000227	0.000195	0.000291	0.000364	0.000250	0.000429
Final Mean Strain	0.0260	0.0470	0.0400	0.0260	0.0220	0.0570
Life Results:						
Initiation (cycles)	2313.	788.	388.	139.	1692.	76.
5% Load Drop (cycles)	5019.	2478.	1000.	458.	3274.	361.
10% Load Drop (cycles)	5552.	2500.	1040.	522.	3846.	367.
50% Load Drop (cycles)	6252.	2543.	1386.	604.	4833.	380.

APPENDIX B-5

PWA 1455 MEAN STRESS TESTING

LOAD CONTROLLED TMF

Specimen Identification	109C	110D	111B	114B	112B
Type of Specimen	MERL 73C	MERL 73C	MERL 73C	MERL 73C	MERL 73C
Test Conditions:					
Cycle Type	IN	IN	IN	IN	OUT
Temperature Range (°C)	538-871	538-871	538-871	538-871	538-871
" " (°F)	1000-1600	1000-1600	1000-1600	1000-1600	1000-1600
Stress Range (Mpa)	671.5	671.3	670.5	604.2	698.1
" " (psi)	97382.6	97366.4	97238.7	87622.9	101251.0
Stress R-Ratio (min/max)	-0.2503	-0.6678	-1.5063	-0.5002	-1.5002
Stress Rate (Mpa/sec)	2.24E+01	2.24E+01	2.23E+01	2.01E+01	2.33E+01
" " (psi/sec)	3.25E+03	3.25E+03	3.24E+03	2.92E+03	3.38E+03
Frequency (cyc/min)	1.000	1.000	1.000	1.000	1.000
Tension Hold (sec)	0.000	0.000	0.000	0.000	0.000
Compression Hold (sec)	0.000	0.000	0.000	0.000	0.000
Stress-Strain Response:					
Strain Range, Init	0.004150	0.004150	0.004040	0.003730	0.004230
Strain Range, Nf/2	0.004250	0.004310	0.003950	0.003740	0.004240
Mean Strain, Init	0.002040	0.001200	-.000090	0.000860	-.000590
Mean Strain, Nf/2	0.006570	0.005010	0.000520	0.007210	-.003790
Inel Stn Rng, Init	0.000200	0.000148	0.000176	0.000154	0.000193
Inel Stn Rng, Nf/2	0.000142	0.000185	0.000189	0.000124	0.000073
Life Results:					
Initiation (cycles)	177.	1914.	5611.	5765.	2684.
5% Load Drop (cycles)	213.	2331.	>16503.[1]	7095.	6709.
10% Load Drop (cycles)	218.	2380.	>16503.[1]	7244.	6850.
50% Load Drop (cycles)	227.	2454.	>16503.[1]	7468.	7062.

Note: 1. Specimen 111B was discontinued at 16,503 cycles with a 0.071 in. crack.

APPENDIX C-1

INCO 718 ISOTHERMAL TESTING

649°C (1200°F) BASELINE

Specimen Identification		71811	71812	71818	7184	7183	71822
Type of Specimen		MERL 75	MERL 75	MERL 75	MERL 75	MERL 75	MERL 75
Test Conditions:							
Temperature	(°C)	649.	649.	649.	649.	649.	649.
"	(°F)	1200.	1200.	1200.	1200.	1200.	1200.
Strain Range		0.006557	0.008040	0.010130	0.006460	0.007950	0.010000
Strain R-Ratio	(min/max)	-0.998	-1.003	-0.992	-0.991	-0.994	-1.001
Strain Rate	(1/sec)	6.56E-03	8.04E-03	1.01E-02	2.20E-04	2.60E-04	3.30E-04
Frequency	(cyc/min)	30.000	30.000	30.000	1.000	1.000	1.000
Tension Hold	(sec)	0.000	0.000	0.000	0.000	0.000	0.000
Compression Hold	(sec)	0.000	0.000	0.000	0.000	.0.000	0.000
Stress-Strain Response:							
Stress Range, Init	(Mpa)	1000.2	1248.4	1497.6	1039.5	1240.4	1454.9
" " "	(psi)	145065.0	181055.0	217200.0	150766.0	179896.0	211005.0
Stress Range, Nf/2	(Mpa)	968.3	1073.5	1166.1	991.4	1102.2	1186.6
" " "	(psi)	140442.0	155696.0	169117.0	143786.0	159862.0	172089.0
Mean Stress, Init	(Mpa)	0.6	-16.0	-56.9	-5.7	-15.1	-3.4
" " "	(psi)	86.4	-2323.9	-8250.2	-829.3	-2187.1	-497.7
Mean Stress, Nf/2	(Mpa)	6.6	-4.3	-20.0	14.3	-0.8	-6.3
" " "	(psi)	951.3	-624.0	-2906.2	2079.3	-117.0	-918.2
Inel Stn Rng, Init		0.000065	0.000213	0.001158	0.000121	0.000132	0.000108
Inel Stn Rng, Nf/2		0.000557	0.001530	0.003049	0.000354	0.001163	0.002717
Life Results:							
Initiation	(cycles)	9633.	2702.	1133.	11066.	2122.	793.
5% Load Drop	(cycles)	13202.	4015.	1720.	13180.	2725.	1020.
10% Load Drop	(cycles)	13400.	4121.	1736.	13224.	2782.	1028.
50% Load Drop	(cycles)	13762.	4323.	1785.	13332.	2868.	1072.

APPENDIX C-2

INCO 718 ISOTHERMAL TESTING

732°C (1350°F) BASELINE

Specimen Identification	71825	71819	71820	71829B[1]	71821	7182	7181	71823
Type of Specimen	MERL 75	MERL 75	MERL 75	MERL 75	MERL 75	MERL 75	MERL 75	MERL 75
Test Conditions:								
Temperature (°C)	732.	732.	732.	732.	732.	732.	732.	732.
" (°F)	1350.	1350.	1350.	1350.	1350.	1350.	1350.	1350.
Strain Range	0.005454	0.006538	0.008050	0.007951	0.010110	0.006460	0.007830	0.010010
Strain R-Ratio (min/max)	-1.005	-1.005	-1.002	-1.005	-0.993	-0.988	-1.007	-0.998
Strain Rate (1/sec)	5.45E-03	6.54E-03	8.05E-03	7.95E-03	1.01E-02	2.20E-04	2.60E-04	3.30E-04
Frequency (cyc/min)	30.000	30.000	30.000	30.000	30.000	1.000	1.000	1.000
Tension Hold (sec)	0.000	0.000	0.000	0.000	0.000	0.000	0.000	0.000
Compression Hold (sec)	0.000	0.000	0.000	0.000	0.000	0.000	0.000	0.000
Stress-Strain Response:								
Stress Range, Init (Mpa)	850.0	1016.6	1195.7	1201.0	1392.4	1012.9	1143.5	1358.7
" " " (psi)	123273.0	147441.0	173409.0	174184.0	201944.0	146908.0	165849.0	197053.0
Stress Range, Nf/2 (Mpa)	825.0	932.5	1055.7	1130.4	1105.8	888.1	956.1	1101.8
" " " (psi)	119658.0	135250.0	153117.0	163940.0	160383.0	128797.0	138668.0	159797.0
Mean Stress, Init (Mpa)	-0.7	-13.4	-15.1	15.9	-14.1	1.4	-15.1	-15.7
" " " (psi)	-94.9	-1945.9	-2187.0	2298.9	-2040.6	198.8	-2193.0	-2281.7
Mean Stress, Nf/2 (Mpa)	0.6	-14.2	-9.7	23.1	-6.7	1.9	9.8	-17.1
" " " (psi)	87.3	-2060.2	-1402.6	3353.7	-965.3	278.3	1414.1	-2473.3
Inel Stn Rng, Init	0.000053	0.000045	0.000316	0.000488	0.001256	0.000125	0.000231	0.000875
Inel Stn Rng, Nf/2	0.000237	0.000631	0.001289	0.000943	0.003172	0.000810	0.001577	0.002912
Life Results:								
Initiation (cycles)	169670.	7052.	2312.	2000.[1]	636.	4719.	1339.	437.
5% Load Drop (cycles)	169670.	8826.	3540.	3123.[1]	1012.	6181.	2792.	572.
10% Load Drop (cycles)	169670.	8955.	3567.	3183.[1]	1050.	6311.	2851.	575.
50% Load Drop (cycles)	169670.	9159.	3612.	3240.[1]	1115.	6506.	2939.	590.

Note: 1. Specimen 71829 was inadvertently run at 1350°F, 0.40% strain range, R=0, with one minute tension hold for 1194 cycles before being run to completion at the conditions shown. These cycles are NOT included in the lives listed here.

APPENDIX C-3

INCO 718 ISOTHERMAL TESTING

316 & 482°C (600 & 900°F) BASELINE

Specimen Identification		71815	71816	71817	71813	71814
Type of Specimen		MERL 75	MERL 75	MERL 75	MERL 75	MERL 75
Test Conditions:						
Temperature	(°C)	316.	316.	316.	482.	482.
"	(°F)	600.	600.	600.	900.	900.
Strain Range		0.006556	0.008036	0.010135	0.006540	0.010068
Strain R-Ratio (min/max)		-1.009	-1.003	-1.013	-0.998	-1.002
Strain Rate	(1/sec)	6.56E-03	8.04E-03	1.01E-02	6.54E-03	1.01E-02
Frequency	(cyc/min)	30.000	30.000	30.000	30.000	30.000
Tension Hold	(sec)	0.000	0.000	0.000	0.000	0.000
Compression Hold	(sec)	0.000	0.000	0.000	0.000	0.000
Stress-Strain Response:						
Stress Range, Init	(Mpa)	1132.1	1381.3	1468.9	1100.5	1430.4
" " "	(psi)	164185.0	200337.0	213034.0	159609.0	207455.0
Stress Range, Nf/2	(Mpa)	1140.3	1335.0	1396.3	1107.9	1369.4
" " "	(psi)	165381.0	193622.0	202503.0	160686.0	198604.0
Mean Stress, Init	(Mpa)	-20.6	-14.7	-21.1	-10.0	-10.6
" " "	(psi)	-2990.4	-2133.8	-3056.6	-1447.5	-1534.2
Mean Stress, Nf/2	(Mpa)	-5.3	-16.9	-23.2	5.6	-13.4
" " "	(psi)	-769.9	-2451.7	-3357.9	807.0	-1936.6
Inel Stn Rng, Init		0.000061	0.000469	0.002025	0.000064	0.001597
Inel Stn Rng, Nf/2		0.000087	0.000775	0.002535	0.000153	0.002345
Life Results:						
Initiation	(cycles)	15839.	6740.	3349.	13617.	2231.
5% Load Drop	(cycles)	21006.	11540.	5201.	19222.	3884.
10% Load Drop	(cycles)	21406.	11639.	5279.	19627.	3938.
50% Load Drop	(cycles)	21999.	11824.	5401.	20234.	4020.

APPENDIX C-4

INCO 718 ISOTHERMAL TESTING

R-RATIO EFFECTS

Specimen Identification	71830	71827	71828	71826	71810
Type of Specimen	MERL 75	MERL 75	MERL 75	MERL 75	MERL 75
Test Conditions:					
Temperature (°C)	316.	649.	649.	732.	732.
" (°F)	600.	1200.	1200.	1350.	1350.
Strain Range	0.006458	0.006448	0.006450	0.006430	0.006430
Strain R-Ratio (min/max)	0.005	0.005	-3390.690	0.001	617.275
Strain Rate (1/sec)	6.46E-03	6.45E-03	6.45E-03	2.10E-04	2.10E-04
Frequency (cyc/min)	30.000	30.000	30.000	1.001	1.001
Tension Hold (sec)	0.000	0.000	0.000	0.000	0.000
Compression Hold (sec)	0.000	0.000	0.000	0.000	0.000
Stress-Strain Response:					
Stress Range, Init (Mpa)	1063.1	1080.3	1081.9	995.2	1011.1
" " " (psi)	154188.0	156675.0	156912.0	144339.0	146649.0
Stress Range, Nf/2 (Mpa)	1049.1	1019.6	1053.7	886.7	897.4
" " " (psi)	152150.0	147872.0	152825.0	128597.0	130156.0
Mean Stress, Init (Mpa)	231.6	237.3	-277.8	254.3	-279.0
" " " (psi)	33588.1	34417.5	-40295.8	36889.0	-40468.0
Mean Stress, Nf/2 (Mpa)	190.2	207.1	-163.3	65.0	-72.1
" " " (psi)	27580.8	30041.3	-23679.1	9422.9	-10457.7
Inel Stn Rng, Init	0.000131	0.000088	0.000097	0.000220	0.000165
Inel Stn Rng, Nf/2	0.000292	0.000344	0.000426	0.000825	0.000770
Life Results:					
Initiation (cycles)	13157.	7608.	20000.	3526.	4646.
5% Load Drop (cycles)	17258.	9767.	29259.	4250.	6435.
10% Load Drop (cycles)	17752.	9835.	29824.	4340.	6479.
50% Load Drop (cycles)	18023.	10011.	31056.	4521.	7260.

APPENDIX C-5

INCO 718 ISOTHERMAL TESTING

HOLD TIME EFFECTS

Specimen Identification		7185	71831	7188	7189	7186	7187
Type of Specimen		MERL 75	MERL 75	MERL 75	MERL 75	MERL 75	MERL 75
Test Conditions:							
Temperature	(°C)	649.	649.	649.	649.	732.	732.
"	(°F)	1200.	1200.	1200.	1200.	1350.	1350.
Strain Range		0.006354	0.006490	0.007820	0.007964	0.006340	0.006461
Strain R-Ratio (min/max)		-0.942	-0.003	-0.948	-1.003	-0.943	-1.004
Strain Rate	(1/sec)	1.84E-04	2.00E-04	2.00E-05	1.74E-05	1.80E-04	1.72E-04
Frequency	(cyc/min)	0.870	0.909	0.066	0.066	0.869	0.800
Tension Hold	(sec)	60.000	65.497	900.000	0.000	60.000	0.000
Compression Hold	(sec)	0.000	0.000	0.000	900.000	0.000	60.000
Stress-Strain Response:							
Stress Range, Init	(Mpa)	1009.8	1103.1	1233.5	1266.0	984.9	974.1
" " "	(psi)	146447.0	159984.0	178891.0	183612.0	142836.0	141281.0
Stress Range, Nf/2	(Mpa)	969.7	1032.5	1155.4	1184.8	922.7	940.7
" " "	(psi)	140641.0	149740.0	167571.0	171830.0	133823.0	136438.0
Mean Stress, Init	(Mpa)	-2.7	253.2	-26.7	28.5	-24.3	4.3
" " "	(psi)	-397.4	36728.3	-3875.4	4138.1	-3525.4	630.6
Mean Stress, Nf/2	(Mpa)	-30.2	118.1	-23.4	131.9	-49.7	113.2
" " "	(psi)	-4382.1	17133.0	-3398.0	19128.8	-7213.0	16423.6
Inel Stn Rng, Init		0.000155	0.000188	0.000319	0.000289	0.000169	0.000172
Inel Stn Rng, Nf/2		0.000367	0.000345	0.000946	0.000647	0.000604	0.000676
Hold Sts Rlx, Init	(Mpa)	-4.8	-36.5	-7.7	+8.7	-6.4	+5.7
" " " "	(psi)	-690.0	-5300.0	-1110.0	+1260.0	-930.0	+830.0
Hold Sts Rlx, Nf/2	(Mpa)	-9.5	-16.8	-15.1	+28.0	-31.9	+33.0
" " " "	(psi)	-1380.0	-2440.0	-2190.0	+4060.0	-4630.0	+4780.0
Life Results:							
Initiation	(cycles)	10593.	6735.[1]	572.	1115.	1531.	1318.
5% Load Drop	(cycles)	13469.	8353.[1]	634.	1582.	2086.	2797.
10% Load Drop	(cycles)	13517.	8531.[1]	655.	1670.	2130.	2856.
50% Load Drop	(cycles)	13668.	8886.[1]	689.	1751.	2219.	3012.

Note: 1. The extensometer slipped on specimen 71831 at 5660 cycles, which ended the test prematurely. The life results shown here are estimates based on the last available inspection results.

APPENDIX D-1
INCO 718 TMF TESTING
OUT-OF-PHASE CYCLES

Specimen Identification	7181T	7182T	7189T	71811T	7185T	71813T	71815T	71816T
Type of Specimen	MERL 73C	MERL 73C	MERL 73C	MERL 73C	MERL 73C	MERL 73C	MERL 73C	MERL 73C
Test Conditions:								
Cycle Type	OUT	OUT	OUT	OUT	OUT	OUT	OUT	OUT
Temperature Range (°C)	316-649	316-649	316-649	316-732	316-732	316-732	316-732	316-732
" " (°F)	600-1200	600-1200	600-1200	600-1350	600-1350	600-1350	600-1350	600-1350
Strain Range	0.006380	0.008000	0.009980	0.005510	0.006510	0.008000	0.006510	0.006550
Strain R-Ratio (min/max)	-0.967	-1.004	-1.006	-0.999	-1.007	-1.007	-0.002	-224.188
Strain Rate (1/sec)	2.10E-04	2.70E-04	3.30E-04	1.80E-04	2.20E-04	2.70E-04	2.20E-04	2.20E-04
Frequency (cyc/min)	1.000	1.000	1.000	1.000	1.000	1.000	1.000	1.000
Tension Hold (sec)	0.000	0.000	0.000	0.000	0.000	0.000	0.000	0.000
Compression Hold (sec)	0.000	0.000	0.000	0.000	0.000	0.000	0.000	0.000
Stress-Strain Response:								
Stress Range, Init (Mpa)	1031.5	1328.8	1569.7	949.7	1155.0	1313.8	1084.1	1128.3
" " " (psi)	149605.0	192725.0	227663.0	137743.0	167509.0	190548.0	157235.0	163638.0
Stress Range, Nf/2 (Mpa)	1063.5	1224.9	1314.3	967.9	1114.1	1160.0	1077.4	1123.9
" " " (psi)	154249.0	177654.0	190619.0	140381.0	161579.0	168238.0	156253.0	163002.0
Mean Stress, Init (Mpa)	57.2	45.9	14.2	96.1	143.2	81.9	285.8	-200.3
" " " (psi)	8299.6	6662.4	2065.2	13931.9	20762.6	11875.2	41451.2	-29044.2
Mean Stress, Nf/2 (Mpa)	152.9	60.0	7.4	187.2	171.2	190.7	273.7	133.1
" " " (psi)	22182.7	8702.5	1077.2	27151.5	24829.9	27664.0	39700.7	19297.0
Inel Stn Rng, Init	0.000111	0.000115	0.000768	0.000031	0.000112	0.000176	0.000141	0.000079
Inel Stn Rng, Nf/2	0.000141	0.001558	0.001531	0.000404	0.000259	0.000053	0.000511	0.000490
Life Results:								
Initiation (cycles)	12311.[1]	3008.	1704.	7969.	1251.	2196.	3349.	2450.
5% Load Drop (cycles)	17456.[1]	4427.	2319.	9555.	2612.	2820.	4050.	4110.
10% Load Drop (cycles)	17824.[1]	4434.	2331.	9570.	2668.	2830.	4065.	4125.
50% Load Drop (cycles)	18375.[1]	4487.	2434.	9601.	2779.	2852.	4084.	4152.

Note: 1. Specimen 7181T failed prematurely at 10,964 cycles in the buttonhead grip.
The lives shown were estimated based on the available inspection results.

APPENDIX D-2
INCO 718 TMF TESTING
IN-PHASE CYCLES

Specimen Identification	7183T	7184T	71810T	71812T	7186T	71814T
Type of Specimen	MERL 73C	MERL 73C	MERL 73C	MERL 73C	MERL 73C	MERL 73C
Test Conditions:						
Cycle Type	IN	IN	IN	IN	IN	IN
Temperature Range (°C)	316-649	316-649	316-649	316-732	316-732	316-732
" " (°F)	600-1200	600-1200	600-1200	600-1350	600-1350	600-1350
Strain Range	0.006450	0.007900	0.009950	0.005440	0.006460	0.007964
Strain R-Ratio (min/max)	-0.993	-0.997	-0.999	-0.993	-1.005	-1.003
Strain Rate (1/sec)	2.20E-04	2.63E-04	3.30E-04	1.80E-04	2.20E-04	2.65E-04
Frequency (cyc/min)	1.000	1.000	1.000	1.000	1.000	1.000
Tension Hold (sec)	0.000	0.000	0.000	0.000	0.000	0.000
Compression Hold (sec)	0.000	0.000	0.000	0.000	0.000	0.000
Stress-Strain Response:						
Stress Range, Init (Mpa)	1051.0	1302.2	1541.1	871.3	1099.5	1287.7
" " " (psi)	152436.0	188865.0	223517.0	126362.0	159464.0	186753.0
Stress Range, Nf/2 (Mpa)	1087.2	1216.8	1370.5	875.9	1141.1	1257.2
" " " (psi)	157683.0	176473.0	198772.0	127041.0	165502.0	182329.0
Mean Stress, Init (Mpa)	-26.7	-29.7	-52.9	-18.6	4.7	-63.4
" " " (psi)	-3874.4	-4312.2	-7677.6	-2696.3	675.7	-9192.9
Mean Stress, Nf/2 (Mpa)	-46.9	-44.3	-72.7	-169.7	-153.6	-140.7
" " " (psi)	-6807.7	-6421.3	-10543.2	-24607.9	-22281.5	-20401.0
Inel Stn Rng, Init	0.000118	0.000191	0.001196	0.000085	0.000101	0.000272
Inel Stn Rng, Nf/2	0.000166	0.000748	0.002250	0.000047	0.000127	0.001333
Life Results:						
Initiation (cycles)	15641.	4186.	518.	18939.	2946.[1]	558.
5% Load Drop (cycles)	16935.	4553.	681.	20574.	3337.[1]	703.
10% Load Drop (cycles)	16950.	4767.	703.	20578.	3408.[1]	720.
50% Load Drop (cycles)	17001.	4983.	740.	20586.	3550.[1]	744.

Note: 1. Specimen 7186T failed prematurely at 2946 cycles due to a crack from the ID.
The lives shown were estimated based on the available inspection results.

APPENDIX D-3

INCO 718 TMF TESTING

ELLIPTICAL CYCLES

Specimen Identification		7188T	71817T	7187T	71818T
Type of Specimen		MERL 73C	MERL 73C	MERL 73C	MERL 73C
Test Conditions:					
Cycle Type		CW	CW	CCW	CCW
Temperature Range	(°C)	316-649	316-732	316-649	316-732
" "	(°F)	600-1200	600-1350	600-1200	600-1350
Strain Range		0.006440	0.006450	0.006450	0.006480
Strain R-Ratio (min/max)		-0.999	-1.002	-0.997	-0.996
Strain Rate	(1/sec)	2.10E-04	2.20E-04	2.20E-04	2.20E-04
Frequency	(cyc/min)	1.000	1.000	1.000	1.000
Tension Hold	(sec)	0.000	0.000	0.000	0.000
Compression Hold	(sec)	0.000	0.000	0.000	0.000
Stress-Strain Response:					
Stress Range, Init	(Mpa)	1045.7	1064.9	1151.3	1042.8
" " "	(psi)	151655.0	154452.0	166982.0	151233.0
Stress Range, Nf/2	(Mpa)	1090.8	1079.3	1153.3	1025.0
" " "	(psi)	158195.0	156540.0	167271.0	148660.0
Mean Stress, Init	(Mpa)	16.6	37.7	19.8	-2.3
" " "	(psi)	2405.0	5473.3	2869.5	-326.7
Mean Stress, Nf/2	(Mpa)	171.7	159.8	93.8	153.9
" " "	(psi)	24905.9	23171.2	13609.6	22324.0
Inel Stn Rng, Init		0.000123	0.000107	0.000111	0.000041
Inel Stn Rng, Nf/2		0.000044	0.000097	0.000230	0.000328
Life Results:					
Initiation	(cycles)	16614.[1]	6022.	11435.	19196.[2]
5% Load Drop	(cycles)	17552.[1]	7780.	13200.	23807.[2]
10% Load Drop	(cycles)	17922.[1]	7800.	13218.	24308.[2]
50% Load Drop	(cycles)	18476.[1]	7821.	13297.	25060.[2]

Notes: 1. Specimen 7188T failed prematurely at 12,158 cycles due to a crack in the buttonhead grip. The lives shown were estimated based on the available inspection results.

2. Specimen 71818T experienced a catastrophic overtemperature at 18,554 cycles when a workman bumped the pyrometer. The lives shown were estimated based on available inspection results.

APPENDIX D-4

INCO 718 TMF TESTING

LOAD CONTROLLED CYCLES

Specimen Identification		71819T	71820T
Type of Specimen		MERL 73C	MERL 73C
Test Conditions:			
Cycle Type		IN	IN
Temperature Range	(°C)	316-649	316-732
" "	(°F)	600-1200	600-1350
Stress Range	(Mpa)	1027.5	890.7
" "	(psi)	149015.0	129178.0
Stress R-Ratio	(min/max)	-0.6655	-0.9973
Stress Rate	(Mpa/sec)	3.43E+01	2.97E+01
" "	(psi/sec)	4.97E+03	4.31E+03
Frequency	(cyc/min)	1.000	1.000
Tension Hold	(sec)	0.000	0.000
Compression Hold	(sec)	0.000	0.000
Stress-Strain Response:			
Strain Range, Init		0.006546	0.005681
Strain Range, Nf/2		0.007282	0.005408
Mean Strain, Init		0.001854	0.000256
Mean Strain, Nf/2		0.007284	0.004059
Inel Stn Rng, Init		0.000318	0.000248
Inel Stn Rng, Nf/2		0.000794	0.000215
Life Results:			
Initiation	(cycles)	3084.	8229.
5% Load Drop	(cycles)	3310.	8400.
10% Load Drop	(cycles)	3340.	8420.
50% Load Drop	(cycles)	3427.	8484.

APPENDIX E-1

INCO 718 MULTIAXIAL TESTING

AXIAL OR TORSION ONLY

Specimen Identification		307	303	310
Type of Specimen		LED 41825	LED 41825	LED 41825
Test Conditions:				
Temperature	(°C)	649.	693.	693.
"	(°F)	1200.	1280.	1280.
Axial Strain Range		0.006580	0.000000	0.000000
Axial Strain R-Ratio	(min/max)	-0.999	0.000	0.000
Axial Strain Rate	(1/sec)	6.58E-03	0.00E+00	0.00E+00
Torsional Strain Range		0.000000	0.013200	0.016260
Torsional Strain R-Ratio	(min/max)	0.000	-1.000	-1.000
Torsional Strain Rate	(1/sec)	0.00E+00	1.32E-02	1.63E-02
Strain Ratio	(torsional/axial)	0.000	0.000	0.000
Strain Phase Angle	(degrees)	0.000	0.000	0.000
Frequency	(cyc/min)	30.000	30.000	30.000
Axial Stress-Strain Response:				
Stress Range, Init	(Mpa)	1001.3	0.0	0.0
" " "	(psi)	145216.0	0.0	0.0
Stress Range, Nf/2	(Mpa)	982.9	0.0	0.0
" " "	(psi)	142549.0	0.0	0.0
Mean Stress, Init	(Mpa)	-2.0	0.0	0.0
" " "	(psi)	-285.0	0.0	0.0
Mean Stress, Nf/2	(Mpa)	-2.2	0.0	0.0
" " "	(psi)	-314.0	0.0	0.0
Inel Stn Rng, Init		0.000046	0.000000	0.000000
Inel Stn Rng, Nf/2		0.000325	0.000000	0.000000
Torsional Stress-Strain Response:				
Stress Range, Init	(Mpa)	0.0	721.0	800.1
" " "	(psi)	0.0	104570.0	116036.0
Stress Range, Nf/2	(Mpa)	0.0	600.2	636.7
" " "	(psi)	0.0	87045.9	92345.4
Mean Stress, Init	(Mpa)	0.0	-0.2	-3.6
" " "	(psi)	0.0	-24.0	-525.0
Mean Stress, Nf/2	(Mpa)	0.0	0.2	-1.5
" " "	(psi)	0.0	25.9	-214.0
Inel Stn Rng, Init		0.000000	0.000996	0.002403
Inel Stn Rng, Nf/2		0.000000	0.002981	0.005272
Life Results:				
Initiation (0.030 in.)	(cycles)	5344.	3975.	2220.
5% Tensile Load Drop	(cycles)	6684.	4572.	3442.
10% Tensile Load Drop	(cycles)	6897.	4674.	3514.
50% Tensile Load Drop	(cycles)	7764.	4848.	3685.
Actual End of Test	(cycles)	8903.	5000.	3691.

APPENDIX E-2

INCO 718 MULTIAXIAL TESTING

IN-PHASE TENSION/TORSION

Specimen Identification		301	308	306
Type of Specimen		LED 41825	LED 41825	LED 41825
Test Conditions:				
Temperature	(°C)	693.	649.	649.
"	(°F)	1280.	1200.	1200.
Axial Strain Range		0.005060	0.006130	0.006010
Axial Strain R-Ratio	(min/max)	-0.998	-0.995	-1.001
Axial Strain Rate	(1/sec)	5.06E-03	6.13E-03	2.00E-04
Torsional Strain Range		0.007500	0.009100	0.008970
Torsional Strain R-Ratio	(min/max)	-1.001	-1.003	-0.999
Torsional Strain Rate	(1/sec)	7.50E-03	9.10E-03	3.00E-04
Strain Ratio	(torsional/axial)	1.482	1.485	1.493
Strain Phase Angle	(degrees)	0.000	0.000	0.000
Frequency	(cyc/min)	30.000	30.000	1.000
Axial Stress-Strain Response:				
Stress Range, Init	(Mpa)	736.8	933.9	922.4
" " "	(psi)	106857.0	135449.0	133777.0
Stress Range, Nf/2	(Mpa)	715.3	828.4	834.4
" " "	(psi)	103744.0	120145.0	121018.0
Mean Stress, Init	(Mpa)	7.3	9.7	-7.8
" " "	(psi)	1057.5	1400.5	-1124.5
Mean Stress, Nf/2	(Mpa)	-17.8	-0.4	-0.4
" " "	(psi)	-2576.5	-61.5	-61.8
Inel Stn Rng, Init		0.000009	0.000119	0.000198
Inel Stn Rng, Nf/2		0.000419	0.000971	0.000743
Torsional Stress-Strain Response:				
Stress Range, Init	(Mpa)	410.8	513.6	508.2
" " "	(psi)	59582.0	74491.9	73708.9
Stress Range, Nf/2	(Mpa)	384.2	447.6	452.0
" " "	(psi)	55720.0	64922.3	65558.1
Mean Stress, Init	(Mpa)	-4.7	-6.0	-7.6
" " "	(psi)	-683.0	-870.0	-1098.5
Mean Stress, Nf/2	(Mpa)	-8.5	-17.1	-8.8
" " "	(psi)	-1233.5	-2478.1	-1271.0
Inel Stn Rng, Init		0.000016	0.000172	0.000675
Inel Stn Rng, Nf/2		0.000697	0.001603	0.001297
Life Results:				
Initiation (0.030 in.)	(cycles)	3865.	3404.	2069.
5% Tensile Load Drop	(cycles)	4550.	4806.	2453.
10% Tensile Load Drop	(cycles)	4629.	4940.	2464.
50% Tensile Load Drop	(cycles)	5102.	5305.	2470.
Actual End of Test	(cycles)	7000.	5800.	2470.

APPENDIX E-3

INCO 718 MULTIAXIAL TESTING

OUT-OF-PHASE TENSION/TORSION

Specimen Identification		302	305	304
Type of Specimen		LED 41825	LED 41825	LED 41825
Test Conditions:				
Temperature	(°C)	693.	693.	693.
"	(°F)	1280.	1280.	1280.
Axial Strain Range		0.006580	0.008090	0.008010
Axial Strain R-Ratio	(min/max)	-0.997	-0.993	-1.000
Axial Strain Rate	(1/sec)	6.58E-03	8.09E-03	2.70E-04
Torsional Strain Range		0.009880	0.012230	0.012070
Torsional Strain R-Ratio	(min/max)	-0.994	-1.003	-1.003
Torsional Strain Rate	(1/sec)	9.88E-03	1.22E-02	4.00E-04
Strain Ratio	(torsional/axial)	1.502	1.512	1.507
Strain Phase Angle	(degrees)	90.000	90.000	90.000
Frequency	(cyc/min)	30.000	30.000	1.000
Axial Stress-Strain Response:				
Stress Range, Init	(Mpa)	975.4	1208.6	1235.8
" " "	(psi)	141459.0	175284.0	179232.0
Stress Range, Nf/2	(Mpa)	961.7	1142.8	1137.8
" " "	(psi)	139471.0	165737.0	165011.0
Mean Stress, Init	(Mpa)	-14.6	-37.4	-46.6
" " "	(psi)	-2124.5	-5424.0	-6762.0
Mean Stress, Nf/2	(Mpa)	-15.9	-21.2	-28.5
" " "	(psi)	-2300.2	-3080.8	-4138.2
Inel Stn Rng, Init		0.000129	0.000176	0.000241
Inel Stn Rng, Nf/2		0.000250	0.000498	0.000985
Torsional Stress-Strain Response:				
Stress Range, Init	(Mpa)	560.9	687.1	672.4
" " "	(psi)	81351.9	99656.9	97525.9
Stress Range, Nf/2	(Mpa)	536.6	667.0	616.2
" " "	(psi)	77829.6	96743.4	89362.0
Mean Stress, Init	(Mpa)	-2.0	-2.8	-8.4
" " "	(psi)	-287.0	-403.5	-1219.0
Mean Stress, Nf/2	(Mpa)	-6.3	-2.8	-9.8
" " "	(psi)	-910.1	-410.0	-1425.1
Inel Stn Rng, Init		0.000610	0.000410	0.000507
Inel Stn Rng, Nf/2		0.000901	0.000682	0.001297
Life Results:				
Initiation (0.030 in.)	(cycles)	1700.	1682.	484.
5% Tensile Load Drop	(cycles)	2064.	1800.	672.
10% Tensile Load Drop	(cycles)	2148.	1850.	679.
50% Tensile Load Drop	(cycles)	2640.	1930.[1]	721.
Actual End of Test	(cycles)	3000.	1863.	800.

Note: 1. Specimen 305 accidentally overloaded at 1863 cycles; 50% life is estimated.

APPENDIX E-4

INCO 718 MULTIAXIAL TESTING

TYPE I TENSION/TORSION

Specimen Identification		309	313	311
Type of Specimen		LED 41825	LED 41825	LED 41825
Test Conditions:				
Temperature	(°C)	649.	649.	649.
"	(°F)	1200.	1200.	1200.
Axial Strain Range		0.004940	0.006040	0.006010
Axial Strain R-Ratio	(min/max)	-1.012	-1.000	-1.001
Axial Strain Rate	(1/sec)	4.94E-03	6.04E-03	2.00E-04
Torsional Strain Range		0.003840	0.004580	0.004690
Torsional Strain R-Ratio	(min/max)	-0.020	-0.018	-0.052
Torsional Strain Rate	(1/sec)	7.68E-03	9.16E-03	3.10E-04
Strain Ratio	(torsional/axial)	1.555	1.517	1.561
Strain Phase Angle	(degrees)	0.000	0.000	0.000
Frequency	(cyc/min)	30.000	30.000	1.000
Axial Stress-Strain Response:				
Stress Range, Init	(Mpa)	773.9	958.3	928.7
" " "	(psi)	112243.0	138978.0	134695.0
Stress Range, Nf/2	(Mpa)	759.3	937.1	924.2
" " "	(psi)	110127.0	135913.0	134036.0
Mean Stress, Init	(Mpa)	4.6	-22.2	-8.2
" " "	(psi)	665.5	-3214.0	-1185.5
Mean Stress, Nf/2	(Mpa)	14.6	37.9	-17.1
" " "	(psi)	2117.0	5500.2	-2482.5
Inel Stn Rng, Init		0.000011	0.000010	0.000077
Inel Stn Rng, Nf/2		0.000025	0.000905	0.000243
Torsional Stress-Strain Response:				
Stress Range, Init	(Mpa)	216.7	274.7	270.0
" " "	(psi)	31429.0	39839.0	39154.0
Stress Range, Nf/2	(Mpa)	223.0	273.8	275.1
" " "	(psi)	32335.4	39713.0	39898.2
Mean Stress, Init	(Mpa)	101.7	120.4	122.6
" " "	(psi)	14747.5	17466.5	17775.0
Mean Stress, Nf/2	(Mpa)	94.4	111.1	96.9
" " "	(psi)	13687.8	16110.6	14049.3
Inel Stn Rng, Init		0.000051	0.000269	0.000027
Inel Stn Rng, Nf/2		0.000083	0.000454	0.000056
Life Results:				
Initiation (0.030 in.)	(cycles)	8890.	4700.	4563.
5% Tensile Load Drop	(cycles)	10650.	6377.	4715.
10% Tensile Load Drop	(cycles)	10950.	6555.	4790.
50% Tensile Load Drop	(cycles)	11950.	7067.	4850.
Actual End of Test	(cycles)	21274.	10150.	6367.

APPENDIX E-5

INCO 718 MULTIAXIAL TESTING

TYPE II TENSION/TORSION

Specimen Identification		314	312	315
Type of Specimen		LED 41825	LED 41825	LED 41825
Test Conditions:				
Temperature	(°C)	649.	649.	649.
"	(°F)	1200.	1200.	1200.
Axial Strain Range		0.004950	0.006110	0.006090
Axial Strain R-Ratio	(min/max)	-0.998	-1.000	-1.001
Axial Strain Rate	(1/sec)	4.95E-03	6.11E-03	2.00E-04
Torsional Strain Range		0.003870	0.004610	0.004500
Torsional Strain R-Ratio	(min/max)	-17.319	-45.127	-122.321
Torsional Strain Rate	(1/sec)	7.75E-03	9.23E-03	3.00E-04
Strain Ratio	(torsional/axial)	1.566	1.509	1.478
Strain Phase Angle	(degrees)	0.000	0.000	0.000
Frequency	(cyc/min)	30.000	30.000	1.000
Axial Stress-Strain Response:				
Stress Range, Init	(Mpa)	787.6	936.7	943.1
" " "	(psi)	114221.0	135850.0	136782.0
Stress Range, Nf/2	(Mpa)	761.0	923.1	933.2
" " "	(psi)	110366.0	133883.0	135349.0
Mean Stress, Init	(Mpa)	1.1	15.9	0.8
" " "	(psi)	153.5	2303.0	120.0
Mean Stress, Nf/2	(Mpa)	-67.8	24.1	5.5
" " "	(psi)	-9831.0	3502.5	797.9
Inel Stn Rng, Init		0.000038	0.000053	0.000101
Inel Stn Rng, Nf/2		0.000023	0.000194	0.000218
Torsional Stress-Strain Response:				
Stress Range, Init	(Mpa)	230.8	279.4	270.3
" " "	(psi)	33477.0	40520.0	39197.0
Stress Range, Nf/2	(Mpa)	217.4	280.6	268.4
" " "	(psi)	31529.4	40693.1	38932.7
Mean Stress, Init	(Mpa)	-101.6	-116.8	-130.7
" " "	(psi)	-14741.5	-16935.0	-18956.5
Mean Stress, Nf/2	(Mpa)	-97.5	-114.1	-135.6
" " "	(psi)	-14134.2	-16548.0	-19659.6
Inel Stn Rng, Init		0.000003	0.000003	0.000019
Inel Stn Rng, Nf/2		0.000440	0.000103	0.000142
Life Results:				
Initiation (0.030 in.)	(cycles)	10000.	5206.	5000.
5% Tensile Load Drop	(cycles)	22540.	5874.	7050.
10% Tensile Load Drop	(cycles)	23000.	5988.	7100.
50% Tensile Load Drop	(cycles)	23424.	6652.	7500.
Actual End of Test	(cycles)	31000.	12480.	7500.

APPENDIX F-1

INCO 718 MEAN STRESS TESTS

649°C (1200°F)

Specimen Identification	578	551	575	567	570	588	563
Type of Specimen	MERL 75	MERL 75	MERL 75	MERL 75	MERL 75	MERL 75	MERL 75
Test Conditions:							
Temperature (°C)	649.	649.	649.	649.	649.	649.	649.
" (°F)	1200.	1200.	1200.	1200.	1200.	1200.	1200.
Strain Range	0.005390	0.006400	0.007960	0.006430	0.007870	0.005450	0.006360
Strain R-Ratio (min/max)	-0.185	-0.107	0.350	0.480	0.816	0.479	0.677
Strain Rate (1/sec)	5.39E-03	6.40E-03	7.96E-03	6.43E-03	7.87E-03	5.45E-03	6.36E-03
Frequency (cyc/min)	30.000	30.000	30.000	30.000	30.000	30.000	30.000
Tension Hold (sec)	0.000	0.000	0.000	0.000	0.000	0.000	0.000
Compression Hold (sec)	0.000	0.000	0.000	0.000	0.000	0.000	0.000
Stress-Strain Response:							
Stress Range, Init (Mpa)	856.6	1027.8	1148.9	1050.1	1164.9	895.4	991.6
" " " (psi)	124240.0	149061.0	166633.0	152298.0	168943.0	129869.0	143820.0
Stress Range, Nf/2 (Mpa)	848.7	979.1	1107.5	1010.5	1107.7	882.0	990.6
" " " (psi)	123082.0	141996.0	160620.0	146552.0	160653.0	127913.0	143664.0
Mean Stress, Init (Mpa)	211.0	180.1	97.2	238.1	154.1	313.3	274.8
" " " (psi)	30597.7	26126.6	14103.0	34529.4	22351.1	45434.4	39847.8
Mean Stress, Nf/2 (Mpa)	204.2	203.6	202.3	344.7	337.6	411.4	410.3
" " " (psi)	29613.9	29523.4	29345.9	49993.5	48964.5	59663.8	59500.6
Inel Stn Rng, Init	0.000032	0.000056	0.000672	0.000025	0.000652	0.000018	0.000015
Inel Stn Rng, Nf/2	0.000027	0.000328	0.001052	0.000165	0.000225	0.000039	0.000049
Final Mean Strain	0.0022	0.0036	0.0104	0.0121	0.0654	0.0081	0.0230
Life Results:							
Initiation (cycles)	63388.	6397.	1663.	3884.	719.	16077.	3590.
5% Load Drop (cycles)	75018.	7986.	2023.	4431.	900.	19864.	4500.
10% Load Drop (cycles)	76064.	8357.	2225.	4700.	950.	20361.	4700.
50% Load Drop (cycles)	78257.	8645.	2375.	5321.	1058.	20879.	4986.

APPENDIX F-2

INCO 718 MEAN STRESS TESTS

732°C (1350°F) - ZERO MEAN & SLOW RATE

Specimen Identification		576[1]	583	592	587
Type of Specimen		MERL 75	MERL 75	MERL 75	MERL 75
Test Conditions:					
Temperature	(°C)	732.	732.	732.	732.
"	(°F)	1350.	1350.	1350.	1350.
Strain Range		0.005410	0.006730	0.005410	0.005430
Strain R-Ratio (min/max)		-0.955	-0.986	-0.197	0.174
Strain Rate	(1/sec)	5.41E-03	6.73E-03	2.25E-03	2.26E-03
Frequency	(cyc/min)	30.000	30.000	12.500	12.500
Tension Hold	(sec)	0.000	0.000	0.000	0.000
Compression Hold	(sec)	0.000	0.000	0.000	0.000
Stress-Strain Response:					
Stress Range, Init	(Mpa)	833.8	1006.5	858.2	837.0
" " "	(psi)	120927.0	145978.0	124474.0	121391.0
Stress Range, Nf/2	(Mpa)	770.0	985.1	826.8	812.2
" " "	(psi)	111674.0	142875.0	119906.0	117793.0
Mean Stress, Init	(Mpa)	1.3	-2.1	127.8	177.8
" " "	(psi)	192.5	-307.6	18534.7	25781.1
Mean Stress, Nf/2	(Mpa)	-32.4	-11.7	134.9	205.6
" " "	(psi)	-4700.7	-1698.2	19561.5	29814.2
Inel Stn Rng, Init		0.000140	0.000360	0.000142	0.000148
Inel Stn Rng, Nf/2		0.000182	0.000447	0.000219	0.000212
Final Mean Strain		0.0000	0.0000	0.0025	0.0055
Life Results:					
Initiation	(cycles)	86447.[1]	4550.	12178.	3854.
5% Load Drop	(cycles)	99086.	6001.	15379.	5224.
10% Load Drop	(cycles)	99389.	6234.	15757.	5324.
50% Load Drop	(cycles)	101702.[1]	6500.	16237.	5586.

Note: 1. Specimen 554 was run at the same nominal conditions as specimen 576; its initiation and 50% load drop lives were 81312 and 96800 cycles, respectively. However, the computer file containing the actual test response data was lost.

APPENDIX F-3

INCO 718 MEAN STRESS TESTS

732°C (1350°F) - 20, 30, & 40 KSI MEAN

Specimen Identification	582	589	558	559	579	573	566	590
Type of Specimen	MERL 75	MERL 75	MERL 75	MERL 75	MERL 75	MERL 75	MERL 75	MERL 75
Test Conditions:								
Temperature (°C)	732.	732.	732.	732.	732.	732.	732.	732.
" (°F)	1350.	1350.	1350.	1350.	1350.	1350.	1350.	1350.
Strain Range	0.005540	0.006440	0.008200	0.009690	0.005390	0.006500	0.008060	0.005480
Strain R-Ratio (min/max)	-0.024	-0.190	0.115	0.432	0.136	0.049	0.470	0.421
Strain Rate (1/sec)	5.54E-03	6.44E-03	8.20E-03	9.69E-03	5.39E-03	6.50E-03	8.06E-03	5.48E-03
Frequency (cyc/min)	30.000	30.000	30.001	30.001	30.000	30.000	30.001	30.000
Tension Hold (sec)	0.000	0.000	0.000	0.000	0.000	0.000	0.000	0.000
Compression Hold (sec)	0.000	0.000	0.000	0.000	0.000	0.000	0.000	0.000
Stress-Strain Response:								
Stress Range, Init (Mpa)	846.6	991.1	1160.6	1246.7	846.0	992.7	1162.8	849.2
" " " (psi)	122779.0	143741.0	168327.0	180813.0	122700.0	143971.0	168637.0	123164.0
Stress Range, Nf/2 (Mpa)	826.4	955.7	1084.4	1178.3	807.5	947.5	1115.0	832.3
" " " (psi)	119855.0	138607.0	157274.0	170894.0	117121.0	137415.0	161715.0	120714.0
Mean Stress, Init (Mpa)	122.0	98.6	72.3	20.7	171.7	140.3	87.2	159.4
" " " (psi)	17687.5	14297.0	10482.2	3005.6	24896.0	20347.5	12640.5	23121.1
Mean Stress, Nf/2 (Mpa)	136.2	135.5	135.0	119.0	203.3	202.6	199.9	276.6
" " " (psi)	19758.4	19645.8	19586.4	17255.2	29481.9	29378.2	28996.8	40121.2
Inel Stn Rng, Init	0.000001	0.000086	0.000463	0.001582	0.000002	0.000019	0.000431	0.000038
Inel Stn Rng, Nf/2	0.000113	0.000342	0.001271	0.001849	0.000081	0.000275	0.000724	0.000067
Final Mean Strain	0.0023	0.0033	0.0087	0.0338	0.0045	0.0046	0.0208	0.0084
Life Results:								
Initiation (cycles)	20786.	3112.	610.	179.	15086.	1924.	308.	4512.
5% Load Drop (cycles)	25447.	4200.	950.	201.	18536.	2734.	500.	5878.
10% Load Drop (cycles)	25741.	4350.	975.	324.	18763.	2891.	520.	6046.
50% Load Drop (cycles)	26995.	4576.	1017.	332.	19592.	2915.	541.	6446.

REFERENCES

Janitor, L. A., and Nelson, R. S., 1989, "CDA - Cyclic Damage Accumulation Life Prediction System - User and Programmer Manual", to be available through COSMIC.

Moreno, V., Nissley, D. M., and Lin, L. S., 1984, "Creep Fatigue Life Prediction for Engine Hot Section Materials (Isotropic) - Second Annual Report," NASA CR-174844.

Nelson, R. S., Schoendorf, J. F., and Lin, L. S., 1986, "Creep Fatigue Life Prediction for Engine Hot Section Materials (Isotropic) - Interim Report," NASA CR-179550.

Nelson, R. S., Levan, G. W., and Schoendorf, J. F., 1992, "Creep Fatigue Life Prediction for Engine Hot Section Materials (Isotropic) - Second Interim Report," NASA CR-189220.

Nissley, D. M., Meyer, T. G., and Walker, K. P., 1992, "Life Predction and Constitutive Models for Engine Hot Section Anisotropic Materials Program - Final Report", CR-189223.

Vanderplaats, G. N., Sugimoto, H., and Sprague, C. M., 1983, "ADS-1: A New General Purpose Optimization Program", IAA 24 Structures, Structural Dynamics and Materials Conference, Lake Tahoe, Nevada.

NASA
National Aeronautics and Space Administration

Report Documentation Page

1. Report No.	2. Government Accession No.	3. Recipient's Catalog No.
NASA CR-189221		

4. Title and Subtitle	5. Report Date
Creep Fatigue Life Prediction for Engine Hot Section Materials (Isotropic) - Final Report	6. Performing Organization Code: 590-21-11

7. Author(s)	8. Performing Organization Report No.
R.S. Nelson, G. W. Levan and P. R. Harvey	PWA-5894-
	10. Work Unit No.

9. Performing Organization Name and Address	11. Contract or Grant No.
United Technologies Corporation Pratt & Whitney Commercial Engineering, East Hartford, CT 06108	NAS3-23288
	13. Type of Report and Period Covered: Contractor Report - Final 5/87-2/89
12. Sponsoring Agency Name and Address National Aeronautics and Space Administration Lewis Research Center 21000 Brookpark Rd. Cleveland, OH 44135	14. Sponsoring Agency Code

15. Supplementary Notes

Project Manager: M.A. McGaw, NASA Lewis Research Center, Cleveland, Ohio

16. Abstract

This Final Report covers the activities completed under the optional program of the NASA HOST Contract, NAS3-23288. The initial effort of this optional program was report-in NASA CR189221,which consisted of high temperature strain controlled fatigue tests to study the effects of thermomechanical fatigue, multiaxial loading, reactive environments, and imposed stresses. The baseline alloy used in the tests included B1900+Hf (with or without coating) and wrought INCO 718. Tests conducted on B1900+Hf included environmental tests using various atmospheres (75 psig oxygen, purified argon, or block exposures) and specimen tests of wrought INCO 718 included tensile, creep, stress rupture, TMF, multiaxial, and mean stress tests. Results of these testings were used to calibrate a CDA model for INCO 718 alloy and to develop modifications or corrections to the CDA model to handle additional failure mechanisms. The Socie parameter was found to provide the best correlation for INCO multiaxial loading. Microstructural evaluations consisting of optical, Scanning Electron Microscopy (SEM), and Transmission Electron Microscopy (TEM) techniques, and surface replication techniques to determine crack initiation lives provided data which were used to develop life prediction models.

17. Key Words (Suggested by Author(s))	18. Distribution Statement
Creep Fatigue, Crack initiation, Thermomechanical fatigue, Multiaxial, Life Prediction, Nickel-base Alloy, Cumulative Damage	

19. Security Classif. (of this report)	20. Security Classif. (of this page)	21. No. of pages	22. Price